A MODEL FOR A CLASS OF COMPACT STARS

Ranjan Sharma

Department of Physics

University of North Bengal

Darjeeling - 734 430

India

A thesis submitted to the

University of North Bengal

for the degree of

Doctor of Philosophy in Science

2002

STOCK TAKING - 2011

Statutory Declarations

Name of the Candidate	:	Ranjan Sharma.
Title of the Thesis	:	*A Model for a Class of Compact Stars.*
Degree	:	Doctor of Philosophy (Ph. D).
Subject	:	Physics
Name of the Guide	:	Prof. S. Mukherjee.
Date of Registration	:	03.05.2000, University of North Bengal.
Place of Research	:	Department of Physics University of North Bengal Darjeeling - 734 430, India.

STATEMENT BY THE CANDIDATE

I would like to state that the research work embodied in this thesis entitled "A Model for a Class of Compact Stars" forms my contribution to the research work carried out under the supervision of Prof. S. Mukherjee at the Department of Physics, University of North Bengal. This work has not been submitted for any other degree to this or any other University. Whenever references have been made to previous works of others, it has been clearly indicated as such and included in the Bibliography.

Signature of Candidate

Name RANJAN SHARMA

Certified by

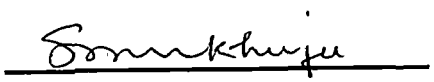

Signature of Guide

Name Prof. S. MUKHERJEE

Professor
Department of Physics,
UNIVERSITY OF NORTH BENGAL.

DEPARTMENT OF PHYSICS
UNIVERSITY OF NORTH BENGAL
P.O. NORTH BENGAL UNIVERSITY
SILIGURI, DIST. DARJEELING (WB)
PIN: 734430 INDIA

Railway Station: New Jalpaiguri (NFR)
Airport: Bagdogra
Phone: +91 (0) 353 551 414
Fax: +91 (0) 353 581 546

E-mail: root @ nbu.ernet.in

(TO WHOM IT MAY CONCERN)

This is to certify that the research work reported in this thesis entitled "A Model for a Class of Compact Stars" by Mr Ranjan Sharma has been carried out by the candidate himself under my supervision and guidance. He has fulfilled all the requirements for the submission of the thesis for Ph. D. degree of the University of North Bengal. Some parts of the research work presented in this dissertation have been performed in collaboration with others. However, even in those works his contribution is very substantial. In character and disposition Mr Ranjan Sharma is fit to submit the thesis for Ph. D. degree.

Date: 25.02.02

(Prof. S. Mukherjee)
Department. of Physics
North Bengal University

Acknowledgments

I wish to acknowledge the assistance I have received from various people and agencies during the course of my research work. To begin with, I must express my deepest gratitude and indebtedness to Prof. S. Mukherjee for shaping me up to this point. His encouragements, suggestions and vision were guiding factors to me throughout the course of my research work. In the Physics Department, I received assistance from all the teachers whenever I sought help from them. I have also received tremendous support from all my friends. In particular, Mr. Subham Majumdar and Mr. Biplab Raychoudhury helped me by providing material and software pakages at various stages of my research work. I would like to thank my co-research workers in the Research Scholar's Hostel, NBU, for boosting me up all the time. In the home front, I was always encouraged by my parents and brothers. I would also like to express my gratitude to Prof. S. D. Maharaj, Prof. M. Dey, Prof. J. Dey, Prof. K. S. Govinder, Dr. M. Govender and Dr. T. K. Dey for useful discussions and collaboration. I am also grateful to the Inter University Centre for Astronomy and Astrophysics (IUCAA), Pune, and its sister organization Iucaa Reference Centre (IRC), NBU, for providing me library and computer facilities. I gratefully acknowledge financial support from the Department of Science and Technology (DST), New Delhi, and the Council of Scientific and Industrial Research (CSIR), New Delhi. True, there are many other people without whose direct or indirect support this work would not have been completed; I apologise for not mentioning their names and thank them all most warmly.

To my parents—-

Contents

Chapter 1

Introduction

'Compact objects' are systems where very high density phases of strongly interacting matter are expected to exist. Neutron stars are compact objects whose masses are comparable to that of the Sun but radii compressed to about 10 km only! Naturally, these gravitationally bound, highly dense objects provide us cosmic laboratories for studying the properties of matter at high densities. As gravity also comes into effect at such a high density, these compact objects are also the meeting points of all the four fundamental forces.

At the final stage of a star's evolution, when all its thermonuclear fuel is exhausted, it cannot withstand the gravitational pull and starts collapsing. As it contracts appreciably from its original size, the density increases and at a sufficiently high density (of the order of nuclear matter density), it produces nonthermal pressure via degenerate fermion and particle interactions to support it against further collapse and becomes a 'compact star'. In 1932, shortly after the discovery of the particle "neutron" by Chadwick, Landau first predicted the possibility of a neutron star; a cold, dense star, whose principal composition are neutrons [1]. In a neutron star, the gravitational attraction is counter balanced by the pressure due to the degenerate neutron gas. The typical mass of a neutron star is about $1 - 2\ M_{\odot}$ ($M_{\odot} = Solar\ mass = 1.989 \times 10^{33}\ gm$),

radius $\sim$ 10 km and mean density $\sim 10^{14}$ $gm\ cm^{-3}$. In 1934, Baade and Zwicky [2] pointed out that neutron stars could be formed during supernova explosion. In 1939, Oppenheimer and Volkoff [3] built a relativistic theory of neutron stars. Our knowledge on these compact objects has improved considerably over the last few decades, thanks to the new generation satellite data as well as our current understanding of basic physics. A good introduction to the physics of neutron stars is given in a book written by Shapiro and Teukolosky [1]. For recent developments in this field, we may refer to some of the recent papers, [4], [5], [6], [7], [8], [9], [10], [11], [12], [13] & [14].

The energy-density inside a cold neutron star may range from a very low density at the suface to about 10^{15} $gm\ cm^{-3}$ at the core of the star. This wide density range may broadly be grouped into three main regimes: (i) below neutron drip density ($\rho_{drip} \sim 4 \times 10^{11}$ $gm\ cm^{-3}$) regime, (ii) neutron drip density to nuclear density ($\rho_{nuc} \sim 2.8 \times 10^{14}$ $gm\ cm^{-3}$) regime, and (iii) supernuclear density regime. To construct a stellar model we need an equation of state (EOS), i.e., $p = p(\rho)$, where, p and ρ denote pressure and energy-density of the stellar material, respectively. Although we have reasonably well-established theoretical knowledge of equations of state of matter upto nuclear matter density, the EOS at supernuclear density remains a field of active research till date [1]. As we cannot reach such a high density in laboratories, we need to build acceptable theories consistent with the observed compact star properties. The macroscopic properties, such as mass and radius of compact objects, are influenced by the composition of its stellar material. As the density inside the core of these compact objects may exceed the normal nuclear matter density (ρ_{nuc}) many exotic phases may exist inside such stars which include condensation of pions and kaons; occurrence of hyperons and more interestingly, a transition from hadronic to quark matter. It can also have mixed phases. Recent progress in high energy particle physics coupled with new observational data has given tremendous impetus in understanding the physics of highly dense compact objects.

Neutron stars are observed as radio pulsars, X-ray pulsars and X-ray bursters. In 1968, Hewish *et al* [15] for the first time observed a pulsar, which was soon identified as a rotating neutron star. Since then, more than thousand pulsars have been discovered [16]. Since more and more observational data are now available, we hope to improve our theoretical understanding of these compact objects.

The gravitational fields for such compact objects are so strong that a general relativistic treatment for such compact objects is required. Consequently, the model for such compact objects are constructed from Einstein's field equations of general relativity:

$$G_{\mu\nu} = R_{\mu\nu} - \frac{1}{2} g_{\mu\nu} R = T_{\mu\nu}, \tag{1.1}$$

where, $G_{\mu\nu}$ is Einstein tensor, $T_{\mu\nu}$, energy-momentum tensor of the stellar matter, $g_{\mu\nu}$, the metric tensor, $R_{\mu\nu}$, the Ricci tensor, and R, the Ricci scalar.

Initial temperature of a neutron star is about $10^{12}\ K$; but very rapidly it cools down below $10^6 K$ [8, 14], mainly due to neutrino emission. As the temperature decreases, matter in a neutron star becomes strongly degenerate due to very high density and hence, neutron stars, in general, are treated as cold ($T = 0$) stars. The themal effects may be treated as small perturbations which will have very little effect on the gross structure of these stars. Also, to develop a theory for these objects, one starts with a non-rotating, static configuration primarily because of the complexity of the theory. For radio pulsars this is a good approximation as most of them are known to be slow rotators [17].

The gross structure of neutron stars has so far been studied by using a variety of equations of state based upon phenomenological as well as realistic models of nuclear forces e.g, [6], [10], [14], [18], [19] & [20]. Our objective here is to develop a model of stars which seem to be more compact than ordinary neutron stars. Specifically, we are interested in those pulsars whose estimated mass and radius can not be explained with normal neutron star equations of state. Obviously, the crucial thing here is the

accuracy of the estimated mass and radius of a star. Although, mass of a compact star can be estimated from binary pulsar observations with very high accuracy [21], there is no direct method to determine the radius of a compact star. However, recent observations of some pulsars in the low-mass X-ray binaries (LMXBs) have been able to put some constraints on their compactness (mass to radius ratio). In some cases, the calculations for radius are also claimed to be very accurate [22]. There are also some proposals that the radius of a neutron star will be directly measured by the observation of gravitational waves from coalescing neutron star/black hole binaries [23], [24]. These observations will hopefully be made in the near future and will be very important to develop detailed models for compact stars. The conclusions that can be drawn at this stage is that some recently observed values for masses and radii are not consistent with the normal neutron star equations of state.

The conjecture, made independently by Witten [25] and Farhi and Jaffe [26], that quark matter (and not ^{56}Fe) might be the true ground state of hadrons, has led to the discussion of an entirely new class of compact stars, popularly called 'strange stars'. These are composed of deconfined u, d & s quarks. Strange stars are expected to form during the collapse of the core of a massive star after the supernova explosion [27]. Another possibility is that some rapidly spinning neutron stars in low mass x-ray binaries (LMXBs) can accrete sufficient mass to undergo a phase transition to become a strange star [28]. The concept of strange stars has later been supported by many authors, e.g., [29], [30], [31], [32] & [33]. Glendenning *et al* [34] and Benvenuto & Althaus [35] analyzed strange matter hypothesis and showed that if Witten's [25] hypothesis is true, we can have an entirely new class of stable white dwarfs called strange dwarfs. Strange matter hypothesis has been used by Madsen [37] to explain the pulsar glitches mechanism. Datta *et al* [38] showed that the very high frequencies in kilohertz quasi-periodic brightness oscillations (kHz QPOs) observed in certain X-ray burst sources (e.g., 4U 1636-53 with frequency 1.22 kHz) can be understood if

one considers (non-magnetized) strange star X-ray binary (SSXB) system rather than neutron star X-ray binary (NSXB) sytem.

Quantum chromodymamics (QCD), the theory of strong interactions, predicts a denconfined quark-gluon phase under extreme conditions of temperature and/or density. In high-energy heavy-ion collisions, a few microseconds ($10^{-5}s$) after the Big Bang or in the core of a very compact star we surely have such extreme conditions. The analysis of pulse timing, brightness, surface temperature and rotational mode instabilities etc. of very well known pulsars also strongly favour such a phase transition. In a recent paper, Kapoor and Shukre [17] took up a good number of modern neutron star equations of state and examining each EOS systematically (making use of the Rankin relation [36]) concluded that they are not good enough to explain the observed mass-radius constraints of known pulsars. They even suggested that pulsars are not neutron stars; rather they are strange stars. Madsen [39] also claimed that millisecond pulsars are most likely to be strange stars rather than neutron stars. These claims have already been supported by various investigators who showed that a number of pulsars, earlier thought to be neutron stars, are actually good strange star candidates. From the semi-empirical mass-radius estimations of X-ray pulsar Her X-1 [40] and X-ray burster 4U 1820-30 [41], Dey *et al* [42] proposed that they are good strange star candidates. Millisecond pulsar SAX J 1808.4-3658 [43], X-ray source 4U 1728-34 [44] and PSR 0943+10 [45] have also been proposed to be strange stars. Very recently, an isolated star RX J185635-3754 has been studied giving it a mass $M = 0.9 \pm 0.2\ M_{\odot}$ and radius $b = 6^{-1}_{+2}\ km$ [47] which may also belong to the class of strange stars as can be seen from the mass-radius curve obtained by Li *et al* [43]. In Table 1.1, we give a list of compact stars whose interior may have strange or other exotic matter.

As the maximum mass and radius of both neutron stars and strange stars are very similar, it is very difficult to distinguish between them. However, the mass-radius curve of a strange star is different from that of a neutron star, vide e.g., Alcock *et*

Pulsar	M ($M_\odot$)	b (km)
Her X-1 ([40])	0.98 ± 0.12	6.7 ± 1.2
4U 1820-30 ([41])	0.8 - 1.8	< 10
4U 1728-34 ([44])	~ 1.1	< 10
SAX J 1808.4-3658 ([43])	1.435(SS1) & 1.323(SS2)	7.07 (SS1) & 6.55(SS2)
PSR 0943+10 ([45])	—	—
PSR 1937+21 ([46])	< 2.4	< 11.5
RX J1856-37 ([47])	0.9 ± 0.2	6^{-1}_{+2}

Table 1.1: Candidates for compact stars composed of strange or other exotic matter. (Li *et al* [43] predicted two masses and radii for SAX J 1808.4-3658 considering two sets of EOS, SS1 & SS2).

al [30, 31, 32]. Neutron star mass generally decreases to a minimum value as radius increases. But strange star mass increases with radius and there is no minimum mass.

As we do not observe quarks as free particles, the quark confinement seems to be a valid proposition, even if the mechanism is not well understood. In 1974, Chodos *et al* [48] proposed a phenomenological model for quark confinement, known as MIT bag model, in which quarks are assumed to be confined in a bag and the confinement is caused by a Universal pressure 'B', called the bag pressure, on the surface of the bag. In this model quark matter energy density has a term denoted by the bag constant B which is the difference in energy densities of the vacua for hadronic matter and the quark matter. The value of bag constant B has not yet been fixed and a representative value of B is 57 $MeV\ fm^{-3}$. Most of the thermodynamical treatments of the strange matter has been carried out in the frame work of MIT bag model. An alternative description of confinement in which the masses of the quarks depend upon the baryon number density was introduced by Fowler *et al* [49]. Using the quark mass density dependent model, Chakrabarty *et al* [50] studied strange quark stars and obtained

results different from that of MIT bag model. But, later Benvenuto and Lugones [51] pointed out that the results were different because of a wrong thermodynamical treatment made in [50]. They studied the stellar properties and also the stability of strange matter at $T = 0$, using the quark mass-density-dependent model for non interacting quarks and obtained mass-radius relations for strange stars very similar to that of MIT bag model. Lugones and Benvenuto [52] did the same calculation for $T > 0$, and showed that at finite temperature too (below a certain critical temperature above which strange matter is unstable), the mass density dependent model gives very similar mass-radius relationship as in MIT bag model. Recently, Peng *et al* [53] modified the thermodynamical treatment discussed in [51] and updated the quark mass scaling and showed that the EOS thus obtained gives dimensionally smaller and less massive strange stars compared to the results of the model in [51] or in MIT bag model. Developments on strange stars has been reviewed by Cheng *et al* [54]. Very recently, Dey *et al* [42] developed a new model for strange stars where the quark interaction is described by an interquark vector potential originating from gluon exchange and a density dependent scalar potential which restores chiral symmetry at a high density. It has been claimed that the model has the ability to describe very compact stars.

The possibility that scalar fields present in the early Universe could condensate to form stars, known as boson stars, has also been explored in recent years. In cosmology, boson stars have been studied in the light of missing non-baryonic dark matter problem [55]. In 1968, Kaup [56] and later Ruffini and Bonazzola [57] first introduced the idea of objects made up of non-interacting massive scalar particles. These stars are supported against collapse by Heisenberg's uncertainty principle, unlike neutron stars which are stabilized by Pauli's exclusion principle. Typically, boson stars are gravitationally bound spherically symmetric configurations of complex scalar fields minimally coupled to gravity as given in general relativity. The physical nature of the spin-0 particle out of which a boson star is formed is still not very clear. As of now, we do not have

enough experimental support to predict the main constituent of a boson star. Most of the recent calculations on boson stars are based on the work formulated by Colpi *et al* [58], who described a boson star by considering a self-interacting complex scalar field Φ and a potential of the form $\frac{\Lambda}{4}|\Phi|^4$, where Λ is the coupling constant. The concept of a boson star was later extended to the case of a combined boson-fermion star by Henriques *et al* [59] and Jetzer[60] to model cold stellar objects composed of both bosons and fermions, parametrized by the central densities of the bosons and fermions.

In view of these varied developments, we wish to study compact objects in a different perspective. As mentioned earlier, the construction of all these highly dense stellar objects demands an EOS, for which one has to depend crucially on the microscopic behaviour of matter at high density and/or temperature. As physics of high density matter is still poorly understood, we shall follow a different technique to study these objects. In our method, we shall reconstruct the supernuclear equations of state directly from the observed properties of compact stars. In 1992, Lindblom [61] developed a method to reconstruct the EOS for nuclear matter from neutron star masses and radii. In a recent paper, Harada [62] also developed a direct method to construct super nuclear EOS from any two of the known properties of compact stars. Although, our idea is similar, the methodology is totally different. We shall prescribe a geometry and then look for suitable matter content that can support such a geometry. Based on a purely geometric approach, macroscopic properties such as mass and radius are the only input parameters required here to determine a class of possible equations of state.

The model was first considered by Vaidya and Tikekar [63]. To find the interior solution of a compact object filled with a perfect fluid-like matter in hydrostatic equilibrium, they made an ansatz for one of the metric coefficients of the relevant metric. The ansatz makes the Einstein's equations easy to solve and also gives physically acceptable solutions capable of describing a class of supercompact objects. Exact solutions of Einstein's equations for this class of stars have been obtained for some specific values

of a parameter λ, e.g., $\lambda = 2$ [63], 7 [64], & 14 [65]. Maharaj & Leach [66] obtained solutions of the same for a set of discrete values of λ. The general solution, for any value of λ, was obtained by Mukherjee *et al* [67]. The general solution greatly enhanced the applicability of the model to realistic cases. In chapter 2 we shall present some of the solutions reported where the authors used the ansatz given by Vaidya and Tikekar [63] and in particular, in section 2.3.4 we shall discuss the solution obtained by Mukherjee *et al* [67]. This general solution will be used extensively by us in the chapters to follow.

We have extended the work of Mukherjee *et al* [67] to the case of a static charged sphere. Earlier work in this field were done by Tikekar [103], Patel *et al* [104], Tikekar and Singh [105] & Patel and Kopper [115]. Essentially we have obtained an exact static spherically symmetric solution of the Einstein's field equations for a source consisting of a perfect fluid and a non-null electromagnetic field whose exterior is described by the usual Reissner-Nordstrom metric [68]. In our method we assumed (in curvature coordinates) a special functional form for the metric function g_{rr} given by Vaidya and Tikekar [63] and then with a particular choice for the electric field intensity E, we determined the remaining metric coefficient g_{tt} in a trigonometric form. Physical significance of the solution has been analysed by calculating the energy density ρ, pressure p and charge density σ of the system. It was found that the solution satifies both strong and weak energy conditions. Where relevant we have regained the uncharged limit of quantities of interest. In particular, we have shown that the causal signals in the charged case are permitted over a wider interval than in the case for uncharged stars.

Although it seems unlikely that there exits a charged astrophysical object, the possibility of a compact star acquiring a net charge by accretion from the surrounding medium has been pointed out recently by Treves and Turolla [69]. Similar observations have also been reported recently by Mak *et al* [70]. These are some of the areas where our general solution may have applications. Recently, Ivanov [71] has reviewed the known solutions for static charged fluid spheres in general relativity which includes our

solution. The solution has been discussed in chapter 3.

In chapter 2, we have shown that the solution given in [67] satisfies the desired physical and regularity conditions. However, the relevant question here is whether the model can describe a realistic star. To answer this question and to show the physical applicability of the model, we have considered some interesting pulsars and from observational data we have shown how the relevant high density equations of state can be reconstructed from the model in a very simple manner. This has also enabled us to study some other properties of these stars. We have considered, in particular, the X-ray pulsar Her X-1 and millisecond pulsar SAX J 1808.4-3658 as their masses and radii are well estimated. These pulsars are interesting because their estimated radii are rather small and these small values cannot be explained by neutron star EOS. This has led various investigators to identify them as strange stars or quark-diquark stars. Employing the strange matter EOS given by Dey *et al* [42], Li *et al* [43] claimed that the low mass X-ray binary (LMXB) pulsar SAX J1808.4-3658 is a strange star. In chapter 4 we have shown that if SAX is a strange star, the relevant EOS can be generated from the solution of Mukherjee *et al* [67].

The equation of state (EOS) in our model, for a suitable choice of the parameter λ, also covers the EOS for a quark-diquark star, a star whose interior has deconfined u, d quarks and diquarks. In chapter 5, we have studied Her X-1 and showed that if Her X-1 is a quark-diquark star, the relevant EOS obtained by Horvath and Pacheco [72] can also be generated by this model. Interestingly, although, the agreement of two equations of state are excellent, the boundary conditions assumed in the two cases are different which led us to make conclusions different from those of Horvath and Pacheco [72].

To study a star one should also check if the stellar configuration is gravitationally stable. Following the earlier work of Knutsen [156] and Tikekar and Thomas [157], which uses the method developed by Chandrasekhar [73], we have shown that the

configurations presented in chapter 4 & 5 to describe SAX J1808.4-3658 and Her X-1, respectively, are stable with respect to small radial oscillations. This has been discussed in chapter 6.

We have observed that the Vaidya-Tikekar [63] model has a scaling property which allows the solution to describe a family of stars of equal compactness ($\frac{M}{b}$) where, M and b are the mass and radius of the star, respectively. In the MIT bag model, scaling property with respect to the bag constant B in the EOS for strange matter has been reported earlier by Witten [25]. The strange matter EOS formulated by Dey *et al* [42] can also be approximated to a linear form as shown by Gondek-Rosińska *et al* [74]. The linearised EOS has the form $p = a(\rho - \rho_0)$, where, ρ and p are energy density and pressure of the star, respectively and a and ρ_0 are two parameters. In the bag model too, exactly the same type of EOS was obtained by Zdunik [75]. The linear form of the EOS allows to scale all the physical parameters of the star with some powers of ρ_0 for a fixed value of a; analogous to the scaling law with respect to the bag constant B. Thus, scaling property in compact stars like strange stars may be thought as due to the EOS being a linear one. But, we have shown that the scaling property in compact stars may rather be thought as a general feature of a spherical distribution in hydrostatic equilibrium. We have demonstrated this by analysing the Tolman-Oppenheimer-Volkoff (TOV) equations and the boundary conditions that are used while solving these equations. A special class of these scaling property is explicitly exhibited by the solution obtained by Mukherjee *et al* [67]. In chapters 4 & 5, we have shown that the solution [67] can be applied to describe strange stars as well as stars whose interior might have other exotic components. Moreover, although for a large value of the parameter λ the EOS becomes almost linear in this model, the same is not true for a smaller value of λ. Scaling property, nevertheless, applies in all the cases. The scaling behaviour in the Vaidya-Tikekar model [63] as well as it's physical implications have been discussed in chapter 7.

In case of compact stars, different possible models have been discussed so far: ordinary neutron star with a deconfined quark core (quark stars having a thin layer of hadronic matter) and bare quark stars, i.e., quark stars with no crust. Also in an ordinary neutron star it may not always be possible to use a single EOS to describe the entire star. The possibility of a compact star having a quark-diquark core surrounded by a low-density envelope of nucleon has already been discussed by Kastor and Traschen [76]. In chapter 8 we have presented a new core-envelope treatment, relevant for compact stars having a deconfined quark core surrounded by less compact hadronic matter, using the solutions obtained by Mukherjee *et al* [67]. Earlier, using TOV equations, Lindblom [77] analysed the features of the mass-radius curve of a relativistic stellar model constructed from an EOS with a first order phase-transition. The basic difference in our approach compared to the earlier workers [76, 77] is that, in our model, we do not make any ad hoc assumption about the EOS. We have constructed the model for a compact star exhibiting a phase transition somewhere inside the star by choosing two different values of the parameter λ (which occur in the Vaidya-Tikekar [63] model) for the two layers separated by a surface where a phase transition may take place and implementing necessary boundary conditions across the surface. It has been found that the core region gives a much softer EOS compared to the envelope region, as expected. Also, we have shown that the central density reached in case of a core-envelope model is larger than that of a star composed of less dense baryonic matter.

The solution obtained by Mukherjee *et al* [67] can also be applied in gravitational collapse problem. The formation of cold compact stellar objects are usually preceded by a period of radiative collapse. The problem of gravitational collapse was first investigated by Oppenheimer and Snyder [78], who considered the contraction of a spherically symmetric dust cloud. In that case the exterior space-time was described by the Schwarzschild metric and the interior space-time was represented by a Friedman-like

solution. Later on, Vaidya [79] derived the line element which describes correctly the exterior gravitational field of a spherically symmetric radiating mass. This has enabled many investigators to model the interior of a radiating star by matching the interior solution to the exterior space-time given by Vaidya (de Oliveira *et al* [80, 81, 82], Kramer [83] and Govender *et al* [84]). The junction conditions for a spherically symmetric shear-free radiating star were derived by Santos [85]. The crucial result that follows from the work of Santos [85] is that the pressure on the boundary of a radiating sphere is non-vanishing in general. Subsequently, different models of radiative gravitational collapse with heat flow were found by utilizing these junction conditions, e.g., [86]. In particular, special attention was given to models in which an initial static stellar configuration started collapsing by dissipating energy in the form of a radial heat flux (Bonnor *et al* [87]). The initial static configuration was taken to be an exact solution of the Einstein field equations before it starts collapsing. In contrast to earlier methods, we started with a final static configuration and looked for solutions for earlier evolutionary stages. In chapter 9, we have presented a simple model of radiative gravitational collapse with a radial heat flux which can describe qualitatively the stages close to the formation of a superdense cold star. Starting with the final static general solution for a cold star, as given by Mukherjee *et al* [67], we have shown that the model can generate solutions for the earlier stages of the star [89].

In this thesis we have ignored two aspects of a neutron star: (a) deformation of the star due to its rotation and (b) the effects of a strong magnetic field. In case of Her X-1, Li *et al* [40] have pointed out that rotation of Her X-1 has negligible effects on its $(M - b)$ relation. Also, considering the rotational effect upto Ω^2 (where Ω is the angular velocity observed at infinity) in case of a slowly rotating boson-fermion star, de Sousa and Silveira [90] observed that field equations remain the same as in the case of a boson-fermion star with no rotation. Hence, they concluded that star properties such as mass and radius of a static model do not differ considerably from that of a slowly

rotating boson-fermion star. Thus, although we assumed a static model for Her X-1, error in our results due to rotation, if any, should be small. Considering strange star EOS under the MIT bag model, Phukon [91] showed that the presence of a magnetic field less than 10^{18} G, does not change the EOS considerably. He found no noticable change in the maximum mass and radius of a strange star for a magnetic field less than 10^{18} G. We may, thus, presume that our results would not differ considerably in the presence of a magnetic field atleast for SAX J1808.4-3658 (magnetic field $\sim 10^8$ G) and Her X-1 (magnetic field $\sim 10^{12}$ G).

In chapter 10 we have concluded by summarizing our results and discussing avenues for further work.

Chapter 2

Vaidya-Tikekar Model: Exact Solutions

2.1 Introduction

The exterior of a static, spherically symmetric distribution of matter is uniquely described by the Schwarzschild metric:

$$ds^2 = -\left(1-\frac{2M}{r}\right)dt^2 + \left(1-\frac{2M}{r}\right)^{-1}dr^2 + r^2\left(d\theta^2 + Sin^2\theta d\phi^2\right), \qquad (2.1)$$

where, M is the mass of the distribution observed by a distant observer. The interior solutions of static perfect fluid spheres, however, are not unique and consequently the problem has been taken up by many authors, e.g., [92] & [93]. There are several techniques to construct models for spherically symmetric objects, e.g., Fodor [94] has prescribed a new algorithm to generate solutions for spherical perfect fluid distribution of matter. Recently, Finch and Skea [95] and Delgaty and Lake [96] have reviewed a large class of interior solutions and pointed out various aspects of those solutions. The large abundance of exact solutions to Einstein's field equations for a static, spherically symmetric perfect fluid star allows us to look for solutions capable of describing realistic stars.

To obtain an exact solution to the Einstein's field equations for a static spherically symmetric perfect fluid configuration, we write the interior metric as (in geometrised units with $8\pi G = c = 1$)

$$ds^2 = -e^{2\gamma(r)}dt^2 + e^{2\mu(r)}dr^2 + r^2(d\theta^2 + \sin^2\theta d\phi^2) \tag{2.2}$$

in standard coordinates $x^i = (t, r, \theta, \phi)$. The quantities $\gamma(r)$ and $\mu(r)$ are the gravitational potentials.

As we consider spherically symmetric objects only, we must have

$$G_{\theta\theta} = G_{\phi\phi}, \tag{2.3}$$

where, $G_{\mu\nu}$ is the Einstein tensor. In addition, we impose the pressure isotropy condition

$$G_{rr} = G_{\theta\theta} = G_{\phi\phi}. \tag{2.4}$$

The perfect fluid spherically symmetric configuration, may, in that case represent a star under certain regularity conditions ([97]), viz.: (1) isotropy of pressure, (2) regularity of the geometry at the origin, (3) positive definiteness of the energy density and pressure at the origin, (4) vanishing of the pressure at some finite radius, (5) monotonic decrease of pressure and energy density with increasing radius, and (6) subluminal speed of sound; although the necessity of condition (6) is arguable in the case of very compact stars [97]. Nevertheless, very few solutions obey these regularity conditions and at the same time represent a realistic situation. We have found a new class of solutions which satisfy all these conditions and is found to be very useful in describing a class of compact stellar objects. Here we mention some of the solutions obeying all these criteria and pick up the general solution given by Mukherjee *et al* [67] which will be used extensively by us in the chapters to follow.

2.2 Equilibrium configuration of a star: Standard approach

The equilibrium structure of a self-gravitating object is derived from the equations of hydrostatic equilibrium. The standard procedure for studying a self-gravitating, static, spherical star is to make use of the Tolman [98], Oppenheimer and Volkoff [3] equations (TOV) given by

$$\frac{dp}{dr} = -(\rho+p)\frac{2M(r)+pr^3}{r^2(1-\frac{2M(r)}{r})} \tag{2.5}$$

$$\frac{dM(r)}{dr} = \frac{1}{2}\rho r^2. \tag{2.6}$$

Here ρ represents the energy density and p is the isotropic pressure, expressed in geometrized units of $length^{-2}$. If the equation of state (EOS) $p = p(\rho)$ is known, all the properties of the star can be determined. One integrates the TOV equations numerically, using the boundary conditions (i) $M(0) = 0$, (ii) $p(0) = p(\rho_c)$, (iii) $p(b) = 0$ and (iv) $e^{2\gamma(b)} = 1 - \frac{2M}{b}$, where b is the radius and $M = M(b)$ is the total mass of the star as measured gravitationally from outside. For a particular EOS and a chosen parameter (e.g., central density) there is one and only one stellar configuration with a particular mass and radius.

The problem is that there are many physical situations in which one simply does not know the equation of state either because of uncertainties in the basic physics (e.g. the physics of matter above nuclear matter density in neutron stars), or in the case of a very compact star where deconfinement is a possibility, it may not be a good suggestion to use a single EOS to describe the entire star. An alternative approach has to be explored in such situations.

2.3 Alternative method

In situations where the equation of state (EOS) of superdense compact objects is uncertain or unknown, it will be useful to follow an alternative approach. One starts here with an ansatz for one of the metric functions and integrate the pressure isotropy condition to determine the other. The solution then characterises a class of static spherically symmetric perfect fluid configuration and provides the relevant EOS. The approach was first considerted by Vaidya and Tikeker [63] who prescribed an ansatz for the geometry for the $t = constant$ hypersurface. The 3-surface has a simple geometrical interpretation. If embedded in a 4-Euclidean space

$$d\sigma^2 = dx^2 + dy^2 + dz^2 + du^2, \tag{2.7}$$

a spheroidal 3-surface is defined by

$$\frac{x^2 + y^2 + z^2}{R^2} + \frac{u^2}{k^2} = 1. \tag{2.8}$$

If we write

$$x = RSin\delta Cos\theta Cos\phi,$$
$$y = RSin\delta Sin\theta Sin\phi,$$
$$z = RSin\delta Cos\theta,$$
$$u = kCos\delta,$$

equation (2.8) becomes,

$$d\sigma^2 = (R^2Cos^2\delta + k^2Sin^2\delta)d\delta^2 + R^2Sin^2\delta(d\theta^2 + Sin^2\theta d\phi^2). \tag{2.9}$$

Again writing, $r = RSin\delta$, we get

$$d\sigma^2 = \frac{1 + \lambda\frac{r^2}{R^2}}{1 - \frac{r^2}{R^2}}dr^2 + r^2(d\theta^2 + Sin^2\theta d\phi^2) \tag{2.10}$$

where we substituted, $\lambda = \frac{k^2}{R^2} - 1$. This 3-surface is spherically symmetric and well behaved for $r < R$ and $\lambda > -1$. For $\lambda = -1$, the hypersurface is flat and $\lambda = 0$ gives spherical space.

The line element for a general static spherically symmetric configuration has the standard form given in (2.2). Capitalizing on the above observation we may now assume the g_{rr} metric component in (2.2) as

$$e^{2\mu} = \frac{1 + \lambda r^2/R^2}{1 - r^2/R^2}. \tag{2.11}$$

The the geometry of the configuration, thus obtained, is governed by the parameters R and λ.

We assume that the space-time region, thus obtained, is filled with a perfect fluid and the energy-momentum tensor for such a fluid has the form

$$T_{ij} = (\rho + p)u_i u_j + p g_{ij} \tag{2.12}$$

where u^i is the 4-velocity of the fluid. Due to spherical symmetry u^i may be chosen as: $u^i = (e^{-\gamma}, 0, 0, 0)$.

The Einstein field equations $G_{ij} = R_{ij} - \frac{1}{2}g_{ij}R = T_{ij}$, for the metric (2.2), then, reduce to

$$\rho = \frac{(1 - e^{-2\mu})}{r^2} + \frac{2\mu' e^{-2\mu}}{r} \tag{2.13}$$

$$p = \frac{2\gamma' e^{-2\mu}}{r} - \frac{(1 - e^{-2\mu})}{r^2} \tag{2.14}$$

$$p = e^{-2\mu}\left(\gamma'' + \gamma'^2 - \gamma'\mu' + \frac{\gamma'}{r} - \frac{\mu'}{r}\right) \tag{2.15}$$

where primes denote differentiation with respect to r.

Equations (2.14) and (2.15) may be combined to give

$$\gamma'' + \gamma'^2 - \gamma'\mu' - \frac{\gamma'}{r} - \frac{\mu'}{r} - \frac{(1 - e^{2\mu})}{r^2} = 0. \tag{2.16}$$

Equation (2.16) results from the pressure isotropy condition. To find the solution to equation (2.16), one has to make some ad hoc assumptions for γ or μ. Assuming

the form of μ as in (2.11), we introduce the transformation

$$\begin{aligned} \psi &= e^{\gamma} \\ x^2 &= 1 - \frac{r^2}{R^2} \end{aligned}$$

so that (2.16) can be written as

$$\left(1 + \lambda - \lambda x^2\right) \psi_{xx} + \lambda x \psi_x + \lambda \left(\lambda + 1\right) \psi = 0. \tag{2.17}$$

Here the suffix x represents differentiation with respect to x. This equation has been comprehensively studied by a number of authors. We give here a few solutions of equation (2.17) which have utilized the ansatz of Vaidya and Tikekar [63]. These solutions may represent a toy model for a class of superdense stars.

2.3.1 The solution of Vaidya and Tikekar [63]

For a particular choice of the curvature parameter $\lambda = 2$, Vaidya and Tikekar [63] obtained an exact solution of equation (2.17), and the line element obtained by them has the form

$$ds^2 = -\left[Ax\left(1 - \frac{4x^2}{9}\right) + B\left(1 - \frac{2x^2}{3}\right)^{3/2}\right]^2 dt^2 + \frac{3 - 2x^2}{x^2} dr^2 + r^2 d\Omega^2. \tag{2.18}$$

where, A and B are constants. $(d\Omega^2 = d\theta^2 + Sin^2\theta d\phi^2)$.

2.3.2 The solution of Tikekar [64]

Tikekar [64] obtained an exact solution of equation (2.17) for $\lambda = 7$ and the line element in this case has the form

$$ds^2 = -\left[C(1 - \frac{7x^2}{2} + \frac{49x^4}{24}) + Dx(1 - \frac{7x^2}{8})^{3/2}\right]^2 dt^2 + \frac{8 - 7x^2}{x^2} dr^2 + r^2 d\Omega^2 \tag{2.19}$$

where, C and D are constants.

2.3.3 The solution of Maharaj & Leach [66]

Maharaj & Leach [66] obtained two catagories of polynomial solutions of equation (2.17) for discrete values of the parameter λ. For $\lambda = (2n-1)^2 - 2$, the solutions are given by:

$$e^{\gamma} = \psi = A\sum_{i=0}^{n} \frac{(n+i-2)!}{(n-i)!(2i)!}(-l)^i x^{2i} + B(1+\lambda-\lambda x^2)^{3/2} \sum_{i=0}^{n-2} \frac{(n+i)!}{(n-i-2)!(2i+1)!}(-l)^i x^{2i+1} \tag{2.20}$$

while for $\lambda = 4n^2 - 2$, the solutions are:

$$\psi = A\sum_{i=0}^{n} \frac{(n+i-1)!}{(n-i)!(2i+1)!}(-m)^i x^{2i+1} + B(1+\lambda-\lambda x^2)^{3/2} \sum_{i=0}^{n-1} \frac{(n+i)!}{(n-i-1)!(2i)!}(-m)^i x^{2i}, \tag{2.21}$$

with,

$$l = 4 - \frac{1}{n(n-1)},$$

$$m = 4 - \frac{4}{4n^2-1}$$

and $n = 2, 3$ etc.

2.3.4 The solution of Mukherjee *et al* [67]

The general solution of equation (2.17) for any value of λ was obtained by Mukherjee *et al* [67]. As we shall use this solution extensively in the chapters to follow, we discuss here various features of this solution.

We straight way start with the equation (2.17). To obtain the general solution, a new variable is defined

$$z = \left(\frac{\lambda}{\lambda+1}\right)^{1/2} x. \tag{2.22}$$

The equation (2.17) then gets the form

$$(1-z^2)\psi_{zz}(z) + z\psi_z(z) + (\lambda+1)\psi(z) = 0 \tag{2.23}$$

where the subscript z denotes differentiation with respect to z.

The solution to this equation for an integer n, where, $n = (\lambda+2)^{1/2}$, can be written as

$$\psi = A_1 T_{n+1}^{-3/2}(z) + A_2(1-z^2)^{3/2} T_{n-2}^{3/2}(z), \tag{2.24}$$

where T_α^β is a Gegenbauer function [99] and A_1 & A_2 are constants.

Differentiating equation (2.24) with respect to z we get,

$$\psi_z = A_1 T_n^{-1/2}(z) + A_2(n+1)(n+3)(1-z^2)^{1/2} T_{n-1}^{1/2}(z). \tag{2.25}$$

We note that $nT_n^{-1/2}(z)$ and $(1-z^2)^{1/2}T_{n-1}^{1/2}(z)$ are actually Tschebyscheff polynomials. For an integer n and real z with $0 < z \leq [\lambda/(\lambda+1)]^{1/2}$, these polynomials can be expressed in terms of trigonometric functions:

$$nT_n^{-1/2}(z) = (2/\pi)^{1/2} \cos(n \cos^{-1} z), \tag{2.26}$$

$$(1-z^2)^{1/2} T_{n-1}^{1/2}(z) = (2/\pi)^{1/2} \sin(n \cos^{-1} z). \tag{2.27}$$

Substituting these values in equation (2.25) and integrating we obtain ψ in terms of trigonometric functions as

$$\psi(z) = e^\gamma = A\left[\frac{\cos[(n+1)\zeta+\delta]}{n+1} - \frac{\cos[(n-1)\zeta+\delta]}{n-1}\right], \tag{2.28}$$

where $\zeta = \cos^{-1} z$, and A and δ are constants. Although the solution (2.28) is obtained by considering initially integral values of n, it can now be continued analytically for any real $\lambda > -2$. Thus we get the general solution for any $\lambda > -2$. Physical considerations may, however, put further constraints on the value of λ.

General features of the solution:

In this model, energy-density ρ and pressure p are given, respectively, by

$$\rho = \frac{1}{R^2(1-z^2)}\left[1 + \frac{2}{(\lambda+1)(1-z^2)}\right] \tag{2.29}$$

$$p = -\frac{1}{R^2(1-z^2)}\left[1 + \frac{2z\psi_z}{(\lambda+1)\psi}\right]. \tag{2.30}$$

The radius of the star, b, is determined by the condition that pressure should vanish at the boundary, i.e., $p = 0$ at $r = b$. From (2.30), this gives

$$z_b \frac{\psi_z(z_b)}{\psi(z_b)} = -\frac{1}{2}(1+\lambda) \tag{2.31}$$

where $z_b = [\lambda/(\lambda+1)]^{1/2}(1 - b^2/R^2)^{1/2}$.

The mass contained inside a radius r is given by

$$M(r) = \frac{1}{2}\int_0^r r'^2 \rho(r')dr' \tag{2.32}$$

which on integration upto $r = b$ yields

$$M(b) = \frac{(1+\lambda)b^3/R^2}{2(1+\lambda b^2/R^2)}. \tag{2.33}$$

From (2.29) and (2.30) we note that ρ is obviously positive for $\lambda > -1$, while $p \geq 0$ requires $z\psi_z/\psi \leq -\frac{1}{2}(\lambda+1)$.

For p to remain finite ψ should not have a zero in the range $z_b \leq z \leq z_0$, where $z_0 = [\lambda/(\lambda+1)]^{1/2}$. We also require that both $d\rho/dz$ and dp/dz should increase monotonically as z increases from z_b to z_0. In Fig.2.1 p is plotted against ρ which clearly shows that there is no singular behaviour for p in the prescribed range.

This model has 4 parameters R, λ, A and δ, of which three, say, R, A and δ, can be determined by the matching conditions: (1) at $r = b$, $p = 0$ and (2) continuity of two metric coefficients across the boundary. The choice of the remaining parameter λ, then, fixes the equation of state. Thus while in the standard approach, the inputs are the central density and the equation of state, in the present model b and λ play similar roles.

Note that $r < R$ corresponds to $b > 2M$ as in the case of the Schwarzschild interior solution. Further the black hole event horizon in the present case can be approached either by letting $r \longrightarrow R$ or $\lambda \longrightarrow \infty$.

To determine the velocity of sound, we differentiate equation (2.28) which gives,

$$u = \frac{\psi_z}{\psi} = \frac{(n^2-1)\Big[\sin[(n-1)\zeta+\delta] - \sin[(n+1)\zeta+\delta]\Big]}{\sqrt{1-z^2}\Big[(n+1)\cos[(n-1)\zeta+\delta] - (n-1)\cos[(n+1)\zeta+\delta]\Big]}. \tag{2.34}$$

From equations (2.29) and (2.30) we get,

$$\frac{dp}{d\rho} = \frac{z(1-z^2)^2u^2 - (1-z^2)u}{z(1-z^2)(1+\lambda)+4z}, \tag{2.35}$$

where, u is defined in equation (2.34). The velocity of sound is defined by $v_s = \sqrt{\frac{dp}{d\rho}}$.

The most stringent constraint in a stellar model comes if we require that the sound propagation be causal; i.e. $\frac{dp}{d\rho} < 1$. This implies

$$\frac{1}{(1-z^2)}\Big(\frac{1}{2z} - D\Big) \leq \frac{\psi_z}{\psi} \leq \frac{1}{(1-z^2)}\Big(\frac{1}{2z} + D\Big), \tag{2.36}$$

where

$$D = [4 + 1/4z^2 + (1+\lambda)(1-z^2)]^{1/2}. \tag{2.37}$$

Again, $p \geq 0$ gives

$$\frac{\psi_z}{\psi} \leq -\frac{\lambda+1}{2z} \quad . \tag{2.38}$$

Combining the two constraints, we get the effective bound

$$\frac{1}{1-z^2}\Big(\frac{1}{2z} - D\Big) \leq \frac{\psi_z}{\psi} \leq -\frac{\lambda+1}{2z}, \tag{2.39}$$

for a realistic model. Eqn. (2.39) readily leads to a lower bound

$$\lambda > \frac{3}{17}. \tag{2.40}$$

This clearly excludes the flat space ($\lambda = -1$).

In Fig.2.1, the slope of the p versus ρ curve is always less than that of $\rho = p$, which shows that $dp/d\rho < 1$ always. Further it lies below and never intersects the $\rho = 3p$ curve indicating $\rho > 3p$ and hence satisfying the strong energy condition.

The constraint (2.39) leads to an upper bound on possible values of $\overline{b} = b/R$, which reads as

$$(1-\overline{b}^2) \geq \frac{\lambda^2 + 5\lambda + 12 - (17\lambda^2 + 82\lambda + 129)^{1/2}}{\lambda(5+\lambda)}. \tag{2.41}$$

In Fig.2.2, the upper bound on $\overline{b}$ is plotted against $\log_{10}\lambda$. The figure shows that for a given $\overline{b}$, there correspond two values of λ.

Equations (2.33) and (2.41) also lead to an upper bound on M/b, which measures the compactness of the star. The upper bound approaches the Schwarzschild limit 1/2 asymptotically as λ tends to infinity. The upper bound on M/b increases monotonically from 0 to $\frac{1}{2}$ as λ is increased from its lowest value $\frac{3}{17}$ as shown in Fig.2.3. This shows that for a given radius b, stars with larger λ will be more compact.

From equation (2.29) we get the central density of the star

$$\rho_c = 3(\lambda + 1)/R^2, \tag{2.42}$$

from which the parameter R can also be determined. In Table 2.1, values of various parameters in this model for different choices of the parameter λ are given. The mass and radius chosen in this case are $M = 0.88\ M_\odot$ and $b = 7.7\ km$, respectively.

We may sum up by observing that

- p is well-behaved in the prescribed range for z. The curve p versus ρ indicates the implicit equation of state for the fluid.
- $dp/d\rho < 1$ always as slope of the solid curve is less than that of $\rho = p$ curve.
- both $\rho > p$ and $\rho > 3p$ (the weak and strong energy conditions) are satisfied as can be seen by comparing with the other two curves in Fig.2.1.

Thus all the physical conditions are satisfied.

2.4 Discussions

To conclude, we have noted that the general soution given by Mukherjee *et al* [67] describes a class of static spherically symmetric distribution of matter in hydrostatic equilibrium, satisfying all physical constraints. Also, as the solution is in simple trigonometric form, the model can be handled easily. Various applications of this model will be taken up in the chapters to follow.

λ	$R(km)$	δ	A	$\left(\frac{dp}{d\rho}\right)_{r=0}$	$\left(\frac{dp}{d\rho}\right)_{r=b}$
2	20.224	2.23367	0.9332	0.3418	0.3518
5	27.545	2.41532	1.6913	0.2714	0.2847
10	36.627	2.49738	2.9926	0.2479	0.2624
20	50.073	2.5449	5.61083	0.2361	0.2511
50	77.488	2.57512	13.4818	0.2291	0.2446
100	108.779	2.58577	26.6039	0.2268	0.2424
200	153.264	2.59118	52.8501	0.2256	0.2413

Table 2.1: Values of various parameter of the model for different choices of the parameter λ for a star of mass $M = 0.88\ M_{\odot}$ & radius $b = 7.7\ km$.

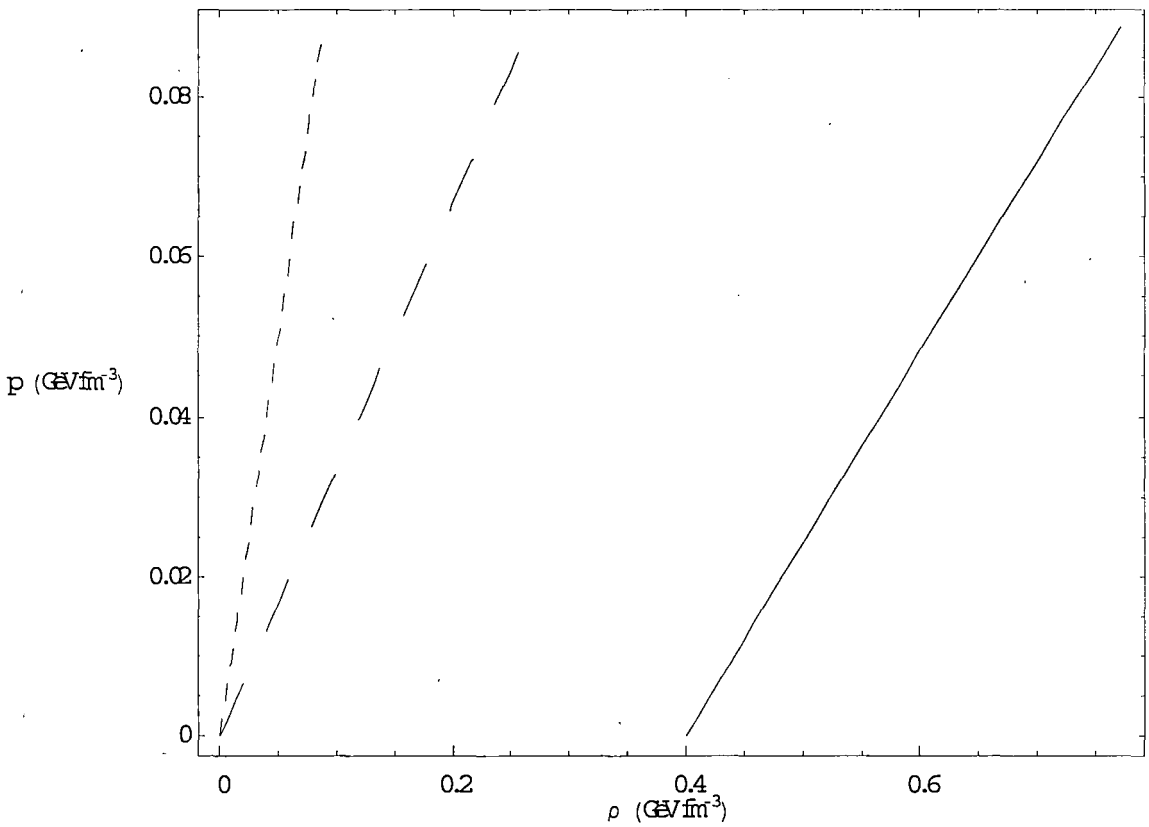

Figure 2.1: Equation of state of a star of mass $M = 0.88\ M_{\odot}$ and radius $b = 7.7\ km$ (solid line), while short and long dashed lines represent $\rho = p$ and $\rho = 3p$ curves, respectively. Here, $\lambda = 100$, $\delta = 2.58577$ and $R = 108.779\ km$.

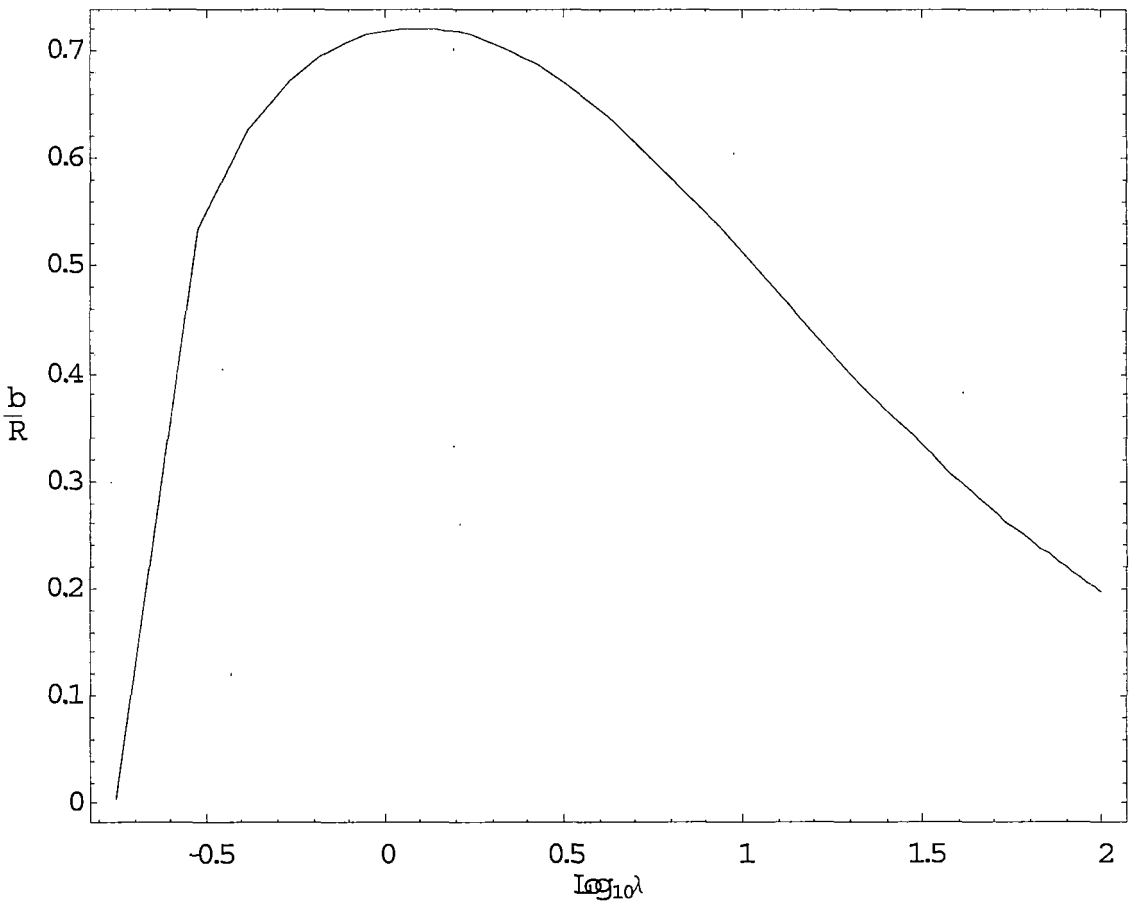

Figure 2.2: Upper bound on the possible values of $\frac{b}{R}$ plotted agained $Log_{10}\lambda$.

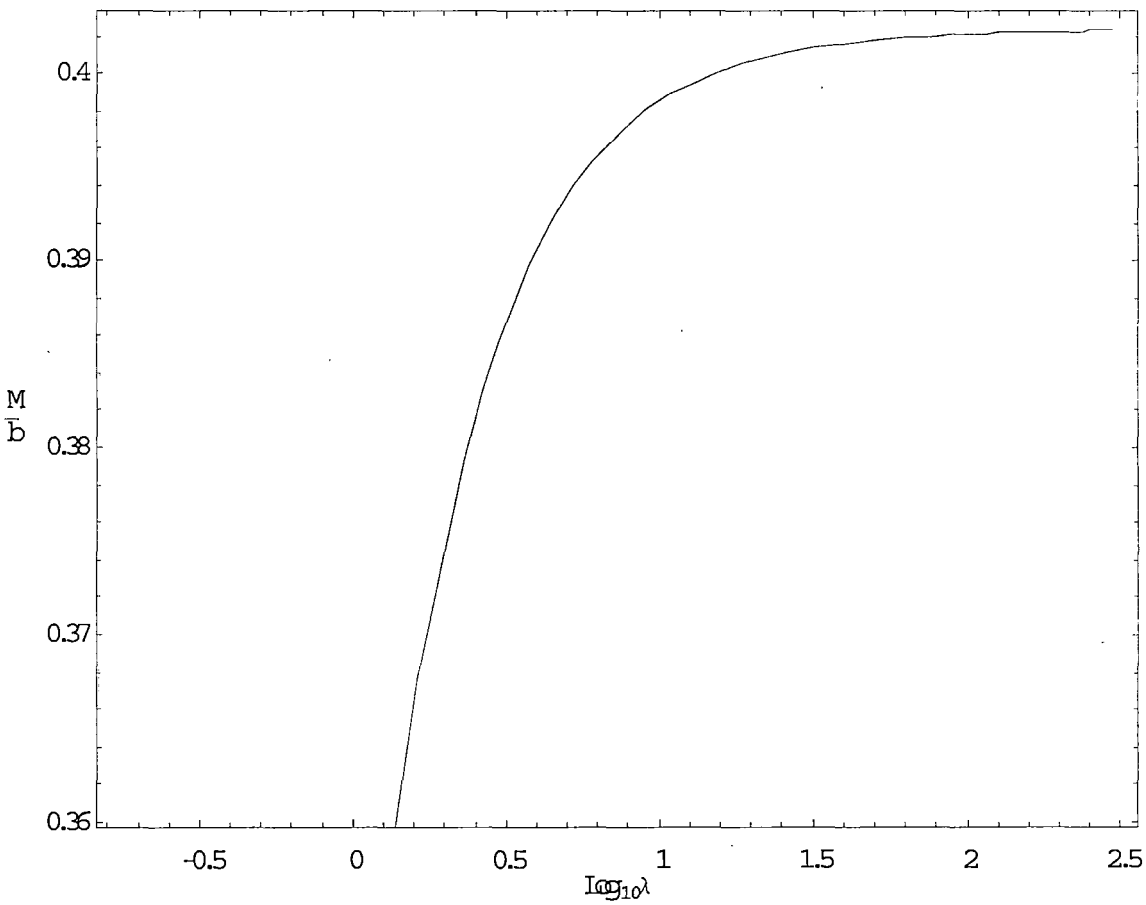

Figure 2.3: Upper bound on the possible values of $\frac{M}{b}$ plotted agained $Log_{10}\lambda$.

Chapter 3

General Solution for a Class of Static Charged Spheres

3.1 Introduction

Exact solutions to the coupled Einstein-Maxwell system of equations are important for many physical applications, in particular in relativistic astrophysics. Such solutions may be used to model relativistic charged stars where the interior of the charged sphere matches with the Reissner-Nordstrom metric at the boundary. It is interesting to observe that, in the presence of charge, the gravitational collapse of a spherically symmetric distribution of matter to a point singularity may be avoided. In this situation the gravitational attraction is counter balanced by the repulsive Coulombian force in addition to the pressure gradient. Consequently the Einstein-Maxwell system, for a charged star, has attracted considerable attention in various investigations. Earlier workers in this field include Bonnor [100], De and Raychaudhari [101] and Cooperstock and Cruz [102], to name a few. Exact solutions of the coupled Einstein-Maxwell equations on the background of spheroidal space-time were obtained by Tikekar [103], Patel *et al* [104] and Tikekar and Singh [105]. Dianyan [106] analyzed the Einstein-Maxwell

system in a higher dimensional space-time. The charged sphere case has also been taken up by Tiwari and Ray [107], Guilfoyle [108] and Rao *et al* [109, 110]. Applications of the Einstein-Maxwell system in inhomogeneous cosmological models have been analyzed by Krasinskii [111]. Considering a particular charge distribution Felice *et al* [112] presented a model for a charged fluid sphere and discussed its stability. Stability of relativistic charged spheres has also been discussed by Anninos and Rothman [113]. In a recent article, Ivanov [71] has reviewed the known solutions for static charged fluid spheres in general relativity.

Although it is most unlikely that there exits a charged large astrophysical object, the possibility of a compact cold star acquiring a net charge by accretion from the surrounding medium has been studied recently by Treves and Turolla [69]. Similar observations have also been reported recently by Mak *et al* [70].

Our objective here is to study the gravitational behaviour of a general class of charged stars for a particular choice of the electric field intensity. In Section 3.2 we present the Einstein-Maxwell field equations for the static, spherically symmetric line element. The set of field equations is reduced to a single differential equation. The general solution of the condition for pressure isotropy is given in Section 3.3 in terms of Gegenbauer functions. We rewrite the general solution in terms of elementary functions. Also we relate our results to the solutions of other investigators. In Section 3.4 we provide a detailed analysis of the quantities of physical interest for a relativistic charged star. Finally in Section 3.5 we discuss the physical viability of our model and consider avenues for further work.

3.2 Einstein-Maxwell equations

We write the line element for static spherically symmetric charged spacetime in the form (in geometrised units with $8\pi G = c = 1$)

$$ds^2 = -e^{2\gamma(r)}dt^2 + e^{2\mu(r)}dr^2 + r^2(d\theta^2 + \sin^2\theta d\phi^2) \tag{3.1}$$

in standard coordinates $x^i = (t, r, \theta, \phi)$. The quantities $\gamma(r)$ and $\mu(r)$ are the gravitational potentials.

The total energy-momentum tensor, for a charged sphere, has the standard form

$$T_{ij} = (\rho + p)u_i u_j + p g_{ij} + 2\left[F_{ik}F_j^k - \frac{1}{4}F_{kl}F^{kl}g_{ij}\right] \tag{3.2}$$

where ρ represents the energy density, p is the isotropic pressure and u^i is the 4-velocity of the fluid. Because of spherical symmetry, the electric field E must be radial, the Maxwell stress tensor has only two non-zero component F_{tr} and F_{rt} and we define the intensity of the electric field as $E^2 = -F_{tr}F^{tr}$. F^{ij} satisfies the following relations:

$$\left(2F^{ij}\sqrt{-g}\right)_{,j} = \sqrt{-g}J^i = \sqrt{-g}\sigma u^i \tag{3.3}$$

$$F_{ij,k} = 0 \tag{3.4}$$

where, J^i and σ denote four-current and proper charge density of the fluid, respectively.

The Einstein-Maxwell equations, for the metric (3.1), then, reduce to

$$\rho + E^2 = \frac{(1 - e^{-2\mu})}{r^2} + \frac{2\mu' e^{-2\mu}}{r} \tag{3.5}$$

$$p - E^2 = \frac{2\gamma' e^{-2\mu}}{r} - \frac{(1 - e^{-2\mu})}{r^2} \tag{3.6}$$

$$p + E^2 = e^{-2\mu}\left(\gamma'' + \gamma'^2 - \gamma'\mu' + \frac{\gamma'}{r} - \frac{\mu'}{r}\right) \tag{3.7}$$

where primes denote differentiation with respect to r.

The quantity

$$q(r) = \frac{1}{2}\int_0^r \sigma r^2 e^{\mu} dr = r^2 E \tag{3.8}$$

defines the total charge contained within the sphere of radius r.

Equations (3.6) and (3.7) may be combined to give

$$\gamma'' + \gamma'^2 - \gamma'\mu' - \frac{\gamma'}{r} - \frac{\mu'}{r} - \frac{(1-e^{2\mu})}{r^2} - 2E^2e^{2\mu} = 0. \tag{3.9}$$

As discussed in chapter 2, in an attempt to reduce the complexity of the field equations Vaidya and Tikekar [63] gave an ansatz for one of the metric coefficients in equation (3.1), given by

$$e^{2\mu} = \frac{1+\lambda r^2/R^2}{1-r^2/R^2}, \tag{3.10}$$

where λ and R are the curvature parameters. This assumption produces relativistic stars with ultrahigh densities and pressures consistent with observations (Rhodes and Ruffini [114]). The assumption has the additional advantage of providing the solution of the field equations with a clear geometrical characterisation. The assumption has been used by Tikekar [103], Patel and Kopper [115] and Tikekar and Singh [105] to describe the behaviour of static charged objects for some restricted values of the parameter λ, e.g., $\lambda = 2$ & 7. Here we would like to generalize these results for an arbitrary λ; the requirements for a realistic solution, e.g., the need for causal signals, however, restrict the value of λ. This issue will be taken up in section 3.4. To solve equation (3.9), we also make the choice for one of the metric coefficients given by equation (3.10).

We now clarify a number of issues that pertain to the physical relevance of this class of static charged spheres. Our choice for the spatial geometry parametrized by λ generates models of static charged spheres which are consistent with densities of superdense stars. For a physically relevant solution, it is often required that an equation of state, relating energy density to the pressure should hold. We observe that the solutions presented here do not satisfy an equation of state, though they are relevant in the description of highly dense stars where we have little information about the matter content, atleast inside the core. However, we should point out that in the uncharged case, the solutions lead to an equation of state as demonstrated by Mukherjee *et al* [67]. In a more general treatment, we would also need to allow for

the electric and magnetic properties of the barotropic matter content. However, in our present investigation, we consider only a special distribution of an electric field.

To carry out the solution, we introduce the transformation

$$\begin{aligned} \psi &= e^{\gamma} \\ x^2 &= 1 - \frac{r^2}{R^2}, \end{aligned}$$

so that (3.9) can be written as

$$\left(1+\lambda-\lambda x^2\right)\psi_{xx} + \lambda x\psi_x + \lambda\left(\lambda+1\right)\psi - \frac{2E^2R^2\left(1+\lambda-\lambda x^2\right)^2}{1-x^2}\psi = 0 \tag{3.11}$$

where we have used (3.10). When $E = 0$, (3.11) becomes

$$\left(1+\lambda-\lambda x^2\right)\psi_{xx} + \lambda x\psi_x + \lambda\left(\lambda+1\right)\psi = 0 \tag{3.12}$$

Equation (3.12) was comprehensively analysed by Maharaj and Leach [66] who found solutions in terms of elementary functions. The general solution, in terms of special functions, was presented by Mukherjee *et al* [67].

To solve the equation (3.11) we make the choice

$$E^2 = \frac{\alpha^2\left(1-x^2\right)}{R^2\left(1+\lambda-\lambda x^2\right)^2} \tag{3.13}$$

where α is a constant. This choice for E generates a model for a charged star which is physically realistic as will be discussed in section 3.4. Also a specific upper bound on α and hence on E is found in this model.

The choice of E, lets us to rewrite equation (3.11) as

$$\left(1+\lambda-\lambda x^2\right)\psi_{xx} + \lambda x\psi_x + \left[\lambda\left(\lambda+1\right) - 2\alpha^2\right]\psi = 0 \tag{3.14}$$

We integrate (3.14) in the next section. The choice (3.13) for the electric field intensity was made so as to retain the characterisation of the solution in terms of the parameter λ. Patel and Koppar [115] chose a similar form for E corresponding to the parameter value $\lambda = 2$.

3.3 General Solution

To obtain the general solution we let

$$z = \left(\frac{\lambda}{\lambda+1}\right)^{1/2} x$$
$$\beta^2 = \lambda + 2 - \frac{2\alpha^2}{\lambda}$$

We can then write (3.14) as the third order equation

$$(1-z^2)\psi_{zzz} - z\psi_{zz} + \beta^2\psi_z = 0 \tag{3.15}$$

If we treat ψ_z as the dependent variable then the general solution of (3.15) is given by

$$\psi_z = A_1 T_\beta^{-1/2}(z) + A_2(1-z^2)^{1/2} T_{\beta-1}^{1/2}(z) \tag{3.16}$$

where $T_\beta^{-1/2}$ and $T_{\beta-1}^{1/2}$ are Gegenbauer functions ([99], p. 547), and A_1 and A_2 are constants. When β is zero or a positive integer then the functions reduce to polynomials. On using the properties of the Gegenbauer functions, we can eliminate the derivative in (3.16) and obtain the representation

$$\psi(z) = C T_{\beta+1}^{-3/2}(z) + D(1-z^2)^{3/2} T_{\beta-2}^{3/2}(z), \tag{3.17}$$

where C and D are constants. We can also represent the solution in the form

$$\psi(\zeta) = A\left[\frac{\cos[(\beta+1)\zeta+\omega]}{\beta+1} - \frac{\cos[(\beta-1)\zeta+\omega]}{\beta-1}\right], \tag{3.18}$$

if we let $\zeta = \cos^{-1} z$ for real z, with $0 < z \leq \beta$. In (3.18), A and ω are constants.

When $\beta^2 = \lambda + 2$ (i.e. $\alpha = 0$) we regain the general solution of Mukherjee *et al* [67] for uncharged spheres. In the case $\beta^2 = 4 - \alpha^2$ (i.e. $\alpha \neq 0$) we regain the particular solution of Patel *et al* [104] for charged spheres with the geometry corresponding to the parameter $\lambda = 2$.

3.4 Physical analysis

The form of the solution enables us to study the physical features in a qualitative fashion. The energy density, pressure and charge density are given, respectively, by

$$\rho = \frac{1}{R^2(1-z^2)}\left[1+\frac{2}{(\lambda+1)(1-z^2)}-\frac{\alpha^2[(\lambda+1)(1-z^2)-1]}{\lambda(1+\lambda)^2(1-z^2)}\right] \tag{3.19}$$

$$p = -\frac{1}{R^2(1-z^2)}\left[1+\frac{2z\psi_z}{(\lambda+1)\psi}-\frac{\alpha^2[(\lambda+1)(1-z^2)-1]}{\lambda(1+\lambda)^2(1-z^2)}\right] \tag{3.20}$$

$$\sigma = \frac{2\alpha z(1-z^2)^{-5/2}}{\sqrt{\lambda}R^2(1+\lambda)^2}\left[2+(\lambda+1)(1-z^2)\right]. \tag{3.21}$$

When $\alpha = 0$ we regain from (3.19) and (3.20) the expressions of Mukherjee *et al* [67] as a special case. A detailed physical study in the particular case $\lambda = 2$ by Patel and Koppar [115] shows that $\rho \geq 0$ and $p \geq 0$ so that the weak energy conditions are satisfied. Our general solution permits a similar analysis to be performed for all real values of λ. The quantities ρ, p, σ have simple forms; they are well-behaved and bounded in the interior of the charged sphere. It is clear that these quantities are finite and regular at the centre. We have shown in Table 3.1, some values of ρ and p for $\lambda = 1$ and $\alpha = 0$ & 0.4. For a high value of $\lambda \geq 50$, the effect of the charge distribution ($\alpha < 0.43$) is negligible.

The radius is fixed by putting $p = 0$ at the boundary $r = b$, which gives the condition

$$\frac{\psi_z(z_b)}{\psi(z_b)} = \frac{\lambda+1}{2z_b}\left[\frac{\alpha^2 b^2}{R^2(1+\lambda)(1-z_b^2)}-1\right], \tag{3.22}$$

where

$$z_b = \left(\frac{\lambda}{\lambda+1}\right)^{1/2}\left(1-\frac{b^2}{R^2}\right)^{1/2},$$

is the value of z at the boundary.

The model has five parameters, A, ω, R ,λ, and α. Two of these may, in principle, be determined by matching the interior solution at $r = b$, to the Reissner-Nordstrom

$\alpha = 0$		$\alpha = 0.4$	
ρ	p	ρ	p
.4567	0	.3800	0
.4842	.0128	.3939	.0037
.5026	.0214	.4089	.0098
.5225	.0307	.4250	.0163
.5441	.0407	.4426	.0233
.5676	.0516	.4617	.0309
.5933	.0635	.4826	.0391
.6188	.0753	.5034	.0472

Table 3.1: Energy-density and Pressure in GeVfm^{-3} for $\lambda = 1$ and $\alpha = 0$ & 0.4, for a typical compact star of mass $M = 0.88\ M_{\odot}$.

metric, given by

$$ds^2 = -\left(1 - \frac{2M}{r} + \frac{q^2}{r^2}\right) dt^2 + \left(1 - \frac{2M}{r} + \frac{q^2}{r^2}\right)^{-1} dr^2 + r^2(d\theta^2 + \sin^2\theta d\phi^2), \quad (3.23)$$

where M and q denote the total mass and charge, respectively, as measured by an observer at infinity. The two parameters A and ω in (3.18) can now be determined conveniently by noting that the equation (3.22) is independent of A, and the relation

$$\psi(z_b) = \left(1 - \frac{b^2}{R^2}\right)^{1/2} \left(1 + \frac{\lambda b^2}{R^2}\right)^{-1/2},$$

is valid. In the uncharged case, given a value of λ (which may be looked upon as specifying an equation of state) one may determine the radius of the star. The mass is already determined by the matching conditions. In the charged case, one needs also to specify either α or q. Thus we have an exactly solvable model.

To see the effect of the charge distribution, we calculate the radius of a typical highly compact star of mass $M = 0.88\ M_{\odot}$. For $\lambda = 1$, if we let the radius in the uncharged

case to be 7.7 km, in the presence of charge with $\alpha = 0.4$, the radius increases to 8.18 km. However if we assume a high value of λ, say $\lambda = 100$, there is practically no effect of charge on the radius. It is, however, useful to study the constraints that are imposed on the parameters from physical considerations.

Since the pressure $p \geq 0$ inside the sphere, we require that

$$\frac{\psi_z}{\psi} \leq \frac{\alpha^2 r^2}{R^2(\lambda+1)2z(1-z^2)} - \frac{\lambda+1}{2z}. \tag{3.24}$$

Again, from (3.19) and (3.20) we obtain the expression

$$\frac{dp}{d\rho} = \frac{z(1-z^2)^2(\psi_z/\psi)^2 - (1-z^2)(\psi_z/\psi) + \alpha^2\left[\frac{2z}{\lambda+1} + \frac{z^3}{\lambda} - \frac{3z}{\lambda}\right]}{z(1-z^2)(\lambda+1) + 4z - \alpha^2\left[\frac{2z}{\lambda+1} - \frac{z}{\lambda} - \frac{z^3}{\lambda}\right]}$$

For causality not to be violated the speed of sound must be less than the speed of light so that $\frac{dp}{d\rho} < 1$. This condition and (3.24) give

$$\frac{1}{(1-z^2)}\left[\frac{1}{2z} - D\right] \leq \frac{\psi_z}{\psi} \leq \frac{\alpha^2 r^2}{R^2(\lambda+1)2z(1-z^2)} - \frac{\lambda+1}{2z} \tag{3.25}$$

where

$$D = \left[4 + \frac{1}{4z^2} + (\lambda+1)(1-z^2) + \frac{4\alpha^2}{\lambda(\lambda+1)}\right]^{1/2}.$$

The constraint (3.25) follows from the joint requirements of positive pressure and causal signals.

From (3.25) we generate a lower bound for the spheroidal parameter

$$\lambda > \frac{-7 + [49 - 17(16\alpha^2 - 3)]^{1/2}}{17}$$

When $\alpha = 0$, we have $\lambda > \frac{3}{17}$, which is the lower bound on the spheroidal parameter for uncharged stars. Otherwise for real λ we require that $\alpha < 0.607$, although for a real and positive λ, $\alpha < 0.43$. This condition on α places an upper bound on the value of the electric field intensity via (3.13). Specifically the bound on E in this model is given by

$$E^2 < \frac{0.185\,[\lambda - (\lambda+1)z^2]}{R^2\,[\lambda + \lambda^2 - \lambda(\lambda+1)z^2]^2}$$

where z lies in the interval (z_0, z_b). Finally we observe that an upper bound on possible values of b/R may be obtained from (3.24). This upper limit on the boundary of the star is given by

$$\frac{b^2}{R^2} \leq \frac{-6\alpha^2 - 12\lambda + 2\alpha^2\lambda - 12\lambda^2 + K}{\alpha^4 - 2\alpha^2\lambda + 5\lambda^2 - 2\alpha^2\lambda^2 + 6\lambda^3 + \lambda^4}$$

where

$$\begin{aligned} K^2 &= (6\alpha^2 + 12\lambda - 2\alpha^2\lambda + 12\lambda^2)^2 \\ &\quad -(3 - 16\alpha^2 - 14\lambda - 17\lambda^2)(\alpha^4 - 2\alpha^2\lambda + 5\lambda^2 - 2\alpha^2\lambda^2 + 6\lambda^3 + \lambda^4) \end{aligned}$$

When $\alpha = 0$ we regain the upper bound on b/R for an uncharged star. We have shown in Table 3.2 the values of b/R for the cases $\alpha = 0$ and $\alpha = 0.4$. In Fig.3.1 we have shown the effects of both λ and α on the upper bound of the possible values of b/R of a charged star. In Fig.3.2 we have plotted the upper bound on $\frac{b}{R}$ against $Log_{10}\lambda$ for two cases: (a) $\alpha = 0$ and (b) $\alpha = 0.4$. We observe that the effect of charge, through the presence of the parameter α, is to raise the upper bound, and this allows for a wider range in the causal behaviour.

The condition $\frac{dp}{d\rho} < 1$ leads to

$$z(1-z^2)^2(\frac{\psi_z}{\psi})^2 - (1-z^2)(\frac{\psi_z}{\psi}) - z(1-z^2)(1+\lambda) - 4z - \frac{4\alpha^2 z}{\lambda(1+\lambda)} < 0. \qquad (3.26)$$

When applied to the centre of the star ($z = z_0$), one gets another interesting constraint on the parameters. Table 3.3 gives the minimum allowed values of $\frac{\psi_z(z_0)}{\psi(z_0)}$ for different λ and two different values of α. Thus, $\frac{\psi_z(z_0)}{\psi(z_0)}$ can attain a lower value for a charged star, indicating a wider range for the parameter ω. For example, for $\lambda = 1$, (a) $\omega > 1.7024$, for $\alpha = 0$ and (b) $\omega > 1.6726$ for $\alpha = 0.4$. The effect decreases with increasing λ. Imposition of other constraints however will further restrict the values of ω.

λ	$\frac{b^2}{R^2}$		
	$\alpha = 0$	$\alpha = 0.2$	$\alpha = 0.4$
.5	.4365	.4600	.5255
1	.5166	.5251	.5502
2	.5000	.5030	.5119
5	.3809	.3815	.3835
10	.2631	.2632	.2636
20	.1611	.1612	.1612
100	.0390	.0390	.0390

Table 3.2: Upper bound on $\frac{b^2}{R^2}$ for different values of α and λ

λ	$\frac{\psi_z(z_0)}{\psi(z_0)}\Big\vert_{Min.}$		
	$\alpha = 0$	$\alpha = 0.2$	$\alpha = 0.4$
.5	-2.2978	-2.3639	-2.5555
1	-3.2762	-3.3102	-3.41072
2	-5.1181	-5.1353	-5.1867
5	-10.5267	-10.5337	-10.5545
10	-19.4957	-19.4991	-19.5096
20	-37.4150	-37.4167	-37.4220
100	-180.7230	-180.7240	-180.7250

Table 3.3: Minimum values of $\psi_z(z_0)/\psi(z_0)$ permitted by causal behaviour

3.5 Discussions

We have found a non-trivial family of a new class of solutions to the Einstein-Maxwell equations for a particular choice of the electric field intensity E (with the associated parameter α) and the general spheroidal parameter λ. This form for E had previously been shown to lead to physically acceptable solutions for $\lambda = 2$ [104]. The generalisation to all allowed values of λ may be useful as uncharged compact stars can be described in this model with large values of λ. Some of these stars could become charged due to accretion [69], [70], in particular charges may accumulate in a shell on the boundary. Description of these stars, in terms of a core-envelope model, may be done by making use of the solution given here. We have also performed a qualitative analysis on the physical properties of the charged sphere. Where relevant we have regained the uncharged limit of quantities of interest. We note the very interesting interplay between λ and the charge parameter α; the presence of charge allows for a wider range for physical parameters. In particular we have shown that $\alpha \neq 0$ permits causal signals over a wider range of values of $\frac{b}{R}$ than is the case for uncharged stars. The upper bound on $\frac{b}{R}$ of the charged star is constrained by both λ and α, as shown in Fig3.1.

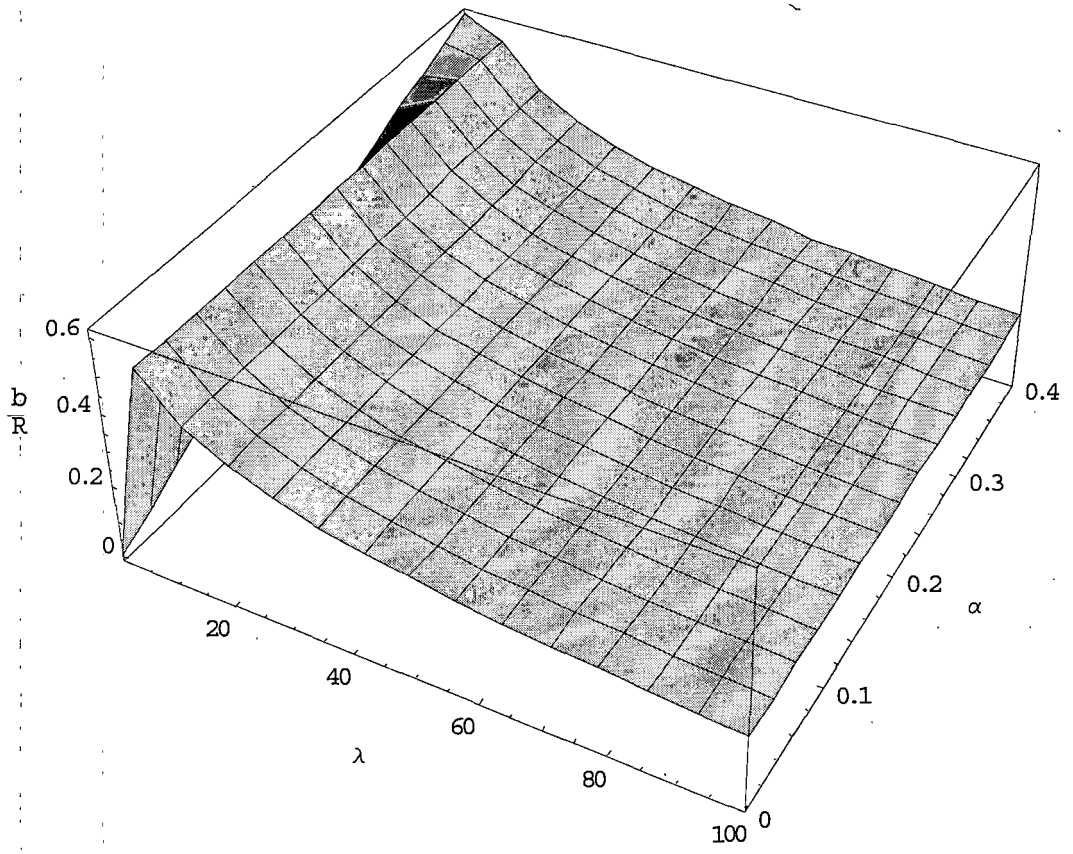

Figure 3.1: Upper bound on the value of $\frac{b}{R}$ plotted against λ & α.

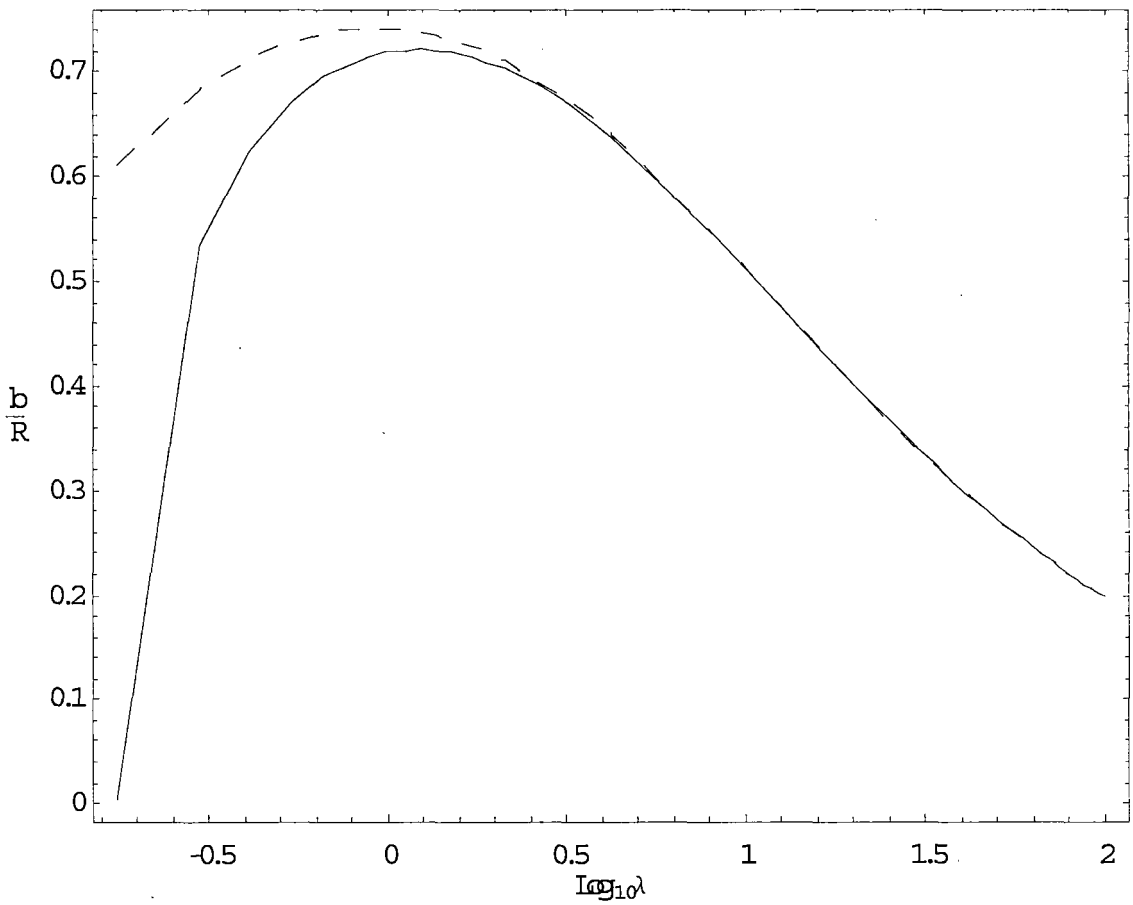

Figure 3.2: Upper bound on the value of $\frac{b}{R}$ plotted against $Log_{10}\lambda$ for $\alpha = 0$ (solid line) and $\alpha = 0.4$ (dashed line).

Chapter 4

Strange Stars

4.1 Introduction

Internal composition of compact objects has become a subject of considerable interest for many years. A neutron has a r.m.s radius of 0.75 fm, and density $\sim 8 \times 10^{14}\ gm\ cm^{-3}$, whereas the central density of a neutron star can be as high as $10^{15}\ gm\ cm^{-3}$. In such a situation, one may expect the hadrons to overlap and hence matter at such a high density is expected to be a soup of quarks. A quark phase softens the EOS of a neutron star leading to a more compact equilibrium configuration as compared to a pure hadronic star of the same mass. The possibility of a new class of stars, popularly called strange stars, composed of stable three flavour *uds*-quark system [25] has given a new spurt of activities in this connection. As the energy per baryon of non strange quark matter consisting of u and d quarks only is greater than the energy per baryon of the nuclei, non strange quark matters are unstable and can not be considered to form a star. The failure to detect free quarks has led to the confinement picture of quarks. In 1974, Chodos *et al* [48] proposed a phenomenological theory (MIT bag model) for quark confinement in which they proposed that the confinement is caused by a Universal pressure B on the surface of any region containing quarks. Collins and

Perry [116] claimed that superdense matter consists of quarks rather than hadrons. Chaplin and Nauenberg [117] estimated that a phase transition from baryon to quark matter is possible if baryon density is about $10-60$ times the baryon density in normal nuclei which virtually rules out the possibility of a quark phase at the core of a neutron star. Keister and Kisslinger [118] had also ruled out the possibility of a pure quark phase in a stable stellar configuration. However, Fechner and Joss [119] showed that above a critical density, which is model dependent, but greater than nuclear matter density (ρ_{nuc}), there might be a phase transition leading to a stable quark star. Whatever might be the case, Witten's [25] strange matter hypothesis has remained a popular topic in the field of compact objects till date, generating various models for compact stars.

Strange star configurations are model dependent. The structure and stability of strange stars have been mostly studied within the framework of a bag model, see e.g., Glendenning *et al* [34] and Kettner *et al* [120]. The most general form of a strange matter EOS under the MIT bag model is given by Farhi & Jaffe [26]

$$p = \frac{1}{3}(\rho - 4B)\,. \tag{4.1}$$

From a calculation based on MIT bag model, Li *et al* [40] suggested that Her X-1 is a strange star. Later on Madsen [39] contradicted the result arguing that strange matter can not be stable at the value of bag constant considered in [40]. Recently, considering a particular interquark potential, Dey *et al* [42] developed an EOS for strange matter. From the semi-empirical mass-radius estimations of X-ray pulsar Her X-1 [40] and X-ray burster 4U 1820-30 [41], Dey *et al* [42] proposed that both of them are good strange star candidates. Using this EOS, Li *et al* [43] claimed that the low-mass X-ray binary (LMXB) pulsar SAX J1808.4-3658 is also a strange star. Very recently, an isolated star RX J185635-3754 has been studied, giving it a mass $M = 0.9 \pm 0.2\ M_{\odot}$ and radius $b = 6^{-1}_{+2}\ km$ [47]. It may also belong to the class of strange stars as can be seen from the mass-radius curve obtained by Li *et al* [43].

In this chapter, we shall apply Vaidya-Tikekar [63] model to study strange stars. In particular, we shall concentrate on SAX J1808.4-3658 and show that, if the claim made by Li *et al* [43] about SAX being a strange star is true, then, without going into the microscopic details, similar results can be obtained directly from the solution given by Mukherjee *et al* [67] for a particular value of λ. Thus SAX J1808.4-3658 belongs to the family of stars described by Vaidya-Tikekar [63] model.

4.2 SAX J1808.4-3658 and the strange star EOS

In the year 1996, SAX J1808.4-3658 (SAX) was discovered by Wijnards and van der Klis with the help of a Wide Field Camera on board *BeppoSAX* [121]. It was described by van der Klis [122] as the "Holy Grail" of X-ray astronomy. It's discovery had been anticipated for about two decades because magnetospheric disk accretion theory as well as evolutionary ideas concerning the genesis of millisecond radio pulsars strongly suggested that such rapid spin frequencies must occur in accreting low-magnetic field neutron stars. SAX is a compact star in low mass X-ray binary with 2.5 ms pulsation; it is an old (10^9 years), low magnetic field (10^8 G) star with 1000 times the solar luminosity at peak (10^{35} erg/sec) with 10^{-4} $M_\odot/year$ accretion rate. From the spectral analysis of data the distance of SAX has been estimated to be $\sim$ 2.5 kpc. These considerations constrain the mass-radius ($M - b$) relations pointing towards the very compact nature of the star, vide Li *et al* [43].

It is not possible to reproduce such compact objects with any conventional known neutron matter EOS. Li *et al* [43] have suggested that it might be a compact strange star made of deconfined u , d & s quarks. In [43], the calculation is based on a model for strange matter derived by Dey *et al* [42], in which one uses an interquark potential which has the following features:

- (1) the model has asymptotic freedom built into it,

- (2) it shows confinement at zero baryon number density ($n_B = 0$) and deconfinement at high n_B,
- (3) the quark mass is chosen as a function of density so as to take care of chiral symmetry restoration (CSR), and
- (4) gives a stable configuration for charge zero, β-stable strange matter.

For completeness we outline here the basic formalism of this model. The calculation is motivated by the large N_c philosophy of 't Hooft [123] as applied to baryons by Witten [124] and uses the Richardson potential [125] which gives the right parameters for mesons [126] and baryons [127]. The robust large N_c phenomenology supports the work and the loop-free treatment lends it an immense simplicity.

In this model the quark interaction is described by a color-Debye-screened interquark vector potential originating from gluon exchange and by a density dependent scalar potential which restores chiral symmetry at high density. The Hamiltonian of the system is given by [42]

$$H = \sum_i (\alpha_i.p_i + \beta_i M_i) + \sum_{i<j} \frac{\lambda(i)\lambda(j)}{4} V_{ij}, \tag{4.2}$$

where, λ-s are the color $SU(3)$ matrices for the two interacting quarks. The interquark interaction is screened which assures deconfinement at a high density. The effective quark mass $M_i(n_B)$ is density dependent and has the form

$$M_i(n_B) = m_i + (310\ MeV) Sech(\gamma \frac{n_B}{n_0}), \tag{4.3}$$

where, $i = u, d, s$, $n_B = (n_u + n_d + n_s)/3$ is the baryon number density, $n_0 = 0.16\ fm^{-3}$, and γ is a numerical parameter. The effective quark mass $M_i(n_B)$ goes from its constituent value at zero density to its current mass m_i as n_B goes to infinity.

The total energy-density of the system is given by,

$$\rho = \rho_{K.E.} + \rho_{P.E.}, \tag{4.4}$$

where the kinetic energy is given by

$$\rho_{K.E.} = \frac{3}{4\pi^2} \sum_{i=u,d,s} \left[k_i^f \left((k_i^f)^2 + \frac{M_i^2}{2} \right) \sqrt{(k_i^f)^2 + M_i^2} - \frac{M_i^4}{2} ln \frac{\sqrt{((k_i^f)^2 + M_i^2)} + k_i^f}{M_i} \right], \tag{4.5}$$

and the potential energy is given by

$$\rho_{P.E.} = -\frac{1}{2\pi^3} \sum_{i,j} \int_{-1}^{+1} dx \int_0^{k_j^f} k_j^2 \int_0^{k_j^f} k_i^2 \times f(k_i, k_j, M_i, M_j, x) \times V \left[D^{-1}, (k_i - k_j)^2 \right] dk_j dk_i, \tag{4.6}$$

where k_i^f is the Fermi momentum of the i-th quark. For the interquark vector potential, one uses the Richardson potential which, in a medium, will be screened due to pair creation and infrared divergence. In equation (4.6) V is the screened Richardson potential given by

$$V_{ij} = \frac{12\pi}{27} \frac{1}{ln\left(1 + \frac{(k_i - k_j)^2 + D^{-2}}{\Lambda^2}\right)} \frac{1}{((k_i - k_j)^2 + D^{-2})}, \tag{4.7}$$

where the inverse screening length D^{-1} has the form

$$(D^{-1})^2 = \frac{2\alpha_0}{\pi} \sum_{i=u,d,s} k_i^f \sqrt{(k_i^f)^2 + m_i^2}, \tag{4.8}$$

where Λ is a scale parameter and α_0 is the perturbative quark gluon coupling constant. Also,

$$f(k_i, k_j, M_i, M_j, x) = \left(e_i.e_j + 2k_i.k_j.x + \frac{k_i^2.k_j^2}{e_i.e_j} \right) \times \frac{1}{(e_i - M_i)(e_j - M_j)}, \tag{4.9}$$

where, $e_i = \sqrt{k_i^2 + M_i^2} + M_i$.

The above formulation, under β-equilibrium and charge neutrality conditions

$$\mu_d = \mu_s, \tag{4.10}$$

$$\mu_d = \mu_u + \mu_e, \tag{4.11}$$

$$2(k_u^f)^3 - (k_s^f)^3 - (k_d^f)^3 - (k_e^f)^3 = 0 \tag{4.12}$$

yield the EOS $p = p(\rho)$, where, μ-s are the chemical potentials of the quarks and the electron. One assumes here that the neutrinos leave the system, i.e., $\mu_\nu = 0$.

The calculated EOS (shortened by the name RsSS) of the strange quark matter is found to lead to the following results:

- (a) the quark matter has more binding than Fe^{56},
- (b) the matter has a large component of strange quarks and
- (c) yields a set of acceptable strange stars with maximum mass (i) $1.44\,M_\odot$ and radius 7.06 km and (ii) mass $1.32\,M_\odot$ and radius 6.53 km, respectively, for two sets of the CSR parameters of the model mentioned in [43] above. For each EOS one can have a series of stars with masses less than the maximum but then, unlike the neutron stars, the radii of these stars will be smaller.

The EOS obtained by Dey *et al* [42] was approximated later into a linearised form by Gondek-Rosińska *et al* [74]. Although the results of Li *et al* [43] and the equation of state given in [74] have influenced considerable activities in this field ([17], [129], [130], [131], [132]), the suggested stellar configuration for SAX needs further confirmation. Here, we present some results by following a general relativistic approach in this connection.

In the standard procedure, given the EOS, one usually determines $(M - b)$ relation for a star by integrating the Tolman-Oppenheimer Volkoff (TOV) equations, using appropriate boundary conditions. But, we shall prescribe here a given geometry and then look for suitable matter which can support this geometry. The EOS obtained from our model takes an almost linear form for a large value of a parameter. Incidentally, the EOS given by Gondek-Rosińska *et al* [74] for SAX agrees very accurately with the EOS predicted by the geometric model. Thus, two equations of state, one obtained from detailed microscopic considerations and another from geometry are found to be

consistent in the sense that both give compact and stable objects with the same mass and radius.

In section 4.3, we shall outline the model based on an ansatz made by Vaidya and Tikekar [63]. This geometrical model has already been discussed in chapter 2. In section 4.4 we shall show that EOS of the ReSS [42] and approximated to a linearized form [74], is also derivable from this model. In section 4.5 we shall conclude by discussing our results.

4.3 Alternative model

Let us assume, for simplicity, that the compact object is static, spherically symmetric and has no magnetic field. The line element for such a configuration has the standard form ($8\pi G = c = 1$)

$$ds^2 = -e^{2\gamma(r)}dt^2 + e^{2\mu(r)}dr^2 + r^2(d\theta^2 + \sin^2\theta d\phi^2) \tag{4.13}$$

The ansatz made by Vaidya and Tikekar [63] is given by

$$e^{2\mu(r)} = \frac{1 + \lambda\frac{r^2}{R^2}}{1 - \frac{r^2}{R^2}}, \tag{4.14}$$

where λ and R are two parameters which characterize the geometry of the star. It is to be noted here that in the eqnuation (4.14) λ denotes physically a measure of compressibility. A large value of λ means a highly compressible matter which, not surprisingly, leads to a compact object.

Assuming that the matter content of the star has a perfect fluid like distribution, the general solution of the field equations obtained Mukherjee *et al* [67] has the form

$$e^{\gamma} = \psi(z) = A\left[\frac{\cos[(n+1)\zeta + \delta]}{n+1} - \frac{\cos[(n-1)\zeta + \delta]}{n-1}\right]. \tag{4.15}$$

All the parameters in equation (4.15) have been defined in chapter 2. As discussed in chapter 2, the solution satisfies strong and weak energy conditions as well as causality

condition and is valid for any value of $\lambda > \frac{3}{17}$ [67]. The energy density ρ, pressure p, mass M and central density ρ_c, are given in equations (2.29), (2.30), (2.33) & (2.42), respectively. The relation between ρ and p, parametrized by the radial coordinate r, is the EOS in this model. The choice of the parameter λ determines the equation of state. For a given mass and radius, there is a one-parameter class of equations of state parametrized by λ. For a chosen value of λ there is only one configuration. In the following section we shall apply these results to see if there is any stable configuration that can support the EOS for strange stars formulated by Dey *et al* [42], by considering the star SAX J1808.4-3658, in particular.

4.4 Numerical Results

To describe a strange star matter distribution, we follow the model formulated by Dey *et al* [42]. Gondek-Rosińska *et al* [74] approximated the EOS given in [42] to a linear form

$$p = a(\rho - \rho_0) \tag{4.16}$$

where a and ρ_0 are two parameters. Equation (4.16) describes a self-bound matter at density ρ_0 at zero pressure with a fixed sound velocity $\sqrt{a}$.

In [42] it has been claimed that X-ray pulsar Her X-1 and X-ray burster 4U 1820-30 are good strange star candidates. Using the model of Dey *et al* [42] (but choosing different sets of parameters), Li *et al* [43] predicted two possible masses for SAX J1808.4-3658; mass 1.435 $M_\odot$ and radius 7.07 km for EOS SS1 and mass 1.323 $M_\odot$ and radius 6.55 km, for EOS SS2. Fitting these two equations of state to the linearized EOS (4.16), one obtains [74]:

- For EOS SS1: Mass $M = 1.435\ M_\odot$, radius $b = 7.07\ km$, $a = 0.463$, density at the boundary $\rho_0 = 1.15 \times 10^{15}\ gm\ cm^{-3}$ and central density $\rho_c = 4.68 \times 10^{15}\ gm\ cm^{-3}$.

- For EOS SS2: Mass $M = 1.323\ M_{\odot}$, radius $b = 6.55\ km$, $a = 0.455$, density at the boundary $\rho_0 = 1.33 \times 10^{15}\ gm\ cm^{-3}$ and central density $\rho_c = 5.5 \times 10^{15}\ gm\ cm^{-3}$.

Case I

Let us now consider the EOS SS1 in our model. Using $M = 1.435\ M_{\odot}$ and $b = 7.07\ km$ as input parameters, we determine the slope $\frac{dp}{d\rho}$ and equating it to 'a', find that $\lambda = 53.34$. The resulting EOS matches very accurately with the EOS SS1. This has been shown in Fig.4.1. The other parameters, in this case, are $R = 43.245\ km$, $\delta = 2.11429$. The central density and surface density obtained in this case are $\rho_c = 4.68 \times 10^{15}\ gm\ cm^{-3}$ and $\rho_b = 1.17 \times 10^{15}\ gm\ cm^{-3}$, respectively.

Case II

If we consider $M = 1.323\ M_{\odot}$ and $b = 6.55\ km$, as input parameters , as in EOS SS2, we find that for $\lambda = 230.58$, the EOS obtained agrees accurately with the EOS SS2. This has been shown in Fig.4.2. The other parameters, calculated in this case are, $R = 82.35\ km$, $\delta = 2.1317$. The central density and surface density obtained in this case are $\rho_c = 5.5 \times 10^{15}\ gm\ cm^{-3}$ and $\rho_b = 1.35 \times 10^{15}\ gm\ cm^{-3}$, respectively.

In Fig.4.3, we have plotted the density variation along the radius for the two cases in our model. Thus we observe that for SAX, the earlier results can easily be obtained by a simple geometrical model outlined in section 4.3. It is a surprising coincidence that a simple model is able to describe a realistic compact star. We have noted earlier that in our model the EOS becomes almost linear for a large value of λ which allows us to reconstruct the linearized EOS obtained by Gondek-Rosińska *et al* [74]. As the differences in the stellar parameters obtained by using the linearized EOS is less than 2% as compared to the (static model) parameters obtained by using Dey *et al* [42] EOS, our model provides a realistic description of SAX in terms of simple analytic functions.

4.5 Discussions

The model worked out in [42, 43] has already been used extensively by many authors. It would be useful to add some comments to indicate how the present work may provide a simple model for studying various problems in the field of compact stars.

SAX and PSR 1937+21 are fast rotors. The ReSS model provides the possibility of withstanding very high rotations which the ordinary neutron stars or even bag SS cannot sustain. The maximum frequencies for the two EOS, SS1 and SS2 are 2.6 and 2.8 kHZ respectively when they are on the mass shed limit (supermassive model) and 1.8 and 2 kHz when they are in the normal evolutionary sequence as shown in [74].

The mass of SAX has recently been investigated by Bhattacharya [129] and the upper limit of the compact mass was found to be 2.27 $M_{\odot}$ with $b = 9.73\ km$. Although these limiting values are not very close to the values considered in case I and case II above, all the cases have comparable compactness (~ 0.2).

Kapoor and Shukre [17] claims a remarkably precise observational relation for pulse core component widths of radio pulsars which enables them to derive stringent limit on pulsar radii, strongly indicating that they are strange stars rather than neutron stars.

Bombaci and Datta [130] have suggested that conversion of normal matter to strange matter may be the central engine for γ ray bursts. Their estimates are based on SS1 and SS2.

EOS SS1 and SS2 were obtained by Dey *et al* [42] by choosing a particular form of the interquark potential whereas the solution of Mukherjee *et al* [67] was obtained following an ansatz made by Vaidya and Tikekar [63] for the geometry of a static, spherically symmetric star. The agreement is striking, though not surprising. The geometry describes (for a large λ) a highly compressible matter with variable density and therefore, a compact object. This model can be used to predict the mass-radius relation of a star. One can, then, examine what kind of micoscopic theories would lead to such an EOS. Here we find that a compact star, like SAX, needs an almost linear

EOS from general relativistic geometric considerations. The coinciding microscopic description are given in references [43], [74].

It is interesting to note that although the EOS given by SS1 and SS2 are essentially different, both allow stellar configurations, consistent with our model for two different values of λ. The model seems to be capable of describing a large class of realistic compact stars.

We know that pulsars are strongly magnetized. Analyzing the observational data, it has been found that most isolated pulsars have magnetic field $\sim 10^{12}\ G$ and most pulsars in the binary systems have magnetic field $\sim 10^{10}\ G$ [91]. In our calculation, we did not consider the effects of the magnetic field. However, considering strange star EOS under the MIT bag model, Phukon [91] showed that the presence of a magnetic field less than $10^{18}\ G$, does not change the EOS considerably. He found no noticable change in the maximum mass and radius of a star of magnetic field $H \leq 10^{18}\ G$. At a very high density ($\rho \geq 10^{15}\ gm\ cm^{-3}$), for a magnetic field of strength $H = 10^{18}\ G$, the energy contribution from the magnetic field was found to be $\sim 24.8\ MeV\ fm^{-3}$, which is still small compared to the value of bag constant $B = 57\ MeV\ fm^{-3}$. Thus, we hope that our results would not differ considerably in the presence of a magnetic field, smaller than $10^{18}\ G$.

The stability of SAX has, earlier, been analyzed by Bhowmick *et al* [134]. Vaidya-Tikekar [63] model permits us to check this claim from a different view point. In chapter 6 we shall show that the model presented here for SAX is gravitationally bound and stable with respect to small radial oscillations.

The model also exhibits an overall scaling behaviour [133] which will be discussed in detail in chapter 7. Physical implications of this scaling property will also be discussed there.

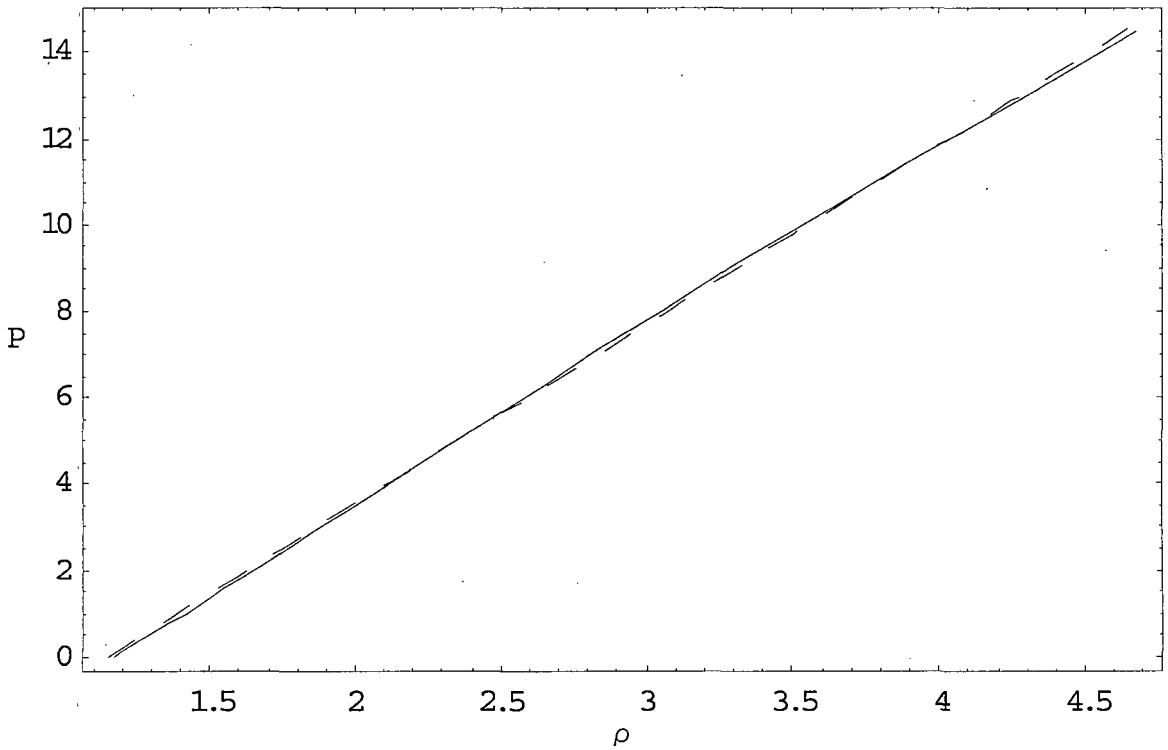

Figure 4.1: Equation of state for $\lambda = 53.34$ (solid line) and linearised EOS SS1 (dashed line). Here energy density (ρ) is expressed in units of 10^{15} $gm\ cm^{-3}$ while pressure (p) is expressed in units of 10^{35} $dyne\ cm^{-2}$.

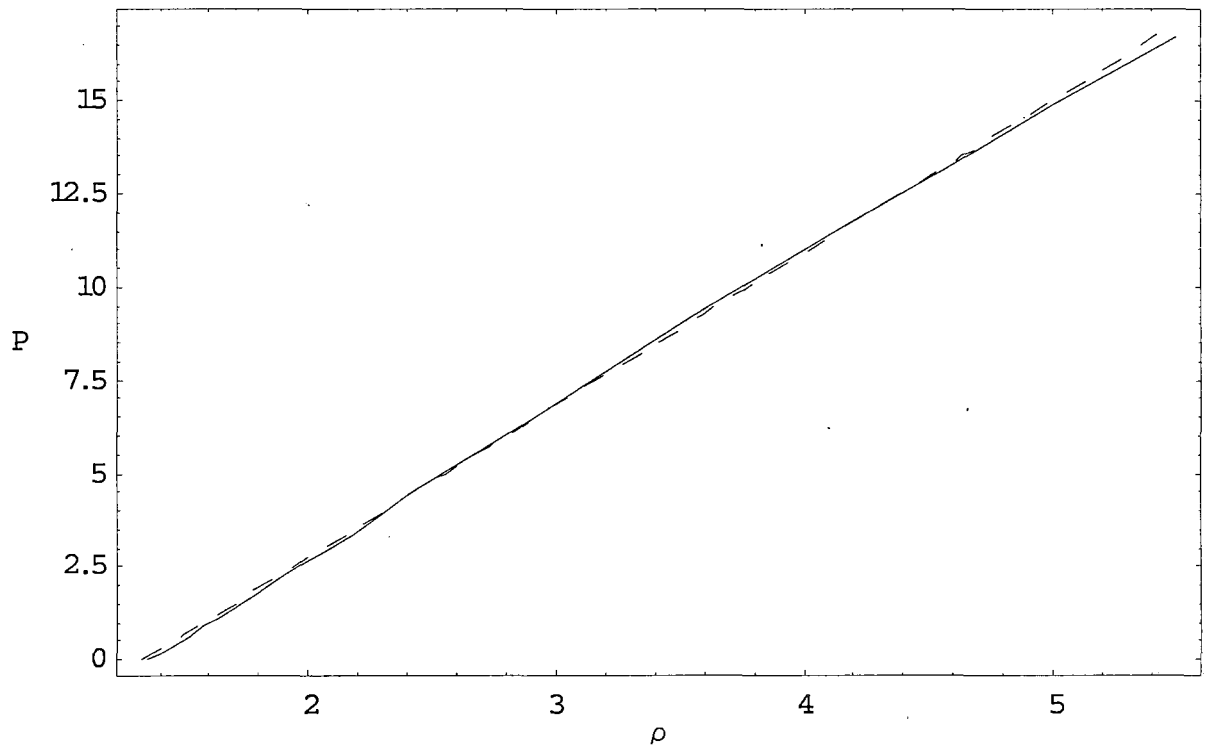

Figure 4.2: Equation of state for $\lambda = 230.58$ (solid line) and linearised EOS SS2 (dashed line). Here energy density (ρ) is expressed in units of 10^{15} $gm\ cm^{-3}$ while pressure (p) is expressed in units of 10^{35} $dyne\ cm^{-2}$.

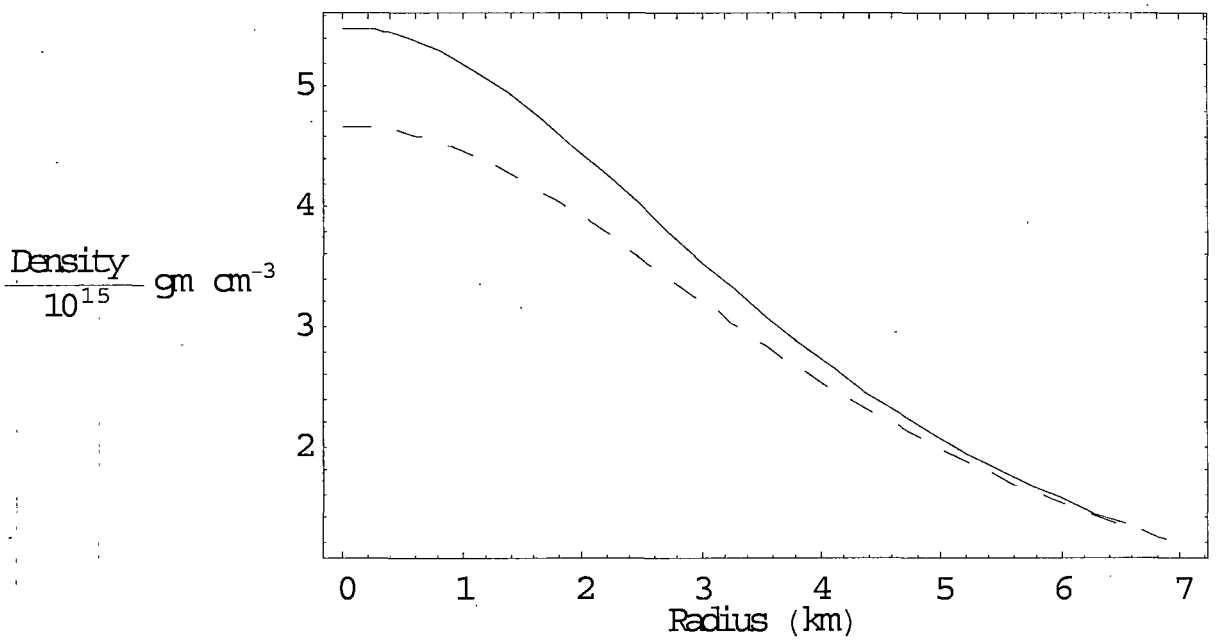

Figure 4.3: Density variation along the radius for $\lambda = 230.58$ (solid line) and $\lambda = 53.34$ (dashed line), in our model.

Chapter 5

Quark-Diquark Stars

5.1 Introduction

One of the most interesting features of a compact star is its mass to radius ratio. The X-ray pulsar Her X-1 is a compact object whose mass-radius constraint has attracted considerable attention in recent years. Her X-1, one of the best studied X-ray pulsars, has a pulse period of 1.24 s, has a strong magnetic field ($\sim 3 \times 10^{12}$ G), and its average luminosity is $\sim 2 \times 10^{37}$ $erg\ s^{-1}$, assuming its distance to be 5 kpc [40]. Based on the observational data (e.g., luminosities, pulse periods, spin up rates etc.), Wasserman and Shapiro [135] constructed semi-empirical mass-radius relations for two X-ray pulsars, Her X-1 and 4U 0115 + 63. Later Li *et al* [40] determined the mass-radius relation of Her X-1 semi-empirically from the observations of its spin variation and cyclotron spectral lines. The estimated mass and radius of Her X-1 are 0.98 ± 0.12 $M_{\odot}$ and $6.7 \pm$ 1.2 km, respectively. If this semi-empirical mass-radius relation for Her X-1, derived by Li *et al* [40], is correct, the question of the composition of Her X-1 becomes very interesting since standard neutron star EOS cannot give this compactness. Schertler *et al* [136] showed that a quark phase softens the equation of state (EOS) of neutron star matter at high densities leading to a more compact equilibrium configuration.

Considering MIT bag model to describe the quark phases, Li *et al* [40] suggested that Her X-1 might be a strange star. But Madsen [128] pointed out that strange matter is unstable for a bag constant $B^{1/4}$ above 164 Mev, considered in [40]. Very recently, Horvath and Pacheco [72] have made the suggestion that Her X-1 might be a mixture of free quarks and diquarks, the latter having a self-interaction described by an effective $\frac{\Lambda}{4}|\Phi|^4$ potential. Kastor and Traschen [76] computed an approximate EOS for a quark-diquark mixture and showed that at a comparatively low density this has the form of a polytrope $p(\rho) = K\rho^{\Gamma}$, with adiabatic index $\Gamma = 2$, where p and ρ denote pressure and energy density of the star and K is a dimensional quantity. The maximum mass and radius obtained by them for a star having a quark-diquark core surrounded by a less dense envelope of nuclear matter were 1.79 $M_{\odot}$ and 11.4 km, respectively. Her X-1, however, is a more compact object. Considering all these aspects, the suggestion of Horvath and Pacheco [72] merits a detailed investigation.

Here, we study the problem of Her X-1 from a different angle. Considering the estimated mass and radius of Her X-1 as input parameters in the model outlined in chapter 2, we find the EOS of the star for $\lambda = 100$, which agrees with the relevant equation of state, given by Horvath and Pacheco [72]. However, the conclusion that can be drawn from our study differs from that of Horvath and Pacheco [72].

5.2 Combined boson-fermion star

The EOS obtained by Horvath and Pacheco [72] was based on earlier works by Ruffini and Bonazzola [57] and Colpi *et al* [58], who studied the equilibrium configuration of a system of massive scalar field. The possibility that scalar fields present in the early Universe could condensate to form stars, known as boson stars, have been studied first by Kaup [56] and Ruffini and Bonazzola [57]. Boson stars are gravitationally bound, spherically symmetric configurations of complex scalar fields minimally coupled to gravity as given in general relativity. Theories of inflation of the Universe prefer

a flat Universe which requires non-baryonic dark matter. Boson stars may provide a considerable fraction of the non-baryonic part of dark matter within the halo of galaxies [55]. The physical nature of the spin 0-particle out of which a boson star is formed is still an open issue. Until now, no fundamental elementary scalar particle has been found in accelerator experiments which could serve as the main constituent of the boson stars. One of the first attempts to incorporate a scalar field in the theory of gravity were made by Brans and Dicke [137]. Colpi *et al* [58] proved that the existence of a self-interaction in the bosonic field Lagrangian could yield higher values for the masses of the configurations. The self-interaction term has the common form $\frac{\Lambda}{4}|\phi|^4$. Since then, many papers have been published on boson stars (e.g, [138] & [139]). A review of these models can be found in [60]. Gleiser [139] investigated the dynamical stability of boson stars against small radial oscillations. Henriques *et al* [59] and Jetzer [60] presented a new model for cold stellar objects composed of both bosons and fermions, parametrized by the central densities of the bosons and fermions. A more realistic description of the system were introduced by de Sousa and Tomazelli [140] who introduced an effective coupling between bosons and fermions. Sahkamoto and Shiraishi [141] gave an exact solution for a non-rotating boson star in $(2+1)$ dimensional gravity with a negative cosmological constant and later extended the work to the case of a boson-fermion star. They also found solutions for rotating boson stars in $(2+1)$ dimensional gravity [142]. There exists a decisive difference between self-gravitating objects made of fermions or bosons: For a many fermion system the Pauli exclusion principle forces the typical fermion into a state with very high quantum number, whereas many bosons can coexist all in the same ground state (Bose-Einstein condensation). This feature is exhibited in the critical particle number N_{crit} for a stable configuration; for fermions $N_{crit} \simeq (\frac{m_{pl}}{m})^3$, whereas, for massive bosons without self-interaction $N_{crit} \simeq (\frac{m_{pl}}{m})^2$, where m_{pl} is the Plank mass.

We assume that boson-fermion stars are static and spherically symmetric with no

magnetic field. We consider the standard line element for such stars,

$$ds^2 = -e^{2\gamma(r)}dt^2 + e^{2\mu(r)}dr^2 + r^2(d\theta^2 + \sin^2\theta d\phi^2). \tag{5.1}$$

The Lagrangian for the bosonic field may be chosen as

$$L_{eff} = \frac{1}{2}\left(\partial_\mu \Phi^* \partial_\nu \Phi - m^2 \Phi^* \Phi\right) - \frac{\Lambda}{4}\left(\Phi^* \Phi\right)^2. \tag{5.2}$$

Here, m is the bosonic mass and Λ is a dimensionless coupling constant.

Energy-momentum tensor for the bosonic field has the form

$$T^B_{\mu\gamma} = \frac{1}{2}\left(\Phi^*_\mu \Phi_\gamma + \Phi_\mu \Phi^*_\gamma\right) - \frac{1}{2} g_{\mu\gamma}\left[g^{\rho\sigma}\Phi^*_\rho \Phi_\sigma + m^2|\Phi|^2 + \frac{1}{2}\Lambda|\Phi|^4\right] \tag{5.3}$$

Energy-momentum tensor for the fermionic field can be written as

$$T^F_{\mu\gamma} = \left(\rho^F + p^F\right) u_\mu u_\gamma + g_{\mu\gamma} p^F \tag{5.4}$$

where, u^μ is the 4-velocity of the fluid. The energy-momentum tensor for a mixed boson-fermion configuration is given by

$$\tau_{\mu\gamma} = T^B_{\mu\gamma} + T^F_{\mu\gamma}. \tag{5.5}$$

The form of the scalar field, giving a spherically symmetric matter distribution, is assumed to be

$$\Phi(r,t) = \phi(r) e^{-i\omega t}, \tag{5.6}$$

which ensures the possibility of a static solution.

For the line element (5.1), the field equations now lead to (introducing $8\pi G$)

$$\frac{(1-e^{-2\mu})}{r^2} + \frac{2\mu' e^{-2\mu}}{r} = 4\pi G\left[2\rho_f + \left(\omega^2 e^{-2\gamma} + m^2\right)\phi^2 + \phi'^2 e^{-2\mu} + \frac{1}{2}\Lambda\phi^4\right] \tag{5.7}$$

$$\frac{2\gamma' e^{-2\mu}}{r} - \frac{(1-e^{-2\mu})}{r^2} = 4\pi G\left[2p_f + \left(\omega^2 e^{-2\gamma} - m^2\right)\phi^2 + \phi'^2 e^{-2\mu} - \frac{1}{2}\Lambda\phi^4\right] \tag{5.8}$$

$$e^{-2\mu}\left(\gamma'' + \gamma'^2 - \gamma'\mu' + \frac{\gamma'}{r} - \frac{\mu'}{r}\right) = 4\pi G\left[2p_f + \left(\omega^2 e^{-2\gamma} - m^2\right)\phi^2 - \phi'^2 e^{-2\mu} - \frac{1}{2}\Lambda\phi^4\right]. \tag{5.9}$$

The scalar wave equation

$$\Phi^{\mu}\Phi_{\mu} - m^2\Phi - \Lambda|\Phi|^2\Phi = 0, \tag{5.10}$$

now takes the form

$$\phi'' + \left(\frac{2}{r} + \gamma' - \mu'\right)\phi' + \left[(\omega^2 e^{-2\gamma} - m^2) - \Lambda\phi^2\right]e^{2\mu}\phi = 0. \tag{5.11}$$

From eqnuations (5.8) & (5.9), we find that the pressure is not isotropic. The pressure anisotropy essentially depends on the self-interaction. But if ϕ' is very small, i.e., if we can neglect ϕ', we get,

$$\gamma'' + \gamma'^2 - \gamma'\mu' - \frac{\gamma'}{r} - \frac{\mu'}{r} - \frac{(1 - e^{2\mu})}{r^2} = 0. \tag{5.12}$$

This equation has already been taken up in chapter 2. Assuming

$$e^{2\mu} = \frac{1 + \lambda r^2/R^2}{1 - r^2/R^2}, \tag{5.13}$$

we get the solution of this equation given by Mukherjee *et al* [67],

$$\psi(z) = e^{\gamma} = A\left[\frac{\cos[(n+1)\zeta + \delta]}{n+1} - \frac{\cos[(n-1)\zeta + \delta]}{n-1}\right]. \tag{5.14}$$

Thus if the scalar field is almost homogeneous, the Vaidya-Tikekar [63] type of model may be used to study the stellar structure. It may so happen that the scalar field is essentially homogeneous inside the star. To see this we rescale our parameters as

$$\Lambda_* = \frac{\Lambda}{4\pi G m^2}, \qquad r_* = \frac{rm}{\sqrt{\Lambda_*}}$$

$$\sigma = \sqrt{\Lambda_*}\phi, \qquad \rho_*^F = \frac{4\pi G\Lambda_*\rho^F}{m^2}$$

$$p_*^F = \frac{4\pi G\Lambda_* p^F}{m^2}, \qquad \Omega = \frac{\omega}{m}$$

In the case large self-interaction, i.e., $\Lambda_* >> 0$, we may neglect terms of $O({\Lambda_*}^{-1})$ and rewrite the equations (5.7)-(5.9) and (5.11) in terms of dimensionless quantities as

$$\frac{(1-e^{-2\mu})}{r_*^2}+\frac{2\mu' e^{-2\mu}}{r_*}=\left[2\rho_*^F+\left(\Omega^2 e^{-2\gamma}+1\right)\sigma^2+\frac{1}{2}\sigma^4\right] \tag{5.15}$$

$$\frac{2\gamma' e^{-2\mu}}{r_*}-\frac{(1-e^{-2\mu})}{r_*^2}=\left[2p_*^F+\left(\Omega^2 e^{-2\gamma}-1\right)\sigma^2-\frac{1}{2}\sigma^4\right] \tag{5.16}$$

$$e^{-2\mu}\left(\gamma''+\gamma'^2-\gamma'\mu'+\frac{\gamma'}{r_*}-\frac{\mu'}{r_*}\right)=\left[2p_*^F+\left(\Omega^2 e^{-2\gamma}-1\right)\sigma^2-\frac{1}{2}\sigma^4\right] \tag{5.17}$$

$$\left[(\Omega^2 e^{-2\gamma}-1)-\sigma^2\right]e^{2\mu}\sigma=0. \tag{5.18}$$

Here a prime denotes differentiation with respect to r_*.

The scalar wave equation (5.18) has two solutions:

- $\sigma(r_*)=0$, which we choose as the exterior solution.
- $\sigma^2=\left(\Omega^2 e^{-2\gamma(r_*)}-1\right)$, which gives the interior solution.

At the boundary of the star, we must have $\sigma=0$ which determines the value of Ω. Earlier workers have treated the scalar wave equation as an eigen value problem for Ω and assuming some specific values of the wave function at the centre with certain boundary conditions, solved the problem. But, in our case, for a large self-interaction, if we consider the solution of Mukherjee *et al* [67], this becomes a simple exercise. The value of Ω in our model has the form $\Omega=e^{\gamma(b)}$, where b is the radius of the star.

Restoration of dimensional parameters and the coordinate variable r gives,

$$\frac{(1-e^{-2\mu})}{r^2}+\frac{2\mu' e^{-2\mu}}{r}=8\pi G\left[\rho^F+\frac{m^4}{4\Lambda}\left(\Omega^2 e^{-2\gamma}-1\right)\left(3\Omega^2 e^{-2\gamma}+1\right)\right] \tag{5.19}$$

$$\frac{2\gamma' e^{-2\mu}}{r}-\frac{(1-e^{-2\mu})}{r^2}=8\pi G\left[p^F+\frac{m^4}{4\Lambda}\left(\Omega^2 e^{-2\gamma}-1\right)^2\right]. \tag{5.20}$$

The above set of equations clearly show that the total energy density and pressure of the star can be decomposed as

$$\rho^{Tot}=\rho^F+\rho^B, \tag{5.21}$$

$$p^{Tot}=p^F+p^B, \tag{5.22}$$

where, bosonic contribution for the energy density and pressure are given, respectively by

$$\rho^B = \frac{m^4}{4\Lambda}\left(\Omega^2 e^{-2\gamma} - 1\right)\left(3\Omega^2 e^{-2\gamma} + 1\right) \tag{5.23}$$

$$p^B = \frac{m^4}{4\Lambda}\left(\Omega^2 e^{-2\gamma} - 1\right)^2. \tag{5.24}$$

From chapter 2, we can write the total energy-density and pressure as,

$$\rho^{Tot} = \frac{1}{R^2(1-z^2)}\left[1 + \frac{2}{(\lambda+1)(1-z^2)}\right] \tag{5.25}$$

$$p^{Tot} = -\frac{1}{R^2(1-z^2)}\left[1 + \frac{2z\psi_z}{(\lambda+1)\psi}\right]. \tag{5.26}$$

Since the metric coefficients γ and μ are known, for a star of given mass and radius, we can calculate ρ^{Tot} and p^{Tot}, for a fixed value of λ, the parameter characterising the EOS of the star.

We shall employ this technique to the case of a quark-diquark star and address the problem of Her X-1, to see if it is a quark-diquark star.

5.3 Quark-diquark EOS

The possibility of diquarks was first put up by Gell-Mann [143]. Since then, over 500 papers on diquarks have been published (see Anselmino *et al* [144]). Ida and Kobayaski [145] and Lichtenberg and Tassie [146] introduced diquarks in order to describe a baryon as a composite state of two particles, a quark and a diquark. Using the model of Colpi *et al* [58], Horvath *et al* [147] formulated an EOS for diquarks and discussed its various features.

Donogue and Sateesh [148] explored the possibility that pairs of quarks might form diquark clusters in the density regime above the deconfinement transition for hadronic matter at finite density. It is believed that hadronic matter at high enough supernuclear density may undergo a transition to a deconfined state of quark and gluons. It has

been suggested that this deconfinement occurs through an intermediate stage, in which nucleons are dissociated but quarks are correlated in spin-singlet pairs called diquarks.

In general, any two-quark system is a diquark. Quarks are color-triplet, spin $\frac{1}{2}$ objects. The possible states of a pair of quarks are thus given by $((M,J) = (\bar{3},0),(\bar{3},1),(6,0)$ & $(6,1))$, where M and J denote the color $SU(3)$ quantum number and spin, respectively. The spin-spin interaction energy between a pair of quarks is given by [149]

$$H_s = -C\sum_{i\neq j} b_i^\dagger \sigma^a \lambda^B b_i b_j^\dagger \sigma^a \lambda^B b_j \tag{5.27}$$

where, i,j labels the interacting quarks, $b_i^\dagger$ is the creation operator for the ith quark, σ^a are the Pauli spin matrices and λ^B-s are Gell-Mann matrices for color $SU(3)$.

This interaction generates a $N-\Delta$ mass difference:

$$< \Delta|H_s|\Delta >= 16C$$
$$< N|H_s|N >= -16C$$

which gives the mass difference, $m_\Delta - m_N = 32C = 300\ MeV$, from which we can calculate the value of C.

Amongst the possible states of a pair of quarks, $(\bar{3},0)$ state gives the maximum binding energy as can be seen below.

$$< \bar{3},0|H_s|\bar{3},0 >= -16C$$
$$< 6,1|H_s|6,1 >= -\frac{8C}{3}$$
$$< \bar{3},1|H_s|\bar{3},1 >= \frac{16C}{3}$$
$$< 6,0|H_s|6,0 >= 8C.$$

Henceforth, by the term diquark we will mean only the $(\bar{3},0)$ state, which is most strongly bound. It will be represented by a scalar field Φ^α, where α is the color index ($\alpha = 1,2,3$).

The mass of the diquark has been derived from the $N - \Delta$ mass difference [148] as

$$m_D \simeq \frac{2}{3}\left[\frac{m_\Delta + m_N}{2}\right] - \left[\frac{m_\Delta - m_N}{2}\right] = 575\ MeV. \tag{5.28}$$

The stability of the diquark as a bound state has been discussed in [149]. However, it has recently been reported that a computer simulated lattice analysis gives for the diquark a mass of around 700 MeV, in vacuum, and it seems to be unbound [151]. However as pointed out in [151], the mass m_D appearing in the effective Lagrangian need not be equal to the vacuum mass. We, in our calculation, will stick to the value of 575 MeV, in accordance with the calculations in [72].

The limitations of QCD perturbative theory has generated many phenomenological models for treating problems in high density physics. MIT bag model [48] is one them. In a bag model, it is assumed that the quarks remain confined in a bag and the confinement is caused by a Universal pressure B on the surface of the bag [48]. One of the many advantages of bag model is that it is fully relativistic. To describe a quark-diquark system we shall assume the bag model.

Let us assume that the X-ray pulsar Her X-1 is a bag containing u and d quarks and diquarks. We choose the diquark field as

$$L_{eff} = \frac{1}{2}\left(\partial_\mu \Phi^* \partial^\mu \Phi - m_D^2 \Phi^* \Phi\right) - \frac{\Lambda}{4}\left(\Phi^* \Phi\right)^2, \tag{5.29}$$

where, the bosonic diquark mass m_D and the dimensionless coupling constant Λ have been estimated, from the calculation of Jaffe and Low [150], to be $575 MeV$ and 111.2, respectively [148].

The equilibrium of the system demands:

$$\mu_u + \mu_e = \mu_d,$$

$$\mu_D = \mu_u + \mu_d,$$

where μ specifies the chemical potential of the species. In section (5.2), we have showed that for large self-interaction ($\Lambda_* \gg 0$), the scalar field is essentially homogeneous

inside the star. Gleiser [139] also pointed out that pressure anisotropy decreases with the increasing value of Λ. In case of diquarks,

$$\Lambda_* = \frac{\Lambda}{4\pi G m_D^2} \sim 10^{30},$$

where we substituted, $\Lambda = 111.2$, $m_D = 575\ MeV$ and $G = m_{Pl}^{-2} \approx 2.2 \times 10^{-5}\ gm$. This shows that we may well neglect the terms involving $O({\Lambda_*}^{-1})$ and take up the model discussed in chapter 5.2 to describe a quark-diquark configuration.

From section 5.2, we get the total energy-density and pressure due to diquark field as

$$\rho^D = \frac{m_D^4}{4\Lambda}\left(\Omega^2 e^{-2\gamma} - 1\right)\left(3\Omega^2 e^{-2\gamma} + 1\right) \tag{5.30}$$

$$p^D = \frac{m_D^4}{4\Lambda}\left(\Omega^2 e^{-2\gamma} - 1\right)^2 \tag{5.31}$$

Following [72] we write the total energy-density and pressure of the system as

$$\rho^{Tot} = m_q(n_u + n_d) + \frac{3}{10}\frac{\pi^{4/3}\hbar^2}{m_q}(n_u^{5/3} + n_d^{5/3}) + \rho_D + B \tag{5.32}$$

$$p^{Tot} = \frac{1}{5}\frac{\pi^{4/3}\hbar^2}{m_q}(n_u^{5/3} + n_d^{5/3}) + p_D - B \tag{5.33}$$

Here B is the bag constant, m_q is the mass of quarks and n_u, n_d and n_D are the number densities of up quark, down quark and diquark, respectively. The first term on the right hand side of equation (5.32) denotes the rest mass energy density of the quarks. Following [72] we take, $B = 57\ MeVfm^{-3}$, $m_q = 360\ MeV$ and $m_D = 575\ MeV$.

Baryon number density of the system is given by

$$n_B = \frac{2}{3}n_D + \frac{1}{3}(n_u + n_d). \tag{5.34}$$

The mixture state has to be electrically neutral, which gives the condition,

$$\frac{1}{3}n_D + \frac{2}{3}n_u - \frac{1}{3}n_d = 0. \tag{5.35}$$

Table 5.1: Values of various parameters for a star of mass $M = 0.88\ M_{\odot}$, and $b = 7.7\ km$, for different values of λ (ρ_c and ρ_b denote central and surface density of the star, respectively).

λ	$R(km)$	δ	A	$\rho_c(GeVfm^{-3})$	$\rho_b(GeVfm^{-3})$
2	20.2238	2.2337	0.9333	0.6637	0.4374
5	27.5447	2.4153	1.6913	0.7156	0.4182
10	36.6273	2.4974	2.9926	0.7419	0.4094
20	50.0726	2.5445	5.6114	0.7579	0.4044
50	77.4878	2.5751	13.4818	0.7686	0.4012
100	108.7790	2.5858	26.6039	0.7723	0.4000
200	153.2640	2.5912	52.8501	0.7743	0.3994

5.4 Results

For a given mass and radius and for a particular choice of the parameter λ, total energy density ρ^{Tot} and pressure p^{Tot} can be calculated using the model discussed in Chapter 2. We assume that the mass and radius of Her X-1 are given by 0.88 $M_{\odot}$ and 7.7 km, respectively (values within the experimental ranges of mass and radius of Her X-1). Values of related parameters for different choices of the parameter λ are shown in Table 5.1.

We find that for $\lambda = 100$ the EOS obtained in this model agrees accurately with the EOS obtained by Horvath and Pacheco [72] for a quark-diquark mixture as shown in Fig.5.1. The predicted EOS is almost linear in both the cases. The variation of $\frac{dp}{d\rho}$ with different λ in our model is shown in Table 5.2.

Equations (5.32)-(5.35) can be solved numerically to get the number densities of quarks and diquarks in equilibrium. In (5.32) and (5.33) ρ^{Tot} and p^{Tot} can be determined from the solutions given by Mukherjee *et al* [67].

Table 5.2: Variation of $\frac{dp}{d\rho}$ for different values of λ for a star of $M = 0.88\ M_{\odot}$ and $b = 7.7\ km$.

λ	$\frac{dp}{d\rho}\|_{r=b}$	$\frac{dp}{d\rho}\|_{r=0}$
2	0.3518	0.3418
5	0.2847	0.2714
10	0.2634	0.2479
20	0.2513	0.2362
50	0.2446	0.2292
100	0.2424	0.2268
200	0.2413	0.2256

The value of Ω, however, depends on the choice of the boundary condition and our choice differs from that of Horvath and Pacheco [72]. It may be noted that a boson star has no well defined boundary. It describes an infinite exponentially decreasing atmosphere. Actually, most of the boson star calculations (e.g.,[60], [72]) are based on the boundary condition, $\sigma(r) \rightarrow 0$ as $r \rightarrow \infty$ and the total mass of a pure boson star is defined as $M = \lim_{r\rightarrow\infty} M(r)$, where $e^{2\gamma(r)} = 1 - \frac{2M(r)}{r}$.

But in the case where there is a fermionic component, which has an almost classical distribution, the reasonable boundary condition should be $\sigma(r = b) = 0$, where b is the radius of the star. We have noted that the imposition of this boundary condition does not allow a large contribution to the energy density by the bosonic component. This is consistent with the observation made by Horvath in an earlier paper [149] that diquark contribution becomes important only below a certain critical density $\rho_* = 7 \times 10^{14}\ gm\ cm^{-3}$.

At the boundary of the star, using equation (5.18) we get, $\Omega = e^{\gamma(b)}$. For $\lambda = 100$, this gives, $\Omega \sim 0.81416$. In Table 5.3 we give the total energy density and pressure as

Table 5.3: Energy-density and pressure contribution from diquarks and fermions

r(km)	ρ^D $(GeV\ fm^{-3})$	p^D $(GeV\ fm^{-3})$	ρ^{Tot} $(GeV\ fm^{-3})$	p^{Tot} $(GeV\ fm^{-3})$
0	0.0552	0.0038	0.7723	0.0885
2	0.0494	0.0031	0.7308	0.0790
4	0.0345	0.0017	0.6263	0.0546
6	0.0155	0.0004	0.5000	0.0243
7.7	0	0	0.4000	0

a function of radius and the contributions from quarks and diquarks.

In Fig.5.1, although we find that the agreement between a quark-diquark EOS and the EOS obtained by using the solution of Mukherjee *et al* [67] spectacular, one should not conclude immediately that Her X-1 is a quark-diquark star. In our calculation, energy density of the quark-diquark star at the boundary is $\sim 0.4\ GeV fm^{-3}$. If one uses the boundary condition, $\sigma(b) = 0$, almost all the contribution comes from the fermionic part. The diquark contribution vanishes at the boundary, while at the centre of the star ($r = 0$), $\rho^D \approx 0.055\ GeV\ fm^{-3}$, $p^D \approx 0.004\ GeV\ fm^{-3}$ where $\rho^{Tot} \approx 0.77\ GeV\ fm^{-3}$ and $p^{Tot} \approx 0.088\ GeV fm^{-3}$. In Fig5.2, we have shown the variation of bosonic scalar field inside the star.

Further, to be realistic, one should consider a core-envelope model, where one considers a core region containing a quark-diquark mixture while the envelope is made of normal neutron matter. This is necessary because in our model $\rho(b) \approx 0.4\ GeV\ fm^{-3}$, which is less than the density required for deconfinement, viz. $\rho_{dc} \approx 0.6\ GeV\ fm^{-3}$ [152]. The junction of the core-envelope region may then be thought of as a layer where the transition from quark phase to the confined hadronic phase occurs. In our model, the matching of the core and the envelope can be achieved easily by choosing for the

two regions appropriate of values of λ and R. This, of course, presumes that the matter content in both the regions can be described by this model with appropriate values of λ. This will be taken up in chapter 8.

5.5 Discussions

We have found that for a large value of λ, our model provides a simple description of a class of compact stars like Her X-1. The EOS in this model agrees very well with the EOS obtained in [72] for a quark-diquark mixture. However, a correct imposition of the boundary condition may require a modification of the parameters given in [72] and hence whether Her X-1 is a quark-diquark star still remains inconclusive. It may be noted that we have not considered a possible rotation of Her X-1. Li *et al* [40] have pointed out that the rotation of Her X-1 is very slow compared to the critical angular velocity $\Omega_{cr} = \sqrt{\frac{GM}{b^3}}$, and hence the effect of this rotation on the $(M - b)$ relation will be negligible. Also, considering the rotational effect up to Ω^2 (where Ω is the angular velocity observed at infinity) in case of a slowly rotating boson-fermion star, de Sousa and Silveira [90] observed that field equations remain the same as in the case of a boson-fermion star with no rotation. Hence, they concluded that properties like mass and radius and the total number of particles of a static model do not differ from that of a slowly rotating boson-fermion star. Thus, although we assumed a static model for Her X-1, error in our results due to rotation, if any, should be small.

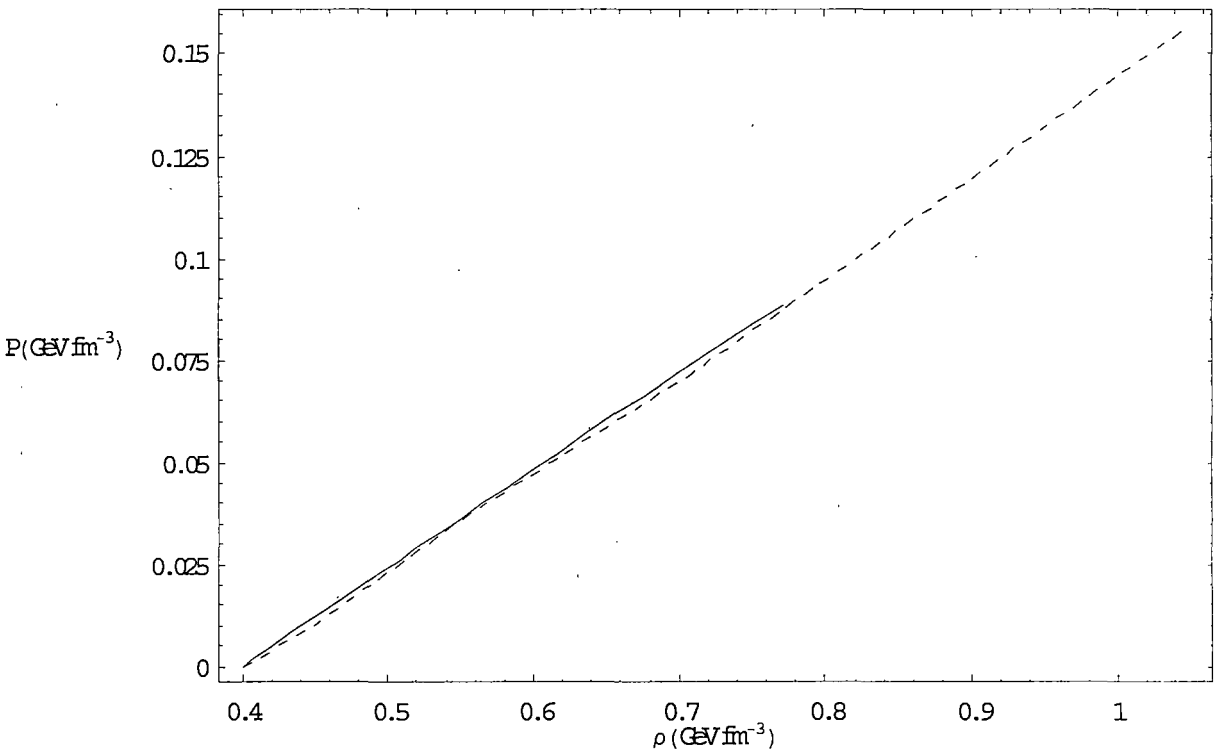

Figure 5.1: (a) EOS of a star of mass $M = 0.88\ M_{\odot}$ and radius $b = 7.7\ km$ in our model (solid line), (b) EOS obtained by Horvath & Pacheco [72] for a quark-diquark mixture state (dashed line).

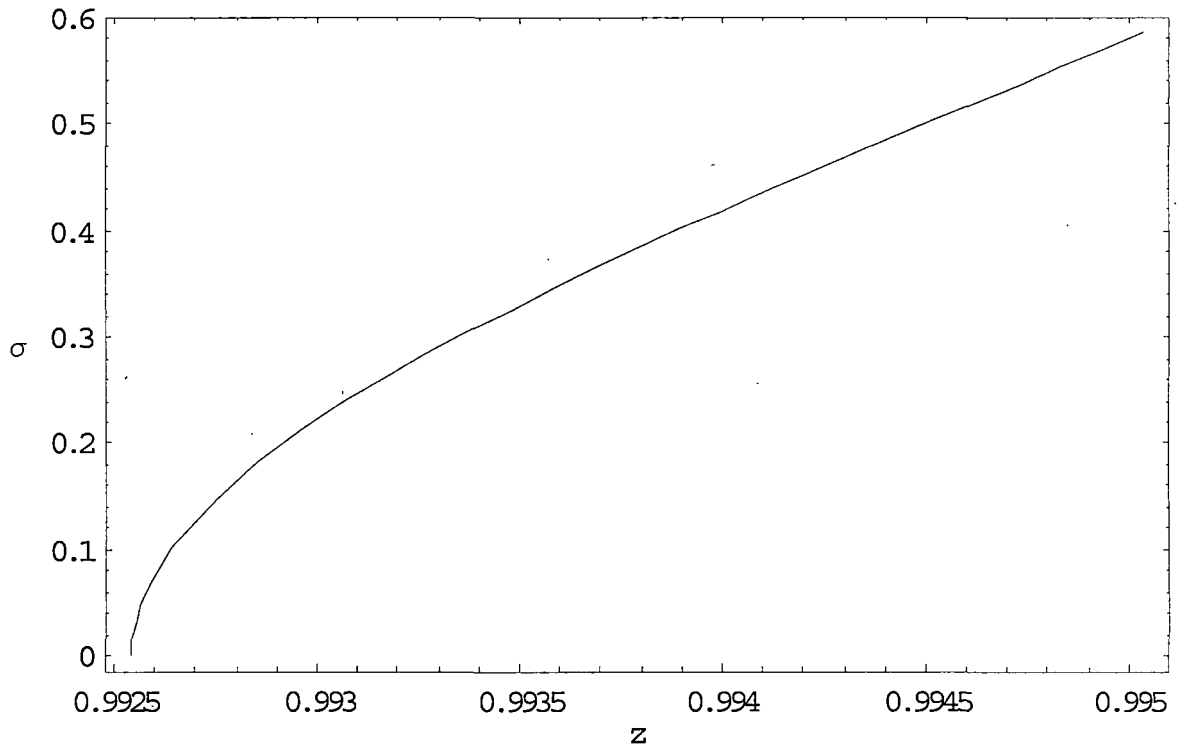

Figure 5.2: Scalar wave function σ plotted against the variable z for a star of mass $M = 0.88\ M_{\odot}$, radius $b = 7.7\ km$ with $\lambda = 100$.

Chapter 6

Stability Analysis

6.1 Introduction

In 1964, Chandrasekhar [73] first developed a method to study the stability of a star against radial oscillations. Bardeen *et al* [153] presented a variety of methods to analyze the stability of a star against radial oscillations.

In our earlier chapters we have shown that the solution of Mukherjee *et al* [67] can be used to generate the EOS for strange matter as well as quark-diquark mixed state in connection with pulsars SAX J1808.4-3658 and Her X-1 respectively. The crucial issue that needs to be studied in this connection is the stability of these solutions. Some of the earlier workers who investigated radial oscillations in strange stars include Glendenning *et al* [34], Kettner *et al* [120] and Cervillera *et al* [154]. Gleiser [139] investigated the dynamical stability of boson stars against radial pulsations. Negi and Durgapal [155] proved the stability of Tolman's type VII solution using the same technique. Using the method developed by Chandrasekhar [73], Knutsen [156] and Tikekar and Thomas [157] proved that Vaidya-Tikekar model [63] is stable for some specific values of the curvature parameter, e.g., $\lambda = 2$ & 7. The general solution of Einstein's field equations [67] helps us to do stability calculations for any value of the

parameter λ. This allows us to extend the stability calculations to realistic stars like SAX J1808.4-3658 or Her X-1. Since we have already shown that for some specific values of λ the model can describe SAX and Her X-1, all we need to do to prove their stability is to show whether the solutions for the relevant values of λ are stable or not. Earlier, Bhowmick *et al* [134] analyzed the stability of SAX J1808.4-3658 and claimed that SAX is a stable star. The calculation presented here permits us to check this claim by using a totally different technique. In this chapter we shall show that the solutions presented in chapter 4 for SAX J1808.4-3658 and also the configuration obtained for Her X-1 in chapter 5, are stable with respect to small radial oscillations.

6.2 Methodology

Let us consider a perturbation of the metric for a spherically symmetric star,

$$ds^2 = -e^{2\gamma(r,t)}dt^2 + e^{2\mu(r,t)}dr^2 + r^2(d\theta^2 + \sin^2\theta d\phi^2), \tag{6.1}$$

where

$$\gamma(r,t) = \gamma_0(r) + \delta\gamma(r,t)$$
$$\mu(r,t) = \mu_0(r) + \delta\mu(r,t).$$

Here γ_0 and μ_0 denote equilibrium configuration, and $\delta\nu(r,t)$ and $\delta\mu(r,t)$ are small perturbations from this configuration. We also perturb the energy density ρ, pressure p and number density n as

$$\rho(r,t) = \rho_0(r) + \delta\rho(r,t)$$
$$p(r,t) = p_0(r) + \delta p(r,t)$$
$$n(r,t) = n_0(r) + \delta n(r,t).$$

The small perturbation in radial parameter r is assumed to be

$$\delta r(r,t) = u_n(r)e^{\gamma_0(r)}e^{-i\omega_n t}/r^2. \tag{6.2}$$

Utilizing energy conservation, baryon number conservation and Einstein's field equations, we get the dynamical equation governing the stellar pulsation in its n-th normal mode ($n = 0$ gives the fundamental mode) which has the Sturm-Liouville's form (the calculation can be found in any standard text book, e.g., [158])

$$P(r)\frac{d^2u_n(r)}{dr^2} + \frac{dP}{dr}\frac{du_n}{dr} + \left[Q(r) + \omega_n^2 W(r)\right] u_n(r) = 0, \tag{6.3}$$

where $u_n(r)$ and ω_n are the amplitude and frequency of the n-th normal mode, respectively. Functions $P(r)$, $Q(r)$ and $W(r)$ are expressed in terms of the equilibrium configuration of the star given by

$$P(r) = \Gamma p_0 r^{-2} e^{\mu_0 + 3\gamma_0} \tag{6.4}$$

$$Q(r) = e^{\mu_0+3\gamma_0}\left[\frac{(p_0')^2}{r^2(\rho_0+p_0)} - \frac{4p_0'}{r^3} - \frac{8\pi}{r^2}(\rho_0+p_0)p_0 e^{2\mu_0}\right] \tag{6.5}$$

$$W = \frac{(\rho_0+p_0)}{r^2} e^{3\mu_0+\gamma_0}. \tag{6.6}$$

For the fundamental mode ($n = 0$), the above equation can be written as

$$\omega_0^2 \int_0^b e^{3\mu_0+\gamma_0}(\rho_0+p_0)\frac{u_0^2}{r^2}dr = \int_0^b e^{\mu_0+3\gamma_0}\frac{(\rho_0+p_0)}{r^2}\times \left[\left(-\frac{4\gamma_0'}{r} - (\gamma_0')^2 + 8\pi p_0 e^{2\mu_0}\right)u_0^2 + \frac{dp_0}{d\rho_0}\left(\frac{du_0}{dr}\right)^2\right]dr, \tag{6.7}$$

where we substituted the varying adiabatic index Γ, given by

$$\Gamma = \frac{(\rho_0+p_0)}{p_0}\frac{dp_0}{d\rho_0}, \tag{6.8}$$

where ρ_0 and p_0 denote energy-density and pressure at equilibrium state and are given by equations (2.29) and (2.30) obtained in chapter 2.

The model will be stable if ω is real. Since integration of the left hand side of equation (6.7) is always positive definite, all we need to do is to show that the right hand side of this equation is positive. To integrate the right hand side of equation (6.7) we employ the method 2-D given by Bardeen *et al* [153]. We take a trial solution for u_0 as a polynomial in r, which can be written conveniently as

$$u_0 = R^3(1-kz^2)^{3/2}\left[1 + a_1(1-kz^2) + b_1(1-kz^2)^2\right], \tag{6.9}$$

where, a_1 and b_1 are arbitrary constants, $k = (1+\lambda)/\lambda$, $z = \sqrt{(1-r^2/R^2)/k}$ and R is the parameter discussed in chapter 2.

At the surface of the star, we impose the condition that the Lagrangian change in pressure vanishes, i.e., $\Delta p \to 0$ as $r \to b$, ($\Delta p \approx \delta p + p_0'\delta r(r,t) = -\frac{1}{r^2}e^{\gamma_0}\Gamma p_0\frac{du_0}{dr}$), which gives

$$\frac{du_0}{dr} = 0$$

at $r = b$. For the trial solution (6.9) this boundary condition gives

$$3 + 5a_1 y + 7b_1 y^2 = 0, \tag{6.10}$$

where $y = \frac{b^2}{R^2}$. In the next section we shall integrate the right hand side of equation (6.7) for different choices of the parameter λ together with the boundary condition (6.10).

6.3 Results

We begin with SAX J1808.4-3658 and consider the configuration SS1. This corresponeds to $\lambda = 53.34$ and gives $b = 7.07\ km$ and $R = 43.245\ km$ and hence $y = \frac{b^2}{R^2} = 0.026728$. Substituting these values we integrate the right hand side of equation (6.7) for different values of a_1 and b_1, large or small, positive or negative, but satisfying equation (6.10). In each case the result is found to be positive, which clearly indicates that the model is stable against small radial pulsations. The results are given in Table 6.1.

If we consider the configuration for the EOS SS2, the relevant parameters are $\lambda = 230.58$, $b = 6.55\ km$, $R = 82.35\ km$ and $y = \frac{b^2}{R^2} = 0.00633$. Employing the same technique we can draw the conclusion this configuration is also stable. The values of the integral of the right hand side of (6.7) for different choices of the parameters a_1 and b_1 are shown in Table 6.2.

Let us now consider the case of Her X-1. In chapter 5 we have already shown that if we take the mass and radius of Her X-1 as $M = 0.88\ M_{\odot}$ and $b = 7.7\ km$, respectively, the corresponding EOS for $\lambda = 100$ agrees well with the EOS obtained by Horvath and Pacheco [72] for a quark-diquark mixture. To prove that our configuration is stable in this case too, we integrate the right hand side of equation (6.7) once again with $\lambda = 100$, $b = 7.7\ km$ and $R = 108.779\ km$. The results are shown in Table 6.3. The results, clearly suggest that the configuration is stable under radial oscillations.

6.4 Discussions

We note that equation (6.7) can also be integrated for different values of the parameter $y = \frac{b^2}{R^2}$. Changing the value of y ($y < 0.5$), Knutsen [156] verified stability of the Vaidya-Tikekar [63] model for $\lambda = 2$ case and showed that the model is stable. Since the solution presented by Mukherjee *et al* [67] can admit any value of $\lambda > \frac{3}{17}$, we can do the same type of calculation for any value of λ subject to the constraint on $y(= \frac{b^2}{R^2})$ given in equation (2.41), which follows from physical consideration. In Table 6.4., the upper bound on the possible values of y for different λ are given. However, in this chapter, we have shown explicitly how the simple analytic solution [67] helps in studying the stability of realistic compact objects, provided an equation of state is available.

b_1	a_1	Integral
1	-22.4858	0.0005
10	-22.8225	0.0005
10^2	-26.1903	0.0004
10^3	-59.8676	0.0004
10^4	-396.641	0.1494
10^5	-3764.37	16.5377
10^6	-37441.7	1670.24
10^{10}	-3.74×10^8	1.67×10^{11}
0	-22.4483	0.0006
-10	-22.0741	0.0006
-10^2	-18.7064	0.0008
-10^3	14.9709	0.0041
-10^4	351.744	0.1861
-10^5	3719.48	16.9049
-10^6	37396.8	1673.91
-10^{10}	3.74×10^8	1.67×10^{11}
10^{-10}	-22.4483	0.0005

Table 6.1: Value of the integral (equation (6.7)) for $\lambda = 53.34$, $y = \frac{b^2}{R^2} = 0.026728$

b_1	a_1	Integral
1	-94.8498	0.00025
10	-94.9295	0.00025
10^2	-95.7266	0.00025
10^3	-103.698	0.00021
10^4	-183.41	0.00002
10^5	-980.534	0.0204
10^6	-8951.78	2.44813
10^{10}	-8.857×10^7	2.495×10^8
0	-94.8409	0.00025
-10	-94.7524	0.00025
-10^2	-93.9552	0.00026
-10^3	-85.984	0.0003
-10^4	-6.2716	0.00098
-10^5	790.852	0.0300
-10^6	8762.09	2.54395
-10^{10}	8.857×10^7	2.496×10^8
10^{-10}	-94.8409	0.00025

Table 6.2: Value of the integral (equation (6.7)) for $\lambda = 230.58$, $y = \frac{b^2}{R^2} = 0.00633$

b_1	a_1	Integral
1	-119.753	0.00174
10	-119.816	0.00174
10^2	-120.447	0.00173
10^3	-126.761	0.00167
10^4	-189.894	0.00113
10^5	-821.232	0.00585
10^6	-7134.61	1.05879
10^{10}	-7.61488×10^7	1.13×10^8
0	-119.746	0.00174
-10	-119.676	0.00174
-10^2	-119.044	0.00175
-10^3	-112.73	0.00181
-10^4	-29.597	0.00257
-10^5	581.741	0.02021
-10^6	6895.12	1.20234
-10^{10}	7.01×10^7	1.13×10^8
10^{-10}	-119.746	0.00174

Table 6.3: Value of the integral (equation (6.7)) for $\lambda = 100$, $y = \frac{b^2}{R^2} = 0.00501062$

λ	$y_{max.}$
1	0.5166
2	0.5000
3	0.4574
4	0.4166
5	0.3810
10	0.2631
20	0.1611
50	0.0742
100	0.0390
200	0.0200

Table 6.4: Upper bound on the possible values of $y = (\frac{b^2}{R^2})$ as a function of λ, as given by equation (2.41).

Chapter 7

Scaling Property in Cold Compact Stars

7.1 Introduction

In the MIT bag model, scaling property with respect to the bag constant B in the EOS for strange matter has been reported earlier by Witten [25]. Following Witten's [25] work, Benvenuto and Horvath [159] and Zdunik [75] also reported some scaling laws in the EOS considered by them for strange stars. The strange matter EOS formulated by Dey *et al* [42] can be approximated to a linear form as shown by Gondek-Rosińska *et al* [74] which is very similar to the EOS obtained by Zdunik [75] for strange matter in the MIT bag model. The linear nature of these equations of state also provides some scaling laws; analogous to the scaling law with respect to the bag constant B. Thus, scaling property in compact stars like strange stars may be thought, at first sight, as due to the equation of state being a linear one. But, in this chapter, we shall show that there is a type of scaling property in compact stars, which is, infact, a general feature of a spherical distribution in hydrostatic equilibrium. We demonstrate this by analysing the Tolman-Oppenheimer-Volkoff (TOV) equations and the boundary conditions that

are used while solving these equations. A special class of these scaling property is explicitly exhibited by the solution considered by Mukherjee *et al* [67]. In chapters 4 & 5, we have shown that this solution can be applied to describe strange stars as well as stars whose interior might have other exotic components. Moreover, although for a large value of the parameter λ the EOS becomes almost linear in this model, the same is not true for a smaller value of λ. Scaling property, nevertheless, applies in all the cases. Physical implications of this scaling property in the Vaidya-Tikekar model [63] will be discussed in this chapter.

7.2 Scaling law in strange star EOS

While studying the expected features of compact stars made of u, d and s quarks (strange stars), Witten [25] first pointed out a scaling property in the mass-radius ($M-b$) relation for such stars. The equation of state for these stars, in the MIT Bag model with massless quarks, can be written as

$$p = \frac{1}{3}(\rho - 4B) \tag{7.1}$$

$$\rho = \frac{9}{4}\pi^{2/3} n^{4/3} + B \tag{7.2}$$

where ρ is the energy-density, p the pressure, B the Bag constant (vacuum energy), and $n_B = \frac{1}{3}(n_u + n_d + n_s)$, the baryon number density. The stars exhibit scaling with respect to the Bag constant

$$M(B) = \sqrt{\frac{B'}{B}} M(B') \tag{7.3}$$

$$b(B) = \sqrt{\frac{B'}{B}} b(B') \tag{7.4}$$

where B and B' are two values of the Bag Constant.

Recently, Gondek-Rosińska *et al* [74] presented a linear EOS for strange matter given by,

$$p = a(\rho - \rho_0),$$

which was obtained by linearizing the EOS for strange matter formulated by Dey *et al* [42]. Similar EOS was obtained by Zdunik [75], who considered MIT bag model to formulate strange matter EOS. The linear nature of the EOS also allows to scale all the physical parameters of a star with some powers of ρ_0 for a fixed value of a, analogous to the scaling law with the bag constant B. This has been discussed by Zdunik [75].

Thus in case of strange stars having a linear EOS, one can always identify a scaling law. We find that this scaling behaviour is not restricted to strange stars alone and it may occur in more general cases. It is not even necessary to consider a linear equation of state.

7.3 Standard approach

To demonstrate the scaling law in a more general way, let us consider a spherically symmetric, static star having an interior metric

$$ds^2 = -e^{2\gamma(r)}dt^2 + e^{2\mu(r)}dr^2 + r^2(d\theta^2 + \sin^2\theta d\phi^2) \tag{7.5}$$

where r is the radial co-ordinate. We have used the conventional units ($c = 8\pi G = 1$).

The standard procedure for determining the $(M - b)$ relation for a star is to make use of the TOV equations given by

$$\frac{dp}{dr} = -(\rho + p)\frac{2M(r) + pr^3}{r^2(1 - \frac{2M(r)}{r})} \tag{7.6}$$

$$\frac{dM}{dr} = \frac{1}{2}\rho r^2 \tag{7.7}$$

For a given EOS ($p = p(\rho)$), macroscopic properties of the star such as mass and radius are determined by integrating the TOV equations numerically, using the boundary conditions (i) $M(0) = 0$, (ii) $p(0) = p(\rho_c)$, (iii) $p(b) = 0$ and (iv) $e^{2\gamma(b)} = 1 - \frac{2M(b)}{b}$, where b is the radius of the star.

We assume that the energy density of the stellar matter depends on a parameter R, which has the dimension of a length. The energy-density and pressure, expressed in geometrized units of length $^{-2}$, assumed finite inside the star, can be written, without loss of generality, as

$$\rho(r) = \frac{1}{R^2} f(r/R), \quad p(r) = \frac{1}{R^2} g(r/R). \tag{7.8}$$

If we now consider a transformation

$$\tilde{r} = r/R, \quad \tilde{M} = M/R, \quad \tilde{\rho} = \rho R^2, \quad \tilde{p} = pR^2$$

the TOV equations and all the boundary conditions remain invariant. The boundary condition $p(b) = 0$, in particular, becomes $\tilde{p}(\tilde{b}) = 0$, and the first zero of $g(x)$ determines $\tilde{b}$ and hence the radius, $b = \tilde{b}R$. The scaling property thus appears once we can identify or construct a parameter R with the dimension of a length in the EOS. As an example, we consider the case of a polytropic equation of state

$$p(\rho) = K\rho^{1+1/n} = K\rho^{\Gamma}, \tag{7.9}$$

where n is the polytropic index and Γ is the adiabatic index. Since K is a dimensional quantity, one can construct the parameter $R_0 = K^{\frac{1}{(2\Gamma-2)}}$, with the dimension of a length and we find a scaling behaviour,

$$M(K) = \left(\frac{K'}{K}\right)^{\frac{1}{2\Gamma-2}} M(K')$$

$$b(K) = \left(\frac{K'}{K}\right)^{\frac{1}{2\Gamma-2}} b(K')$$

where K and K' are two values of the parameter K.

7.4 Scaling law in Vaidya-Tikekar [63] model

The scaling property mentioned above is explicitly built in Vaidya and Tikekar [63] model. In particular, we consider the solutions given by Mukherjee *et al* [67] to prove

Distance	$\frac{dp}{d\rho}$	
r (km)	$\lambda = 2$	$\lambda = 100$
0	.3418	.2268
2	.3437	.2296
4	.3484	.2363
6	.3525	.2423
7.7	.3518	.2424

Table 7.1: Variation of $\frac{dp}{d\rho}$ along the radius of a star of $M = 0.88\ M_{\odot}$, $b = 7.7\ km$, for $\lambda = 2$ ($R = 20.224\ km$) and $\lambda = 100$ ($R = 108.779\ km$).

our point. A simple way to study the relevant scaling property here is to note that in the model discussed in chapter 2, R has the dimension of a length and to define

$$\tilde{\rho} = \rho R^2, \quad \tilde{p} = pR^2,$$
$$\tilde{M} = \frac{M}{R}, \quad \tilde{r} = \frac{r}{R}, \ \& \ \tilde{b} = \frac{b}{R}.$$

The model can now be written in terms of $\tilde{\rho}$, $\tilde{p}$, $\tilde{M}$, $\tilde{r}$ and $\tilde{b}$, and it becomes independent of R. The elimination of the parameter R from the EOS implies the existence of a homologous family of stars, (for $R > b > 2M$), unless restricted by other physical constraints. The family of stars are represented by $\tilde{M}$, $\tilde{b}$, $\tilde{\rho}$ and $\tilde{p}$. λ here helps to parametrize the equation of state, given implicitly by the equations (2.29) and (2.30) in chapter 2. To see this in a simple way, we can write,

$$\frac{dp}{d\rho} = \frac{d\tilde{p}}{d\tilde{\rho}} = \frac{z(1-z^2)^2(\psi_z/\psi)^2 - (1-z^2)(\psi_z/\psi)}{z(1-z^2)(\lambda+1)+4z}. \tag{7.10}$$

We have shown in Table 7.1, values of $\frac{dp}{d\rho}$ for different λ. It is seen that at a small λ, the relevant stellar matter has almost a radiation like behaviour which becomes less

stiff as λ increases. Note that the EOS in our model is not exactly linear, at least for a small λ, but the scaling property nevertheless works.

The scaling law discussed so far can also be expressed in terms of the central density of the star. In section 2.2.4, we obtained central density as

$$\rho_c = \frac{3(\lambda+1)}{R^2}. \tag{7.11}$$

Inserting the expression for R in the above mentioned scaling formulae, we can rewrite the scaling formulae, as

$$\tilde{\rho} = \rho\left(\frac{\rho_c}{h}\right),\ \tilde{p} = p\left(\frac{\rho_c}{h}\right),\ \tilde{M} = M\left(\frac{\rho_c}{h}\right)^{1/2},\ \tilde{b} = \left(\frac{\rho_c}{h}\right)^{1/2},$$

where, $h = 3(\lambda+1)$.

Thus if mass $\tilde{M}_1$ and radius $\tilde{b}_1$ of a star are known for a central density ρ_{c1}, then for a central density ρ_{c2} the rescaled mass $\tilde{M}_2$ and radius $\tilde{b}_2$ can be written as

$$\tilde{M}_1 = \left(\frac{\rho_{c1}}{\rho_{c2}}\right)^{1/2}\tilde{M}_2$$
$$\tilde{b}_1 = \left(\frac{\rho_{c1}}{\rho_{c2}}\right)^{1/2}\tilde{b}_2.$$

Thus the star $\tilde{M}_2$, $\tilde{b}_2$ will also be described by this model with the same λ.

The scaling property can be generalized easily to the case of a charged sphere too, as mentioned in chapter 3. This happens because all field equations and boundary conditions in this model can be given in terms of z, and the reduced quantities $\tilde{\rho} = \rho R^2$, $\tilde{p} = pR^2$, $\tilde{\sigma} = \sigma R^2$, $\tilde{M} = \frac{M}{R}$, $\tilde{b} = \frac{b}{R}$. In other words, the model is fully described in terms of $\tilde{\rho}$, $\tilde{p}$, $\tilde{\sigma}$, $\tilde{M}$, and $\tilde{b}$ and the parameter R does not appear anywhere. It is obvious that the expressions (3.18)-(3.26) in chapter 3 and boundary conditions have the required scaling behaviour. Thus we observe that the class of charged stars described in this model have a similar scaling behavoiur. Note that the electric field also needs a scaling here.

The expressions for ρ and p in chapter 2, may be obtained in many ways. In Bag model, one has to include the contribution of vacuum energy density in the expressions for ρ and p and for a strange star the equation of state is a linearized relation between ρ and p [74]. In chapter 4, we have shown that our model can be used to reconstruct strange natter EOS. We have also shown in chapter 5 that a quark-diquark EOS can also be constructed by this model [162]. It appears that scaling behaviour has a physical relevance and one may expect to find a large class of cold stars more compact than ordinary neutron stars.

7.5 Discussions

We have noted that a cold compact star should have a scaling property, whenever one can identify a parameter with the dimension of a length. The result does not depend on the specific form of the equation of state. It is rather a general feature of a spherical distribution that is in hydrostatic equilibrium. We have also shown that our model exhibits this scaling property explicitly. For example, if we have a star with mass M, radius b, and charge q, there may also be a star with mass, radius and charge given by ξM, ξb and ξq, where ξ is a constant. Making a contact with the physical value of any one of these reduced quantities, one determines the appropriate value of ξ and hence the physical values of other quantities. Thus the scaling follows once we can identify a suitable dimensional parameter in the equation of state. Different parameters may be available in different cases but the results may be trivial in some cases. Also, the scaling behaviour will be restricted within a range determined by physical constraints (e.g. $R > b > 2M$ as well as $\frac{dp}{d\rho} < 1$). The nature of interaction among the constituents of the stellar matter may impose further constraints. Thus the scaling behaviour will perhaps be realistic only for scaling parameters ($\sim \frac{\tilde{b}}{b}$) whose values are close to 1, so that the underlying physical processes and interactions do not become different from those in the unscaled case.

Chapter 8

Core-Envelope Model for Compact Stars

8.1 Introduction

Macroscopic features of a supercompact star such as mass and radius are dependent crucially on the composition of the stellar material. To construct a stellar model we use an equation of state (EOS), i.e., $p = p(\rho)$, where ρ and p denote energy-density and pressure of the stellar material, respectively. To determine the mass and radius of the star one integrates the Tolman-Oppenheimer-Volkoff (TOV) equations numerically, using appropriate boundary conditions. However, a case of special interest occurs if the interior of a star has a deconfined quark core surrounded by an envelope of normal baryonic matter. In such a case it is not be possible to use a single EOS to describe the entire star and the situation becomes much more complicated. In this case, the construction of a stellar model demands two input parameters, namely central density and density at the junction and the equations of state of the two layers composed of two different kinds of material.

The possibility of a quark phase in the interior of a compact star has already been

pointed out independently by Witten [25] and Farhi and Jaffe [26]. This possibility has generated speculations of an entirely new class of compact stars known as strange stars. In chapter 1 we have noted the suggestions by various investigators that some pulsars could be strange stars, e.g., 4U 1820-30 (Bombaci, 1997 [130]) Her X-1 (Dey *et al*, 1998 [42]), , SAX J 1808.4-3658 (Li *et al*, 1999 [40]), 4U 1728-34 (Li *et al*, 1999 [43]) and PSR 0943+10 (Xu *et al*, 1999 [45]). However, whether strange stars are bare or they have a normal nuclear crust has remainsd an unsolved issue till date [30], [160], [161]. Most of the strange star calculations are based on a single EOS, although there are suggestions that a strange star can have a low density crust if a sufficient gap of electron layer is assumed between the core and the nuclear crust [54, 91, 120]. A compact star may have other exotic components too. For example, Horvath and Pacheco [72] have claimed that Her X-1 is a star composed of a mixture of quark-diquark matter. In the model bosonic diquarks have been described by a self-interacting complex scalar field Φ and a potential of the form $\frac{\Lambda}{4}|\Phi|^4$, where Λ is the coupling constant. The calculation was based on the earlier work in this field by Kaup [56], Ruffini and Bonazzola [57], Colpi *et al* [58]. Kastor and Traschen [76] explored the possibility of a compact star having quark-diquark core surrounded by a low-density envelope of nucleon. Drago & Lavagno [164] presented a new model for compact stars having deconfined quark cores surrounded by a less dense mixed phase.

Following these developments, it will be intereseting to explore an alternative method to construct a model for a star having two layers; a deconfined quark core enveloped by a normal baryonic matter. This can easily be implemented using the solution of Mukherjee *et al* [67] under Vaidya-Tikekar model [63]. The solution has already been discussed in chapter 2. A parameter λ, in this model specifies the equation of state(EOS) of the star. Earlier, the Vaidya-Tikekar [63] model was used to construct a core-envelope model where an anisotropic solution for the core region was assumed [65]. Using TOV equations, Lindblom [77] analysed the features of the mass-

radius curve of a relativistic stellar model constructed from an EOS with a first order phase-transition. In our work, without using TOV equations, we can construct a model exhibiting a phase transition, by choosing different values of the parameter λ.

As of now, we do not have enough experimental support to predict exactly at which point a hadronic phase transition occurs. Weber [7] gave a wide range for such a phase transition ($\rho_{DC} \approx 0.28 - 0.98\ GeV\ fm^{-3}$). In a recent CERN pre-print, Heinz [152] analysed quark-gluon phase transition and showed that an energy density of about $0.6\ Gev\ fm^{-3}$ is needed to make this phase transition possible. As we are yet to reach a concensus on this issue, we in our calculation, will consider $0.6\ GeV\ fm^{-3}$ as a representative value for such a phase transition. Although we shall not discuss the explicit nature of the exotic phases for the two layers, the effect of a phase transition can easily be seen from the change in softness/stiffness of the EOS of the entire body.

8.2 Core-envelope model

We start with a static, spherically symmetric star having a line element of the form

$$ds^2 = -e^{2\gamma(r)}dt^2 + e^{2\mu(r)}dr^2 + r^2(d\theta^2 + \sin^2\theta d\phi^2), \tag{8.1}$$

where,

$$e^{2\mu} = \frac{1 + \lambda r^2/R^2}{1 - r^2/R^2}, \tag{8.2}$$

and

$$e^{\gamma} = \psi(z) = A\Big[\frac{\cos[(n+1)\zeta + \delta]}{n+1} - \frac{\cos[(n-1)\zeta + \delta]}{n-1}\Big]. \tag{8.3}$$

All the parameters have been defined in chapter 2. For a given mass and radius of this class of stars, we have shown in Table 8.1, values of $\frac{dp}{d\rho}$ for different choices of the parameter λ. It is evident that at a small λ, the relevant stellar matter has almost a radiation like behaviour which becomes less stiff as λ increases. Thus the solution can be utilized to construct models for stars having concentric layers of different material components distinguished by the parameter λ.

λ	$R\ (km)$	δ	A	$\left(\frac{dp}{d\rho}\right)_{r=0}$	$\left(\frac{dp}{d\rho}\right)_{r=b}$
2	20.224	2.23367	0.9332	0.3418	0.3518
5	27.545	2.41532	1.6913	0.2714	0.2847
10	36.627	2.49738	2.9926	0.2479	0.2624
20	50.073	2.5449	5.61083	0.2361	0.2511
50	77.488	2.57512	13.4818	0.2291	0.2446
100	108.779	2.58577	26.6039	0.2268	0.2424
200	153.264	2.59118	52.8501	0.2256	0.2413

Table 8.1: Values of $\frac{dp}{d\rho}$ for different choices of the parameter λ for a star of mass $M = 0.88\ M_{\odot}$ & radius $b = 7.7\ km$.

For simplicity we consider a two-fluid model where the inner core and the outer crust of the star will be described by two values of the parameter λ. We consider a star of mass M and radius b km, whose core and envelope regions are defined as :

- Core: $0 \leq r \leq a$
- Envelope: $a \leq r \leq b$

Let λ_C and λ_E specify the equations of state of the core and envelope regions, respectively. For the solution in the core region $(0 \leq r \leq a)$, we write the constants as A_C, δ_C and R_C, while for the envelope region $(a \leq r \leq b)$, constants are A_E, δ_E and R_E.

8.2.1 Boundary conditions

We apply the following boundary conditions in our model: at $r = a$,

$$e^{\gamma_C(r=a)} = e^{\gamma_E(r=a)} \tag{8.4}$$

$$e^{\mu_C(r=a)} = e^{\mu_E(r=a)} \tag{8.5}$$

$$p_C(r=a) = p_E(r=a) \tag{8.6}$$

and at the boundary of the star, $r = b$,

$$e^{2\gamma_E(r=b)} = \left(1 - \frac{2M}{b}\right) \tag{8.7}$$

$$e^{2\mu_E(r=b)} = \left(1 - \frac{2M}{b}\right)^{-1} \tag{8.8}$$

$$p_E(r = b) = 0. \tag{8.9}$$

8.3 Numerical analysis

To get a qualitative feeling of the model, we now consider a couple of simple cases where we have assumed two stars of different masses and radii undergoing a phase transition.

8.3.1 Case I

Let us consider a star of mass $M = 1\ M_\odot$ and radius $b = 7.5\ km$ which has a deconfined core surrounded by a less dense hadronic matter. We also assume that the deconfinement occurs at $\rho_{dc} = 0.6\ GeV\ fm^{-3}$. From Table 8.1, we find that a larger value of λ gives a much softer EOS. Hence, we assume that the core region of the star is described by a value greater than the value of λ at the envelope region. To be specific, we take $\lambda_C = 100$ and $\lambda_E = 2$, arbitrarily. Note that although we are treating λ_C and λ_E as free parameters in this model, these values are fixed once we identify the exact composition of the two layers.

We now satisfy the boundary conditions (8.4)-(8.9) numerically and find that the junction will be at a radial distance $a = 6.20193\ km$. The other parameters are determined as $R_C = 96.9532\ km$, $R_E = 17.7912\ km$, $\delta_C = 2.51408$, $\delta_E = 2.17076$, $A_C = 25.229$ & $A_E = 0.900734$. The resulting EOS is shown in Fig.8.1.

We note that at $r = 6.20193\ km$ (junction), pressure is continuous, but there is a sharp discontinuity in energy-density which clearly suggests a phase transition. Also

the slope of the core region EOS is ≈ 0.26 whereas its corresponding value at the envelope region is ≈ 0.38. The central density of the star of such a configuration is $\approx 0.972\ GeV\ fm^{-3}$. If the star would have been composed of only one kind of matter described by $\lambda = 2$, the central density would have been $\approx 0.858\ GeV\ fm^{-3}$. This shows that a higher value of λ at the core of the star increases the central density of the star considerably.

8.3.2 Case II

In [162], it has been shown that the EOS obtained for $\lambda = 100$, $R = 108.779\ km$ and $\delta = 2.58577$ in the model discussed in chapter 2, matches accurately with the EOS for a quark-diquark mixture obtained by Horvath and Pacheco [72]. In [162], it has been pointed out that energy contributions form diquarks should vanish when pressure goes to zero which was not considered in [72]. Motivated by this observation we now construct another model in which we make an ad hoc choice for the inner core, viz. $\lambda_C = 100$, $R_C = 108.779\ km$ and $\delta = 2.58577$. For the less dense outer layer we arbitrarily take $\lambda_E = 5$. The envelope may have a quark-hadron mixed phase, a purely hadronic phase or any other exotic phase. Note that, as we have already assumed the values of two unknown parameters, we do not make additional assumption for mass and radius.

Matching conditions, then yield, $R_E = 26.858\ km$, $\delta_E = 2.41552$, $A_C = -9.6654$ and $A_E = 1.69184$. The mass and radius in this case turn out to be $\approx 0.857\ M_\odot$ and $\approx 7.5\ km$, respectively. The resulting EOS is shown in Fig.8.2.

Form Fig8.2, we find that at a distance of $\approx 4.42\ km$ form the centre and energy density of $\approx 0.6\ GeV\ fm^{-3}$, a phase transition occurs. The slope of the core EOS is ≈ 0.23 whereas the slope of the envelope EOS is ≈ 0.28. The central density of the star is $\approx 0.772\ GeV\ fm^{-3}$. If the entire star would have been composed of the matter described by $\lambda = 5$, the central density would have been $\approx 0.753\ Gev\ fm^{-3}$.

Alternatively, if the star would have been composed entirely one kind of matter specified by $\lambda = 100$, the total mass and radius of the star would have been 0.88 $M_{\odot}$ and 7.7 km, respectively.

8.4 Discussions

We have studied compact stars having two layers - a highly dense core surrounded by a comparatively less dense envelope. This is a simplified model in the sense that in our model we have considered only two zones. In principle the model can also be extended to the case of a star having more than two concentric layers of different composition. Our approach may be contrasted with that of Kastor and Traschen [76] who used two equations of state to integrate the TOV equations.

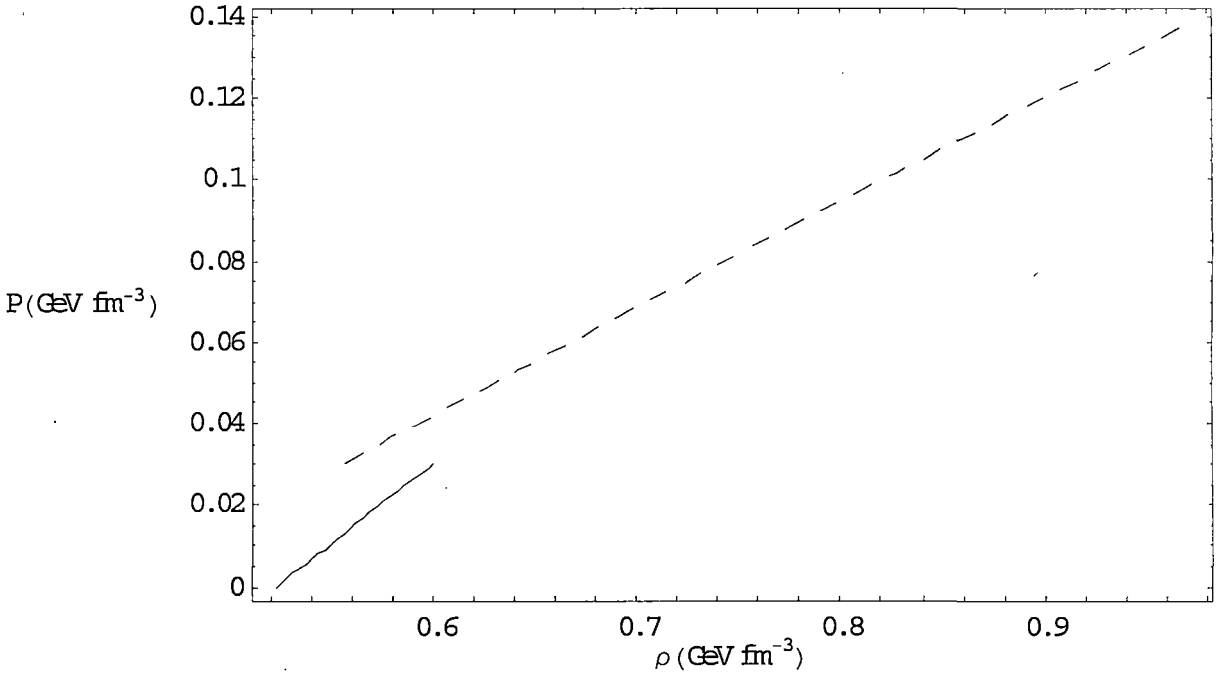

Figure 8.1: Equation of state for the core region with $\lambda = 100$ (dashed line) and EOS for the envelope with $\lambda = 2$ (solid line).

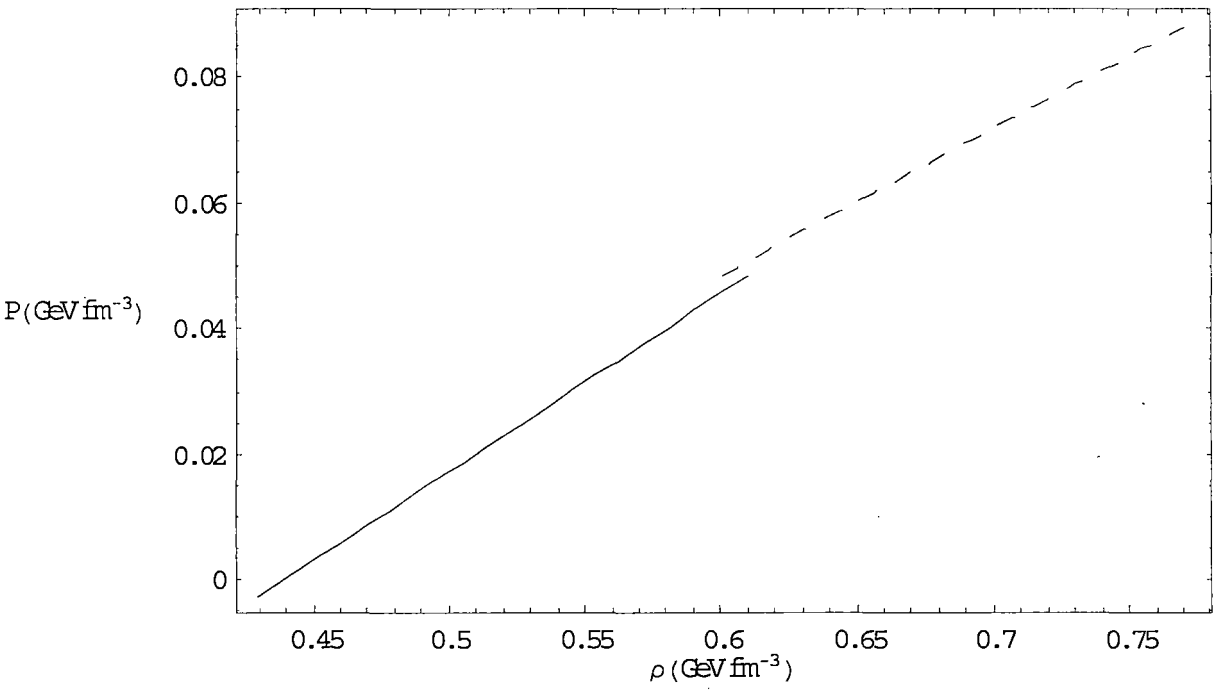

Figure 8.2: Equation of state for the core region with $\lambda = 100$ (dashed line) and EOS for the envelope region with $\lambda = 5$ (solid line).

Chapter 9

Radiating Spherical Collapse with Heat Flow

9.1 Introduction

The theory of gravitional collapse has many interesting applications in astrophysics where the formation of cold compact stellar objects are usually preceded by a period of radiative collapse. The problem of gravitional collapse was first investigated by Oppenheimer and Snyder [78], who considered the contraction of a spherically symmetric dust cloud. In that case the exterior spacetime was described by the Schwarzschild metric and the interior space-time was represented by a Friedman-like solution. Later on, Vaidya [79] derived the line element which describes correctly the exterior gravitational field of a spherically symmetric radiating mass. This has enabled many investigators to model the interior of a radiating star by matching the interior solution to the exterior space-time given by Vaidya [79], e.g., [80], [81], [82], [83] & [84]. The junction conditions for a spherically symmetric shear-free radiating star was completely derived by Santos [85]. The crucial result that follows from Santos is that the pressure on the boundary of a radiating sphere is nonvanishing in general. Subsequently, many

models of radiative gravitational collapse with heat flow were found by utilising these junction conditions. In particular, special attention was given to models in which an initial static stellar configuration started collapsing by dissipating energy in the form of a radial heat flux (Bonnor *et al* [87]). The initial static configuration was taken to be an exact solution of the Einstein field equations. In a recent paper Schäfer and Goenner [86] presented a model of a highly idealized spherically object radiating away its mass with constant luminosity. The body starts collapsing at time $t = -\infty$ with both infinite mass and radius and contracts to a point at time $t = 0$ without forming an event horizon.

Our aim here is to consider the evolution of a star undergoing a radiative gravitional collapse with its final state being that of a superdense star. We want to study this evolutionary process starting from the final non radiating state and interpolating to earlier times when it was emitting radiation.

In Section 9.2 we present the relevant background material and the line element for the interior space time. Einstein equations for an energy momentum tensor with heat flux are solved without assuming a particular form for the final static configuration. The Vaidya solution is introduced in Section 9.3 and the matching condition is utilized to determine approximately the temporal evolution of the model. In Section 9.4 we use the solution of Mukherjee *et al* [67] to describe the final state of the star and find out the evolution of the star making use of the knowledge of the final static configuration. Although we are using a simple model, the results obtained analytically are expected to provide the general trends of results for realistic stars. In Section 9.5 we summarize our results.

9.2 Interior spacetime

Let us assume that a general shear-free metric of the form

$$ds^2 = -A^2(t,r)dt^2 + B^2(t,r)(dr^2 + r^2 d\Omega^2) \tag{9.1}$$

represents the interior spacetime of a star. The choice of a shear-free metric is motivated by the simplicity of the resulting equations, which remain tractable throughout. Moreover, as observed by Bonnor *et al* [87], it is possible to show through Raychaudhuri's equation that the slowest possible collapse is for shear-free fluids. Thus our results will be appropriate in any case if the collapse is not very fast. Also, the choice of a shear-free metric will later on help us to apply the same junction conditions derived by Santos [85] in our model.

The energy momentum tensor for the interior matter distribution is taken to be

$$T_{\mu\nu} = (\rho + p)u_\mu u_\nu + p g_{\mu\nu} + q_\mu u_\nu + q_\nu u_\mu \tag{9.2}$$

where the flow vector satisfies

$$q^\mu u_\nu = 0,$$

u^μ being a timelike four velocity vector. Following Bonnor *et al* [87], we choose the metric functions as follows:

$$A(r,t) = A_0(r) + \epsilon a(r)T(t) \tag{9.3}$$

$$B(r,t) = B_0(r) + \epsilon b(r)T(t) \tag{9.4}$$

and the energy density ρ and the isotropic pressure p as

$$\rho(r,t) = \rho_0(r) + \epsilon\bar{\rho}(r,t) \tag{9.5}$$

$$p(r,t) = p_0(r) + \epsilon\bar{p}(r,t) \tag{9.6}$$

The radial heat flux is of the order of $\epsilon(0 < \epsilon \ll 1)$. However, unlike the case studied by Bonnor *et al* [87], A_0 and B_0 describe here the final static solutions of the

cold star. Einstein's field equations for the static configuration give the relations:

$$\rho_0 = -\frac{1}{B_0^2}\left[2\left(\frac{B_0''}{B_0}\right) - \left(\frac{B_0'}{B_0}\right)^2 + \frac{4}{r}\left(\frac{B_0'}{B_0}\right)\right] \tag{9.7}$$

$$p_0 = \frac{1}{B_0^2}\left[\left(\frac{B_0'}{B_0}\right)^2 + 2\frac{A_0'}{A_0}\frac{B_0'}{B_0} + \frac{2}{r}\left(\frac{A_0'}{A_0} + \frac{B_0'}{B_0}\right)\right] \tag{9.8}$$

where prime($'$) denotes differentiation with respect to r.

The pressure isotropy equation is given by

$$\left(\frac{A_0'}{A_0} + \frac{B_0'}{B_0}\right)' - \left(\frac{A_0'}{A_0} + \frac{B_0'}{B_0}\right)^2 - \frac{1}{r}\left(\frac{A_0'}{A_0} + \frac{B_0'}{B_0}\right) + 2\left(\frac{A_0'}{A_0}\right)^2 = 0 \tag{9.9}$$

We assume that the presure isotropy condition is satisfied for a known static solution (A_0, B_0). The perturbed field equations up to first order in ϵ can be written as

$$\bar{\rho} = -3\rho_0\frac{b}{B_0}T + \frac{1}{B_0^3}\left[-\left(\frac{B_0'}{B_0}\right)^2 b + 2\left(\frac{B_0'}{B_0} - \frac{2}{r}\right)b' - 2b''\right]T \tag{9.10}$$

$$\bar{p} = -2p_0\frac{b}{B_0}T + \frac{2}{B_0^2}\left[\left(\frac{B_0'}{B_0} + \frac{1}{r} + \frac{A_0'}{A_0}\right)\left(\frac{b}{B_0}\right)' + \left(\frac{B_0'}{B_0} + \frac{1}{r}\right)\left(\frac{a}{A_0}\right)'\right]T - 2\frac{b}{A_0^2 B_0}\ddot{T} \tag{9.11}$$

$$q = \frac{2\epsilon}{B_0^2}\left(\frac{b}{A_0 B_0}\right)'\dot{T} \tag{9.12}$$

where an overhead dot denotes differentiation with respect to t.

The condition of pressure isotropy for the perturbed matter distribution can be written as

$$\left[\left(\frac{a}{A_0}\right)' + \left(\frac{b}{B_0}\right)'\right]' - 2\left[\left(\frac{a}{A_0}\right)' + \left(\frac{b}{B_0}\right)'\right]\left(\frac{A_0'}{A_0} + \frac{B_0'}{B_0}\right) - \frac{1}{r}\left[\left(\frac{a}{A_0}\right)' + \left(\frac{b}{B_0}\right)'\right] + 4\frac{A_0'}{A_0}\left(\frac{a}{A_0}\right)' = 0 \tag{9.13}$$

The general solution to this equation is

$$\frac{b}{B_0} = C_0\int rA_0^2B_0^2dr + C_1 - \int rA_0^2B_0^2\int A_0^{-4}\left(\frac{(\frac{a}{A_0})'A_0^2}{rB_0^2}\right)'drdr \tag{9.14}$$

or, equivalently,

$$\frac{a}{A_0} = C_0\int\frac{rB_0^2}{A_0^2}dr + C_1 - \int\frac{rB_0^2}{A_0^2}\int A_0^4\left(\frac{(\frac{b}{B_0})'}{rA_0^2B_0^2}\right)'drdr \tag{9.15}$$

where C_0 and C_1 are constants.

Equations (9.14) or (9.15) gives a relation between $a(r)$ and $b(r)$. For specific calculations, however, it will be helpful to follow an alternative approach. We write $\left(\frac{a}{A_0}\right)' = X(r)$ and $\left(\frac{b}{B_0}\right)' = Y(r)$ and rewrite equation (9.13) as

$$\frac{(X+Y)'}{X+Y} - \left(\frac{2A_0'}{A_0} + \frac{2B_0'}{B_0} + \frac{1}{r}\right) + 4\frac{A_0'}{A_0}\frac{X}{X+Y} = 0. \tag{9.16}$$

Equation (9.16) can be integrated easily if we assume

$$\frac{X}{X+Y} = A_0\frac{dg(A_0)}{dA_0} \tag{9.17}$$

which gives

$$X = k_1 r A_0^3 B_0^2 y e^{-4g(A_0)} \tag{9.18}$$

and

$$Y = \left(\frac{1}{yA_0} - 1\right) X \tag{9.19}$$

where k_1 is an integration constant and $y = \frac{dg(A_0)}{dA_0}$.

Thus we get

$$\frac{a}{A_0} = k_1 \int r A_0^3 B_0^2 y e^{-4g(A_0)} dr + k_2 \tag{9.20}$$

where k_2 is another integration constant.

The right hand side of equation (9.20) can be integrated for different choices of the function $g(A_0)$. It is instructive to consider a simple case:

$$g(A_0) = \frac{1}{2} Ln A_0 \tag{9.21}$$

This gives

$$\frac{a}{A_0} = \frac{b}{B_0} = \frac{k_1}{2} \int r B_0^2 dr + k_2. \tag{9.22}$$

It may be useful to calculate the total energy entrapped within the surface Σ of the star. Up to first order in ϵ, this is given by

$$m(r_\Sigma, t) = m_0(r_\Sigma) + \epsilon \bar{m}(r_\Sigma, t) \tag{9.23}$$

where,

$$m_0(r_\Sigma) = -\left(r^2 B_0' + r^3 \frac{B_0'^2}{2B_0}\right)_\Sigma \tag{9.24}$$

$$\bar{m}(r_\Sigma, t) = \left[\left(-r^2 b' - r^3 \frac{B_0'^2}{2B_0}\left(2\frac{b'}{B_0'} - \frac{b}{B_0}\right)\right) T(t)\right]_\Sigma \tag{9.25}$$

where r_Σ corresponds to the boundary. The evaluation of $m_0(r_\Sigma)$ and $\bar{m}(r_\Sigma, t)$ will be taken up in section 9.4.

9.3 Junction conditions

The boundary of the collapsing star divides spacetime into two distinct regions, the interior spacetime described by the metric (9.1) and the exterior spacetime. Since the collapsing star is radiating energy, the exterior spacetime is described by Vaidya's outgoing metric

$$ds^2 = -\left(1 - \frac{2m(v)}{r}\right) dv^2 - 2dvdr + r^2(d\theta^2 + \sin^2\theta d\phi^2) \tag{9.26}$$

$m(v)$ being an arbitrary function of the retarded time v. The solution (9.26) is the unique spherically symmetric solution of the Einstein field equations for radiation in the form of a null fluid. The Vaidya solution is often used to describe the exterior gravitational field of a radiating star, e.g. de Oliveira *et al* [80, 81, 82], Kolassis *et al* [88] and Kramer [83].

In order to facilitate the smooth matching of the interior space-time to the Vaidya exterior, we utilise the junction conditions deduced by Santos [85]. We can rewrite equation (9.11) and (9.12) as

$$\bar{p} = -2p_0 \frac{b}{B_0} T + 2\frac{b}{A_0^2 B_0}\left(\alpha T - \ddot{T}\right) \tag{9.27}$$

$$q = \frac{4b\epsilon}{A_0^2 B_0^2} \beta \dot{T} \tag{9.28}$$

where

$$\alpha = \frac{A_0^2}{bB_0}\left[\left(\frac{B_0'}{B_0} + \frac{1}{r} + \frac{A_0'}{A_0}\right)\left(\frac{b}{B_0}\right)' + \left(\frac{B_0'}{B_0} + \frac{1}{r}\right)\left(\frac{a}{A_0}\right)'\right] \tag{9.29}$$

$$\beta = \frac{A_0^2}{2b}\left(\frac{b}{A_0 B_0}\right)'. \tag{9.30}$$

To find $T(t)$ we make use of the junction condition $p_\Sigma = (qB)_\Sigma$ together with $(p_0)_\Sigma = 0$ which gives

$$\alpha_\Sigma T - \ddot{T} = 2\beta_\Sigma \dot{T} \tag{9.31}$$

where Σ represents the boundary of the star. The solution of (9.31) is given by

$$T(t) = T_0 Exp\left[-\left(\beta_\Sigma + \sqrt{\alpha_\Sigma + {\beta_\Sigma}^2}\right)t\right] \tag{9.32}$$

which satisfies the boundary conditions

$$T(t)|_{t=\infty} = 0 \text{ and } T(t)|_{t=0} = T_0 \tag{9.33}$$

where T_0 is a constant. Since we expect $T(t)$ to decrease as t increases, we must have $\alpha_\Sigma > 0$. This will be taken up in the next section.

9.4 Final static solution

We assume that the line element (9.1) represents a static solution at large time i.e. at $t \to \infty$, and the metric coefficients are then represented by A_0 and B_0, the static part of equations (9.3) and (9.4), respectively.

For the static solution we take the soutions of Mukherjee *et al* [67] of the Vaidya-Tikekar [63] model, viz.

$$ds^2 = -e^{2\gamma(\bar{r})}dt^2 + e^{2\mu(\bar{r})}d\bar{r}^2 + \bar{r}^2(d\theta^2 + \sin^2\theta d\phi^2) \tag{9.34}$$

where

$$e^{2\mu(\bar{r})} = \frac{1+\lambda\bar{r}^2/R^2}{1-\bar{r}^2/R^2} \tag{9.35}$$

and

$$e^{\gamma(\bar{r})} = A\left[\frac{\cos[(n+1)\zeta+\delta]}{n+1} - \frac{\cos[(n-1)\zeta+\delta]}{n-1}\right] \tag{9.36}$$

In equations (9.35) and (9.36), A, δ and R are constants, $\zeta = \cos^{-1} z$, $n^2 = \lambda + 2$ and $z^2 = (\frac{\lambda}{\lambda+1})(1 - \frac{\bar{r}^2}{R^2})$.

The solution satisfies strong and weak energy conditions as well as causality condition and is vaid for any value of $\lambda \geq \frac{3}{17}$ [67]. In earlier chapters we have shown that this model can describe cold compact stars like Her X-1 and SAX J1808.4-3658. The model also has a scaling property which allows it to describe a class of stars with the same compactness [133]. Moreover, the stability of the stellar configurations for various λ can be verified easily in this model, as shown in chapter 6. Thus although the solution provides a simple model of a star, its simple analytic form is found to be very useful in studying the gross features of a star with an EOS specified by the parameter λ.

However, to make use of this solution, we need to transform the metric (9.1) to the form given by (9.34), i.e. change the radial coordinate r to $\bar{r}$. Comparing equations (9.1) and (9.34), we get,

$$\bar{r} = rB_0(r) \text{ and } e^{\mu(\bar{r})}d\bar{r} = B_0(r)dr \tag{9.37}$$

Using equations (9.35) and (9.37), we get the inverse transformation relation as

$$r = k_3 exp\left[-tanh^{-1}\left(\frac{sin\chi}{\sqrt{1+\lambda cos^2\chi}}\right) - \sqrt{\lambda}sin^{-1}\left(\sqrt{\frac{\lambda}{\lambda+1}}sin\chi\right)\right] \tag{9.38}$$

where $\chi = cos^{-1}\left(\frac{\bar{r}}{R}\right)$ and k_3 is an integration constant.

The integration in equation (9.22) is over r, but using equation (9.37) we can integrate it over $\bar{r}$ so that the final results are expressed in terms of $\bar{r}$. We get,

$$\frac{a}{A_0} = \frac{b}{B_0} = -\frac{k_1}{4l^2}R^2\sqrt{\lambda}\left[sin^{-1}(lx) + lx\sqrt{1-l^2x^2}\right] + k_2 \tag{9.39}$$

where $l = \sqrt{\frac{\lambda}{\lambda+1}}$, $x = \sqrt{1 - \frac{\bar{r}^2}{R^2}}$.

This gives us an analytic solution for the early evolutionary stages of the star. However, to get an idea about the behaviour of the solution, we need to take specific cases and do some numerical work. This will be taken up in the next section.

9.5 Results and discussions

As an example, we consider a star whose final state has a mass $m = 0.88\ M_{\odot}$ and radius $b = 7.7$ km. Note that, these values fall well within the estimated mass and radius of the well known pulsar Her X-1 [40]. Moreover, with a particular choice of the parameter λ ($\lambda = 100$), it has been shown in chapter 5 that the equation of state obtained by using the static solution, agrees accurately with the equation of state obtained by Horvath and Pacheco [72] for a quark-diquark mixture. Matching the static solution to the Schwarzchild exterior solution and using the boundary condition $p_0 = 0$ at $\bar{r} = b$ (note that in the evolutionary stage pressure does not vanish at the boundary), we calculate the values of the constants as $R = 108.779$ km, $\delta = 2.58577$ and $A = 26.6039$.

We, now choose the constants k_1, k_2 & k_3 in such a way that our model describes the expected early evolutionary stages of the star. The time dependence of $T(t)$, heat flux $q(t)$ and mass $m(r,t)$ are shown in Fig.9.1, Fig.9.2 and Fig.9.3, respectively, where we considered two exemplary cases: (1) $k_1 = 1$, $k_2 = 10^5$ & $k_3 = 1$ (solid line) and (2) $k_1 = 1$, $k_2 = 10^{5.2}$ and $k_3 = 1$ (dashed line). Arbitrary choices of these values may not give realistic results. In Fig.9.1 & 9.2, we find that both $T(t)$ and $q(t)$ decreases with time, as expected. Also, in Fig.9.3, the mass of the star decreases with increasing time and as time goes to infinity the mass saturates to it final static value of $0.88\ M_{\odot}$.

Thus, our model gives a description of the evolution of a radiating star. For a known static configuration of a star, this model generates solutions for the earlier stages of the star by a perturbative approach. This may be looked upon as complementary to the approach of Bonnor *et al* [87]. Possibly, the two methods, when combined carefully, will be able to give a total picture of the radiative collapse of a star, which ends up as a cold compact star. In our method, we have made use of the general solution given by Mukherjee *et al* [67]. Although we chose a simple form of $g(A_0)$ more general cases may also be studied.

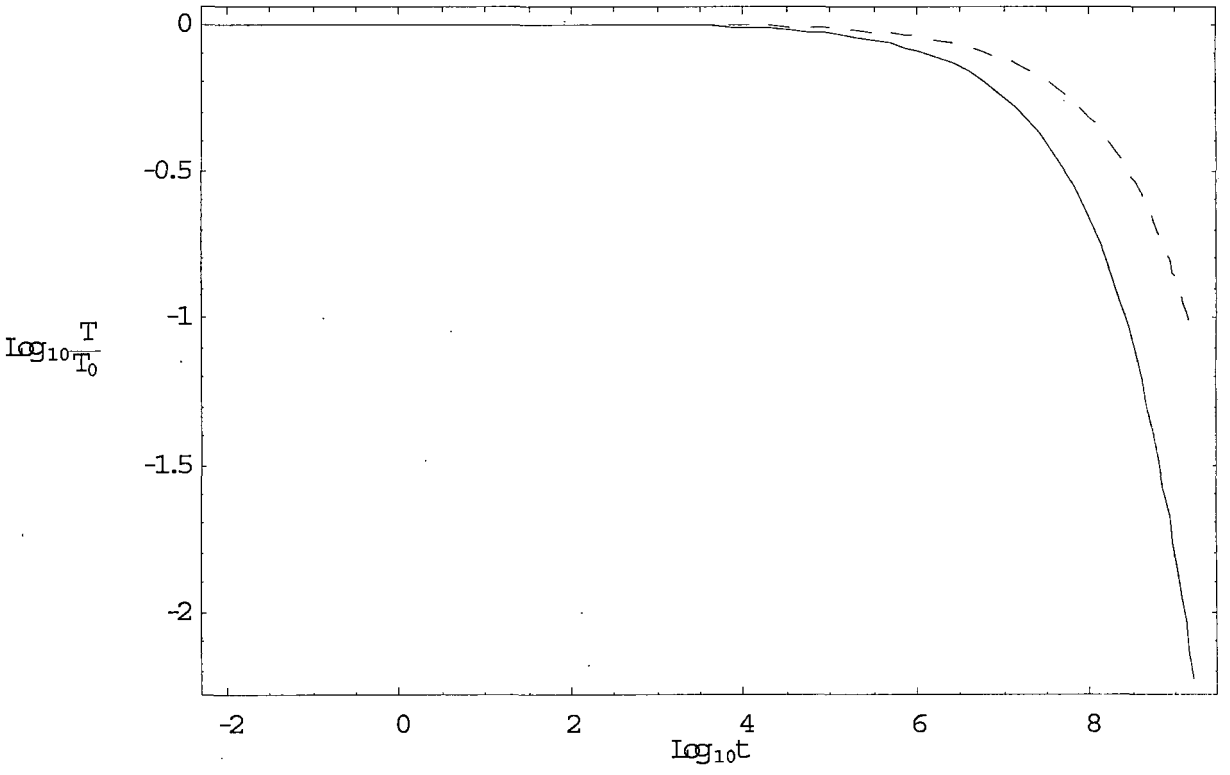

Figure 9.1: Evolution of T(t). The solid line is for $k_1 = 1$, $k_2 = 10^5$ & $k_3 = 1$, while the dashed line corresponds to $k_1 = 1$, $k_2 = 10^{5.2}$ & $k_3 = 1$.

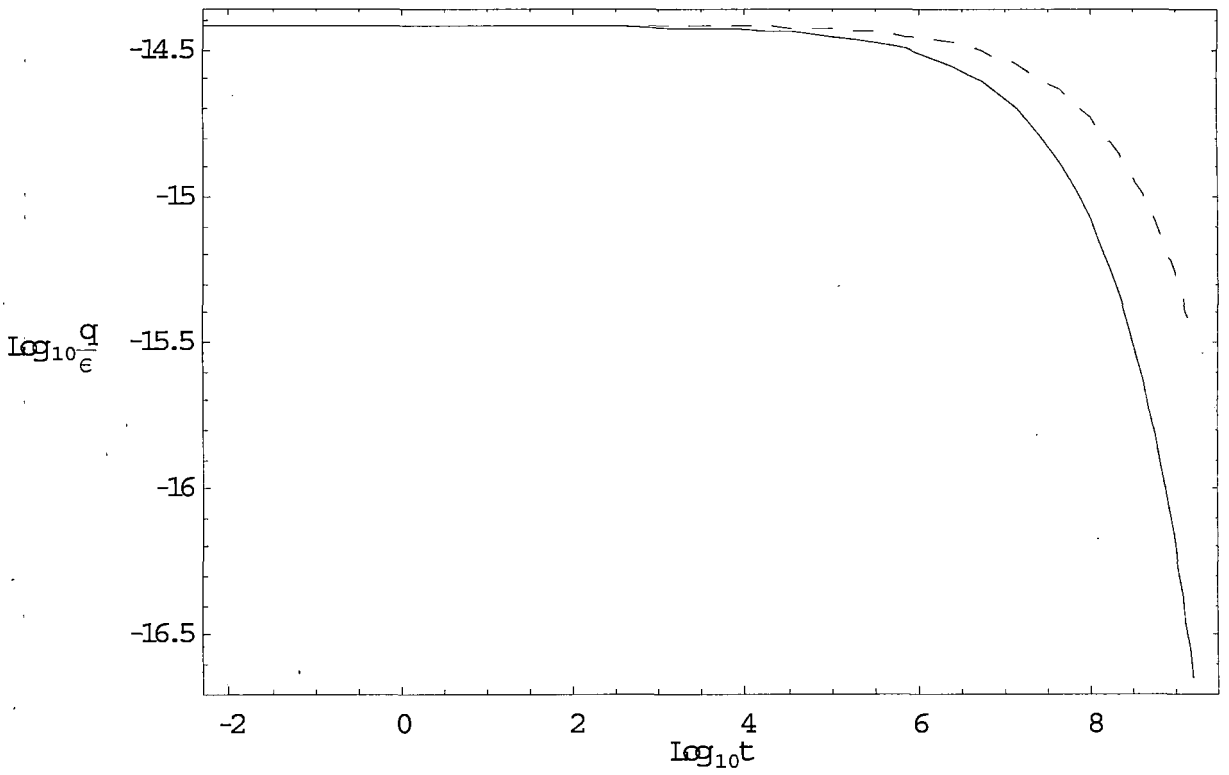

Figure 9.2: Variation of heat flux q as a function of t. The solid line is for $k_1 = 1$, $k_2 = 10^5$ & $k_3 = 1$, while the dashed line corresponds to $k_1 = 1$, $k_2 = 10^{5.2}$ & $k_3 = 1$.

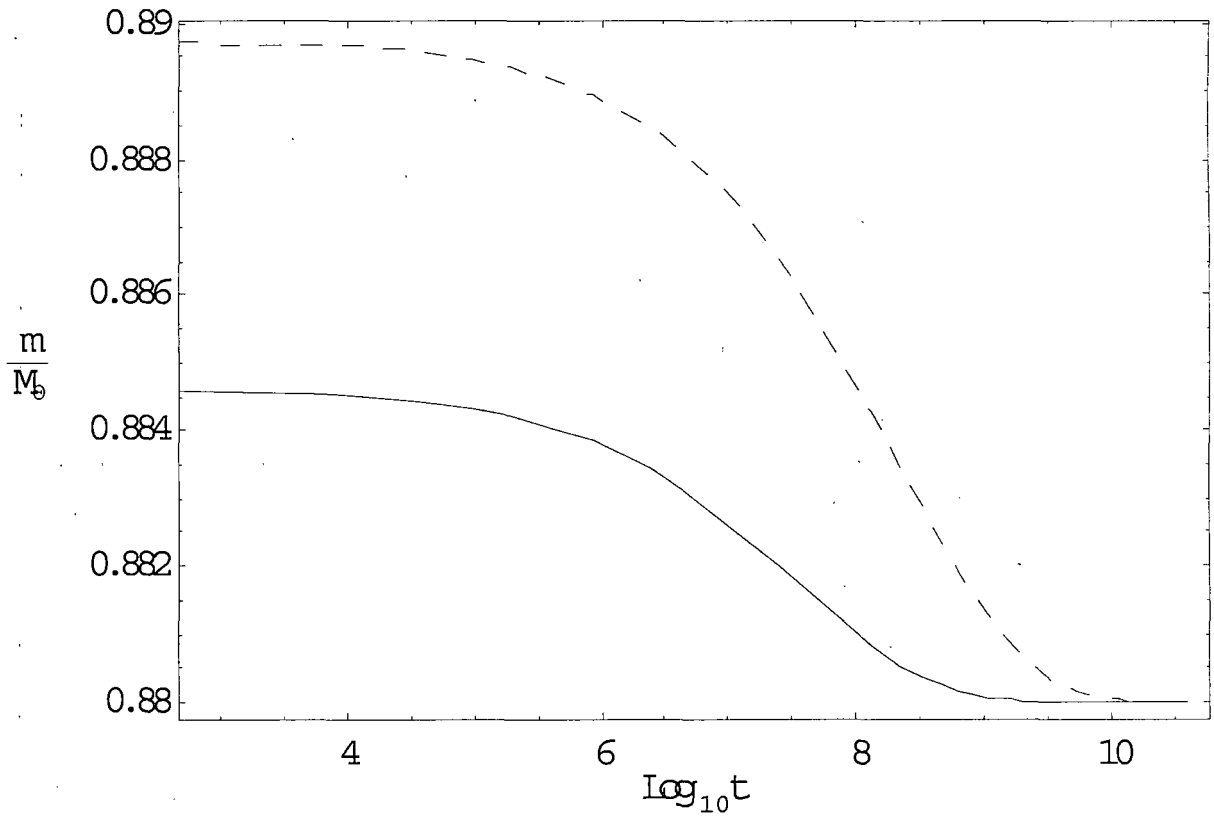

Figure 9.3: Evolution of mass of a star whose final static configuration has mass $m = 0.88\ M_{\odot}$. The solid line is for $k_1 = 1$, $k_2 = 10^5$ & $k_3 = 1$, while the dashed line corresponds to $k_1 = 1$, $k_2 = 10^{5.2}$ & $k_3 = 1$.

Chapter 10

Concluding Remarks

In this chapter we would like to summarize our results and point out areas for future work. We have shown many physical applications of a class of solutions obtained by Mukherjee *et al* [67] based on an ansatz made by Vaidya and Tikekar [63] for the geometry of a static spherically symmetric star. Within the framework of Vaidya-Tikekar model [63], we have studied various possibilities of cold compact stars, namely, (i) charged stars, (ii) quark stars (strange stars), (iii) combined boson-fermion stars (quark-diquark stars) and (iv) stars with a phase transition. Our results may be outlined as follows:

- We have shown that the solution is very useful in describing ultra-compact objects. We have developed a direct method to reconstruct super nuclear equations of state; e.g., strange matter EOS and quark-diquark EOS, by considering only two values of the observables of a star, namely mass and radius, and a parameter λ. The parameter λ appears from the geometry of the star and for a given mass and radius, characterizes the EOS of the star. To demonstrate the physical applicability of the solution, we have considered a couple of interesting cases. We have shown that if SAX J1808.4-3658 is a strange star, the relevant EOS obtained by Dey *et al* [42] can be reconstructed from the solution given in [67] for

the masses and radii given in [43]. Similarly, if Her X-1 is a quark-diquark star as suggested by Horvath and Pacheco [72], the relevant EOS can also be obtained in this model. Although a realistic description of a star, a very complex system, is not expected by this simple description, we have been able to capture the gross features of the composition of the star. This will provide a useful first step in our search for a complete understanding of the composition of very compact stars and of the physical processes that lead to the observed compactness of these objects.

- We have verified the stability of the relevant stellar configurations obtained by using this model. Earlier, the stability of Vaidya-Tikekar [63] model were analysed for some restricted values of the parameter λ, namely, $\lambda = 2$ [156] & 7 [157], because of the non-availability of solutions for other values of λ. But, using the general solution obtained by Mukherjee *et al* [67], the stability of the model can be verified for different choices of the parameter λ. We have verified the stability of the model for large values of the parameter λ, namely, $\lambda = 53.34,\ 100$ & 230.58, which were found to be relevant for the description of compact objects in our study.

- We have observed that the Vaidya-Tikekar [63] model has a scaling property which allows the solution to describe a family of stars of equal compactness. Following the observations made by Witten [25] and Zdunik [75] the scaling property in compact stars like strange stars might be thought of being associated with the equation of state and its linearity. But we have shown that a cold compact star should have a scaling property, whenever one can identify a parameter with the dimension of a length in the EOS. The result does not depend on the specific form of the equation of state. It is rather a general feature of spherical distribution that is in hydrostatic equilibrium. We have shown that Vaidya-Tikekar [63] model can be applied to describe strange stars as well as stars whose interior might have other exotic components. Moreover, although for a large value of the

parameter λ the EOS becomes almost linear in this model, same is not true for a smaller value of λ. Scaling property, however, applies to all the cases.

- We have extended the solution to the case of a static charged spherical distribution of matter and obtained a new class of solutions for such bodies. Physical properties of such charged bodies have been analysed. The solution may be useful, in core-envelope model, in describing the outer envelope of a star which may become charged due to accretion [69], [70].

- The model has been used to describe stars having two layers of different material composition, say, a deconfined quark core surrounded by a comparatively less dense baryonic envelope. This has been done by choosing solutions for two different values of the parameter λ for the two layers separated by a surface where a phase transition may take place and satisfying necessary boundary conditions across the surface. This model can be used in the case of compact stars where phase transition is a possibility.

- The model has also been utilised to study the late evolutionary stages of a collapsing star, becoming ultimately a cold compact star.

Although, we have demonstrated some applications of the solution of Mukherjee *et al* [67], the applicability of these class of solutions may be much wider. The solution, being simple and analytic, can provide a description of the gross features of cold compact stars. One will, no doubt, need to consider a more complex description for a realistic star. We would like to point out here some areas where the model may have further applications as well as areas where the model can be improved upon.

- In some cases, pressure anisotropy may be a feature to be considered [165]. However, the anisotropy can be studied by generalizing the model and at present, we are looking into this possibility.

- In our study, we have neglected the rotational effects on the gross observational properties of compact objects. It has been pointed out by Li *et al* [40] (in case of Her X-1), and by de Sousa and Silveira [90] in case of combined boson fermion stars, that the effects are small. However, for a more realistic description, we should extend the model to the case of a rotating star and investigate the effects of rotation on the physical properties of the star.

- Although considering a strange matter EOS under the MIT bag model, Phukon [91] showed that gross features of the star remain almost unaltered for a magnetic field of strength upto 10^{18} G, it will be interesting to investigate the deformation in the metric coefficients due to the presence of a strong magnetic field in this model.

- Finally, since the model can describe some of the general features of interesting X-ray pulsars like Her X-1, in terms of analytic functions, it may be useful in explaining some special features like quasi periodic oscillations, bursts etc., by a simple perturbative approach.

To summarize, based on available data on pulsars, we have been able to study various properties of compact objects, making use of a simple model. Knowing fully well that the model is too simple, we have emphasized on what can be achieved from the model, rather than what we cannot know from the model. We hope that this simple analytic model will be able to provide some guidance to more realistic and detailed numerical study to understand present and future observational data on compact objects.

Bibliography

[1] Shapiro S L & Teukolosky S A: *Black Holes, White Dwarfs and Neutron Stars: The Physics of Compact Objects*, (Wiley, New York, 1983).

[2] Baade W & Zwicky F (1934) *Phys. Rev.* **45**, 138.

[3] Oppenheimer J R & Volkoff G M (1939) *Phys. Rev.* **55**, 374.

[4] Steiner A, Prakash M & Lattimer J M (2000) *Phys. Lett.* **B486**, 239; *nucl-th/0003066.*

[5] Prakash M, Lattimer J M, Pons J A, Steiner A W & Reddy S (2001) *Lect. Notes Phys.* **578**, 364; *astro-ph/0012136.*

[6] Sahu P K (2000) *Phys. Rev. C* **62**, 045801; *nucl-th/0007067.*

[7] Weber F (1999) *Acta. Phys. Polon.* **B30**, 3149; *astro-ph/9910371.*

[8] Haensel P, *astro-ph/9605164.*

[9] Balberg S & Shapiro S L, *astro-ph/0004317.*

[10] Akmal A, Pandharipande V R & Ravenhall D G (1998) *Phys. Rev. C* **58**, 1804; *nucl-th/9804027.*

[11] Kutschera M (1998) *Acta. Phys. Polon.* **B29**, 25; *astro-ph/9801235.*

[12] Pethick C J, Akmal A, Pandharipande V R & Ravenhall D G, *astro-ph/9905177.*

[13] Yasuhira M, *nucl-th/0010030.*

[14] Heiselberg H & Pandharipande V (2000) *Ann. Rev. Nucl. Part. Sci.* **50**, 481; *astro-ph/0003276.*

[15] Hewish A, Bell S J, Pilkington J D H, Scott P F & Collins R A (1968) *Nature* **217**, 709.

[16] Heiselberg H, *astro-ph/0201465.*

[17] Kapoor R C & Shukre C S (2001) *Astron. & Astrophys.* **375**, 405.

[18] Lattimer J M & Prakash M (2000) *Phys. Rep.* **333**, 121; *astro-ph/0002203.*

[19] Leung Y C & Wang C G (1973) *Astrophys. J* **181**, 895.

[20] Schertler K, Greiner C & Thoma M H, *astro-ph/9801200.*

[21] Thorsett S E & Chakrabarty D (1999) *Astrophys. J* **512**, 288; *astro-ph/9803260.*

[22] Rutledge R E, Bildsten L, Brown E F, Pavlov G G & Zavlin V E (2001) *Astrophys. J* **551**, 921.

[23] Vallisneri M (2000) *Phys. Rev. Lett.* **84**, 3519; *gr-qc/0202037.*

[24] Saijo M & Nakamura T (2001) *Phys. Rev. D* **63**, 064004.

[25] Witten E (1984) *Phys. Rev. D* **30**, 272.

[26] Farhi E & Jaffe R L (1984) *Phys. Rev. D* **30**, 2379.

[27] Dai Z G, Peng Q H & Lu T (1995)*Astrophys. J* **440**, 815.

[28] Cheng K S & Dai Z G (1996) *Phys. Rev. Lett.* **77**, 1210; (1998) *Phys. Rev. Lett.* **80**, 18.

[29] Haensel P, Zdunik J L & Schaeffer R (1986) *Astron. & Astrophys.* **160**, 121.

[30] Alcock C, Farhi E & Olinto A (1986) *Astrophys. J.* **310**, 261.

[31] Alcock C, Farhi E & Olinto A(1986) *Phys. Rev. Lett.* **57**, 2088.

[32] Alcock C & Olinto A(1988) *Ann. Rev. Nucl. Part. Sci.***38**, 161.

[33] Glendenning N K (1990) *Mod. Phys. Lett. A* **5**, 2197.

[34] Glendenning N K, Kettner Ch. & Weber F (1995) *Phys. Rev. Lett.* **74**, 3519; (1995) *Astrophys. J* **450**, 253.

[35] Benvenuto O G & Althaus L G (1996) *Astrophys. J.* **462**, 364.

[36] Rankin J M (1990) *Astrophys. J.* **352**, 247.

[37] Madsen J (1988) *Phys. Rev. Lett.* **61**, 2909.

[38] Datta B, Thampan A V & Bombaci I, *astro-ph/9912173.*

[39] Madsen J (1998) *Phys. Rev. Lett.* **81**, 3311.

[40] Li X.-D, Dai Z.-G & Wang Z.-R (1995) *Astron. & Astrophys.* **303**, L1.

[41] Bombaci I (1997) *Phys. Rev. C* **55**, 1587.

[42] Dey M, Bombaci I, Dey J, Ray S & Samanta B C (1998) *Phys. Lett. B* **438**, 123; Addendum: (1999) B **447**, 352; Erratum: (1999) B **467**, 303; (1999) *Indian J. Phys.* **73B**, 377.

[43] Li X.-D, Bombaci I, Dey M, Dey J & van den Heeuvel E P J (1999) *Phys. Rev. Lett.* **83**, 3776.

[44] Li X.-D, Ray S, Dey J, Dey M & Bombaci I (1999) *Astrophys. J* **527**, L51.

[45] Xu R X, Qiao G J & Zhang B (1999) *Astrophys. J* **522**, L109.

[46] Xu R X, Xu X B & Wu X J (2001) *Chin. Phys. Lett.* **18**, 837; *astro-ph/0101013.*

[47] Pons J A, Walter F M, Lattimer J M, Prakash M, Neuhäuser R & Penghui An, *astro-ph/0107404.*

[48] Chodos A, Jaffe R L, Johnson K, Thorn C B & Weisskopf V F (1974) *Phys. Rev. D* **9**, 3471.

[49] Fowler G N, Raha S & Weiner R M (1981) *Z. Phys.* **C9**, 271.

[50] Chakrabarty S, Raha S & Sinha B (1989) *Phys. Lett. B* **229**, 112.

[51] Benvenuto O G & Lugones G (1995) *Phys. Rev. D* **51**, 1989.

[52] Lugones G & Benvenuto O G (1995) *Phys. Rev. D* **52**, 1276.

[53] Peng G X, Chiang H C & Ning P Z (2000) *Phys. Rev. C* **62**, 025801; *hep-ph/0003027.*

[54] Cheng K S, Dai Z G & Lu T (1998) *Int. J. Mod. Phys. D* **7**, 139.

[55] Mielke E W & Schunck F E (2000) *Nucl. Phys.* **B564**, 185; *gr-qc/0001061*; *gr-qc/9801063.*

[56] Kaup D J (1968) *Phys. Rev.* **172**, 1331.

[57] Ruffini R & Bonazzola S (1969) *Phys. Rev.* **187**, 1767.

[58] Colpi M, Shapiro S L & Wasserman I (1986) *Phys. Rev. Lett.* **57**, 2485.

[59] Henriques A B, Liddle A R & Moorhouse R G (1990) *Nucl. Phys.* **B337**, 737; (1989) *Phys. Lett.* **B233**, 99.

[60] Jetzer P (1992) *Phys. Rep.* **220**, 163.

[61] Lindblom L (1992) Astrophys. J **398**, 569.

[62] Harada T (2001) *Phys. Rev. C* **64**, 048801; *astro-ph/0108410.*

[63] Vaidya P C & Tikekar R (1982) *J. Astrophys. Astron.* **3**, 325.

[64] Tikekar R (1990) *J. Math. Phys.* **31**, 2454.

[65] Sabu M C (1998): *A Study of Some Spacetimes of Gravitational Significance*, Ph D. thesis, Sardar Patel University, India.

[66] Maharaj S D & Leach P G L (1996) *J. Math. Phys.* **37**, 430.

[67] Mukherjee S, Paul B C & Dadhich N K (1997) *Class. Quantum Grav.* **14**, 3475.

[68] Sharma R, Mukherjee S & Maharaj S D (2001) *Gen. Rel. Grav.* **33**, 999.

[69] Treves A & Turolla R (1999) *Astrophy. J.* **517**, 396.

[70] Mak M K, Dobson Jr Peter N & Harko T (2001) *Europhys. Lett.* **55**, 310; *gr-qc/0107011.*

[71] Ivanov B V, *gr-qc/0109010.*

[72] Horvath J E & Pacheco J A D F (1998) *Int. J. Mod. Phys. D* **7**, 19.

[73] Chandrasekhar S (1964) *Phys. Rev. Lett.* **12**, 114; *Astrophys. J* **140**, 417.

[74] Gondek-Rosińska D, Bulik T, Zdunik L, Gourgoulhon E, Ray S, Dey J & Dey M (2000) *Astron. & Astrophys.* **363**, 1005.

[75] Zdunik J L (2000) *Astron. & Astrophys.* **359**, 311; *astro-ph/0004375.*

[76] Kastor D & Traschen J (1991) *Phys. Rev. D* **44**, 3791.

[77] Lindblom L (1998) *Phys. Rev. D* **58**, 024008.

[78] Oppenheimer J R & Snyder H (1939) *Phys. Rev.* **56**, 455.

[79] Vaidya P C (1951) *Proc. Indian Acad. Sci.* **A33**, 264.

[80] de Oliveira A K G, Santos N O & Kolassis C A (1985) *Mon. Not. R. Astron. Soc.* **216**, 1001.

[81] de Oliveira A K G, de Pacheco J A F & Santos N O (1986) *Mon. Not. R. Astron. Soc.* **220**, 405.

[82] de Oliveira A K G, Kolassis C A & Santos N O (1988) *Mon. Not. R. Astron. Soc.* **231**, 1011.

[83] Kramer D (1992) *J. Math. Phys.* **33**, 1458.

[84] Govender M, Maharaj S D & Maartens R (1998) *Class. Quantum Grav.* **15**, 323.

[85] Santos N O (1985) *Mon. Not. R. Astron. Soc.* **216**,403.

[86] Schäfer D & Goenner H F (2000) *Gen. Rel. Grav.* **32**, 2119.

[87] Bonnor W B, de Oliveira A K G & Santos N O (1989) *Phys. Rep.* **181**, 269.

[88] Kolassis C A, Santos N O & Tsoubelis D (1988) *Class. Quantum Grav.* **5**, 1329.

[89] Govender M, Govinder K S, Maharaj S D, Sharma R, Mukherjee S & Dey T K (2002) *Radiative spherical collapse with heat flow* (communicated).

[90] de Sousa C M G & Silveira V (2001) *Int. J. Mod. Phys. D* **10**, 881; *gr-qc/0012020.*

[91] Phukon T C (2000) *Phys. Rev. D* **62**, 023002.

[92] Buchdahl H A (1959) *Phys. Rev.* **116**, 1027.

[93] Kramer D, Stephani H, Herlt E & MacCallum M: *Exact Solutions of Einstein's Field Equations*, (Cambridge University Press, Cambridge, 1980).

[94] Fodor G, *gr-qc/0011040.*

[95] Finch M R & Skea J E F (1998) *A Review of the Relativistic Static Fluid Sphere*, unpublished, http:// www.dft.if.uerj.br/users/JimSkea/papers/pfrev.ps

[96] Delgaty M S R & Lake K (1998) *Computer Physics Communications* **115**, 395; *gr-qc/9809013.*

[97] Rahman S & Visser M, *gr-qc/0103065.*

[98] Tolman R C (1939) *Phys. Rev.* **55**, 364.

[99] Morse P M & Feshbach H: *Methods of Theoretical Physics*,(Mc Graw-Hill Book Co., 1953) Vol 1, p-782.

[100] Bonnor W B (1960) *Z. Phys.* **160**, 59; (1965) *Gravitation & Cosmology* **4**, 294.

[101] De U K & Raychaudhari A K(1968) *Pro. R. Soc. London Ser.* **A 303**, 97.

[102] Cooperstock F I & Cruz de la V (1977) *Gen. Rel. Grav.* **9**, 835.

[103] Tikekar R (1984) *Gen. Rel. Grav.* **16**, 445; (1984) *J. Math. Phys.* **25**, 1481.

[104] Patel L K, Tikekar R & Sabu M C (1997) *Gen. Rel. Grav.* **29**, 489.

[105] Tikekar R & Singh G P (1998) *Gravitation & Cosmology* **4**, 294.

[106] Dianyan Xu (1988) *Class. Quantum Grav.* **5**, 871.

[107] Tiwari R N & Ray S (1997) *Gen. Rel. Grav.* **29**, 683.

[108] Guilfoyle B S (1999) *Gen. Rel. Grav.* **31**, 1645.

[109] Rao J K & Trivedi M M(1998) *Pramana* **51**, 663.

[110] Rao J K, Annapurna M & Trivedi M M (2000) *Pramana* **54**, 215

[111] Krasinskii A (1997): *Inhomogeneous Cosmological Models* (Cambridge University Press, Cambridge.)

[112] de Felice F, Siming L & Yunquiang Y (1999) *Class. Quantum Grav.* **16**, 2669.

[113] Anninos P & Rothman T (2002) *Phys. Rev. D* **65**, 024003; *gr-qc/0108082.*

[114] Rhodes C E & Ruffini R (1974) *Phys. Rev. Lett.* **32**, 324.

[115] Patel L K & Koppar S S (1987) *Aust. J. Phys* **40**, 441.

[116] Collins J C & Perry M J (1975) *Phys. Rev. Lett.* **34** 1353.

[117] Chaplin G F & Nauenberg M (1976) *Nature* **264**, 235.

[118] Keister B D & Kisslinger L S (1976) *Phys. Letts.* **64B**, 117.

[119] Fechner W B & Joss P C (1978) *Nature* **274**, 347.

[120] Kettner Ch., Weber F, Weigel M K & Glendenning N K (1995) *Phys. Rev. D* **51**, 1440.

[121] In 't Zand J M M *et al* (1998) *Astron. & Astrophys.* **331**, L25; *astro-ph/0104285.*

[122] van der Klis M (2000) *Ann. Rev. Astron. & Astrophys.* **38**, 717; *astro-ph/0001167.*

[123] 't Hooft G (1974) *Nucl. Phys. B* **72**, 461; (1974) B **75**, 461.

[124] Witten E (1979) *Nucl. Phys.* **B160**, 57.

[125] Richardson J L (1979) *Phys. Letts. B* **82**, 272.

[126] Crater H W & van Alstine P (1984) *Phys. Rev. Lett.* **53**, 1527.

[127] Dey J, Dey M & LeTourneux J (1986) Phys. Rev. D **34**, 2104; Dey J, Dey M, Mukhopadhyaya G & Samanta B C (1991) *Can. J. Phys.* **69**, 749; Dey J, Tomio L, Dey M & Frederico T (1991) *Phys. Rev.* **C44**, 2181; Ray K, Dey J & Dey M (2000) *Mod. Phys. Lett. A* **15**, 683.

[128] Madsen J (1997) *Astron. & Astrophys.* **318**, 466; *astro-ph/9601129.*

[129] Bhattacharyya S (2001) *Astrophys. J* **554**, L185; *astro-ph/0105223.*

[130] Bombaci I & Datta B (2000) *Astrophys. J* **530**, L69.

[131] Ray S, Dey J & Dey M (2000) *Mod. Phys. Lett. A* **15**, 1301.

[132] Dar A & De Rújula A, *astro-ph/0002014*; Ouyed R, Dey J & Dey M, *astro-ph/0105109*; Blaschke D, Bombaci I, Grigorian H & Poghosyan G, *astro-ph/0110443*; Toledo Sanchez G & Piekarewicz J, *nucl-th/0109017*; Dey M, Sinha M, Ray S & Dey J, *astro-ph/0108082*; Xu R X, Xu X B & Wu X J, *astro-ph/0101013*, (2001) *Chin. Phys. Lett.* **18**, 837; Xu R X & Busse F H, *astro-ph/0101011*; Poghosyan G, Grigorian H & Blasckhe D, *astro-ph/0101002*; Armstrong T A *et al*, *nucl-ex/0010017*, (2001) *Phys. Rev. C* **63**, 054903; Blaschke D, Grigorian H & Poghosyan G, *astro-ph/0008005*; Xu R X, Zhang B & Qiao G J, *astro-ph/0006021*, (2001) *Astropart. Phys.* **15**, 101; Ray S, Dey J, Dey M, Ray K & Samanta B C, *astro-ph/0003472*; Bhattacharya S, Thampan A V & Bombaci I (2001) *Astro. Astrophys.* **372** 925; Zdunik J L, Haensel P, Gondek-Rosińska D & Gourgoulhon E, *astro-ph/0002394*, (2000) *Astron. & Astrophys.* **356**, 612.

[133] Sharma R, Mukherjee S & Maharaj S D (2000)*Mod. Phys. Lett. A* **15**, 1341.

[134] Bhowmick S, Dey J, Dey M, Ray S & Ray R, *astro-ph/0103389.*

[135] Wasserman I & Shapiro S L (1983) *Astrophys. J.* **265**, 1036.

[136] Schertler K, Greiner C, Schaffner-Bielich J & Thoma M H (2000) *Nucl. Phys.* **A677**, 463; *astro-ph/0001467.*

[137] Brans C H & Dicke R H (1961) *Phys. Rev.* **124**, 925.

[138] Schunck F E & Torres D F (2000) *Int. J. Mod. Phys. D* **9**, 601.

[139] Gleiser M (1998) *Phys. Rev. D* **38**, 2376.

[140] de Sousa C M G & Tomazelli J L (1998) *Phys. Rev. D* **58**, 123003.

[141] Sakamoto K & Shiraishi K (1998) *JHEP* **9807**, 015; *gr-qc/9804067*; (1998) *Phys. Rev. D* **58**, 124017; *gr-qc/9806040*.

[142] Sakamoto K & Shiraishi (2000) *Phys. Rev. D* **62**, 124014; *gr-qc/9910113*.

[143] Gell-Mann M (1964) *Phys. Lett.* **8**, 214.

[144] Anselmino M, Predazzi E, Ekelin S, Fredriksson S & Lichtenberg D B (1993) *Rev. Mod. Phys.* **65**, 1199.

[145] Ida M & Kobayashi R (1966) *Prog. Theor. Phys.* **36**, 846.

[146] Lichtenberg D B & Tassie L J (1967) *Phys. Rev.* **155**, 1601.

[147] Horvath J E, de Freitas Pacheco J A & de Araújo J N C (1992) *Phys. Rev. D* **46**, 4754.

[148] Donoghue J F & Sateesh K S (1988) *Phys. Rev. D* **38**, 360.

[149] Horvath J E (1992) *Phys. Lett. B* **294**, 412.

[150] Jaffe R L & Low F E (1979) *Phys. Rev. D* **19**, 2105.

[151] Horvath J E & Lugones G, *astro-ph/0112159*.

[152] Heinz U (2001) *Nucl. Phys.* **A685**, 414; *hep-ph/0009170*.

[153] Bardeen J M, Thorne K S & Meltzer D W (1966) *Astrophys. J.* **145**, 505.

[154] Cervillera L P N, Aquilano R O & Vucetich H (1998) *Mod. Phys. Lett. A* **13**, 1253.

[155] Negi P S & Durgapal M C (1999) *Gen. Rel. Grav.* **31**, 13.

[156] Knutsen H (1988) *Mon. Not. R. Astr. Soc.* **232**, 163.

[157] Tikekar R & Thomas V O (1998) *Pramana* **50**, 1.

[158] Misner C W, Thorne K S & Wheeler J A : *Gravitation*, (W. H. Freeman & Co. New York, 1973.)

[159] Benvenuto O G & Horvath J E (1991) *Mon. Not. R. Astr. Soc.* **250**, 679.

[160] Xu R X, Qiao G J & Zhang B, *astro-ph/9909484.*

[161] Usov V V (1998) *Phys. Rev. Letts.* **80**, 230.

[162] Sharma R & Mukherjee S (2001) *Mod. Phys. Lett. A* **16**, 1049.

[163] Sharma R, Mukherjee S, Dey M & Dey J (2002) *A general relativistic model for SAX J 1808.4-3658*, (communicated).

[164] Drago A & Lavagno A (2001) *Phys. Letts. B* **511**, 229; *hep-ph/0103209.*

[165] Mak M K & Harko T, *gr-qc/0110103.*

List of Publications:

1. *Her X-1: A Quark-Diquark Star?,*
   Sharma R & Mukherjee S, Mod. Phys. Lett. A (2001) **16**, 1049.

2. *General solution for a class of static charged spheres,*
   Sharma R, Mukherjee S & Maharaj S D , Gen. Rel. Grav. (2001) **33**, 999.

3. *Scaling Property in Cold Compact Stars,*
   Sharma R, Mukherjee S & Maharaj S D , Mod. Phys. Lett. A (2000) **15**, 1341.

4. *Radiative spherical collapse with heat flow,*
   Govender M, Govinder K S, Maharaj S D, **Sharma R**, Mukherjee S & Dey T K (2001) (*communicated).*

5. *A general relativistic model for SAX J 1808.4-3658,*
   Sharma R, *Mukherjee S, Dey M & Dey J (2001)* (communicated).

6. *A Core-Envelope Model for Compact Stars,*
   Sharma R & Mukherjee S, (2001) (*communicated).*